An uncertain view of the global EDM landscape

12 May 2025

Skyler Degenkolb, *Universität Heidelberg*

arxiv:2403.02052

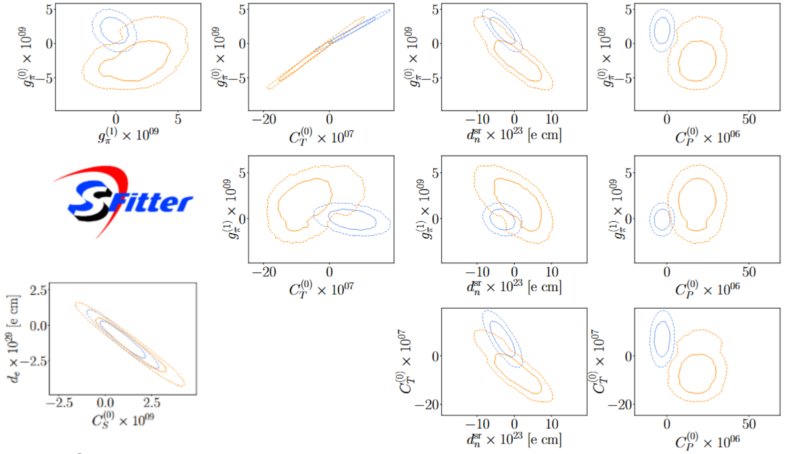

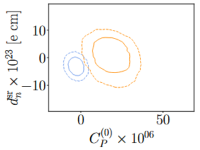

N. Elmer, SMD,
T. Modak, M. Muehlleitner, T. Plehn

$\{d_e, C_S, C_T, C_P, g_\pi^{(0)}, g_\pi^{(1)}, d_n^{sr}\}$

11 experiments / 7-8 parameters

Hadronic-level global analysis of EDMs

arxiv:2504.13030

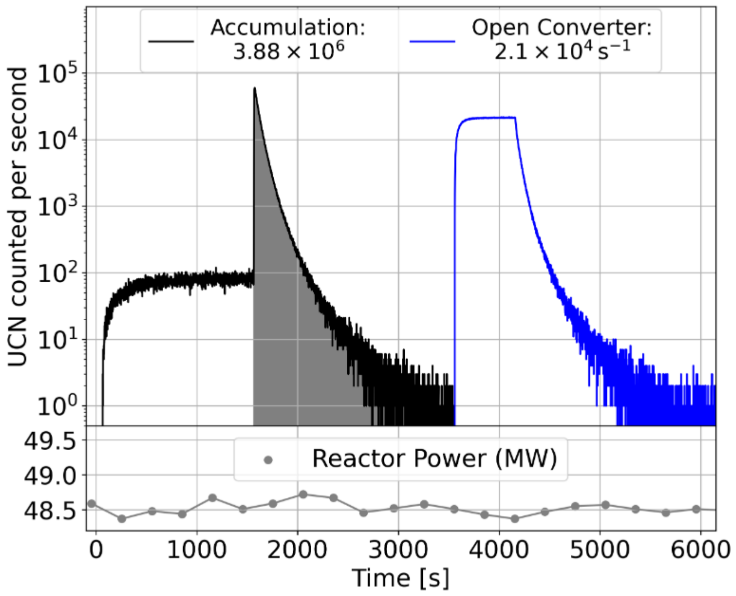

SuperSUN: ultracold neutrons for PanEDM

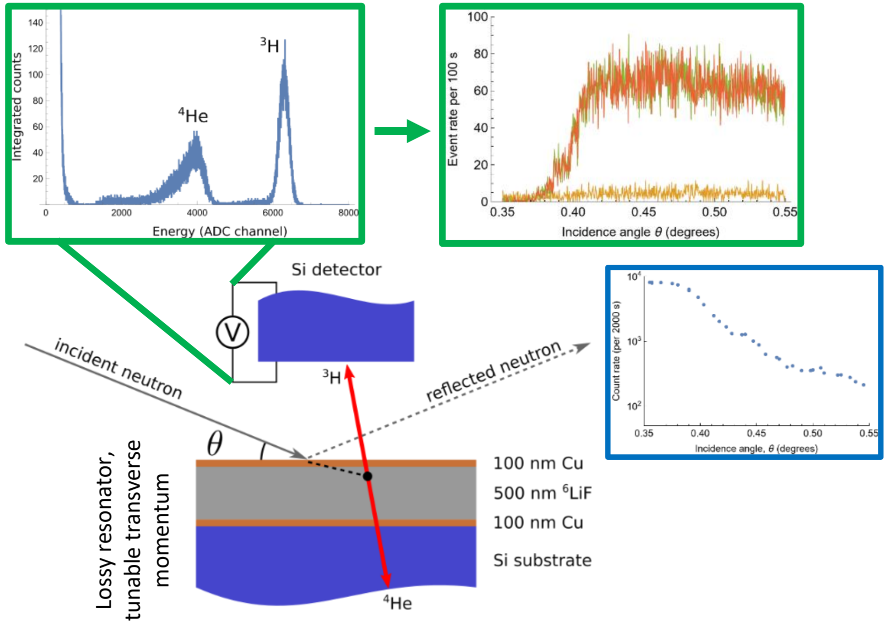

New methods: quantum sensing, QC

An uncertain view of the global EDM landscape

12 May 2025

Skyler Degenkolb, *Universität Heidelberg*

arxiv:2403.02052

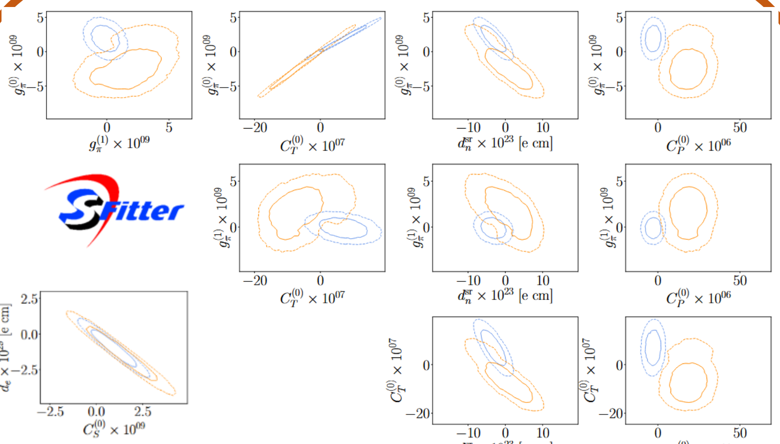

N. Elmer, SMD,
T. Modak, M. Muehlleitner, T. Plehn

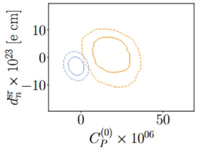

$\{d_e, C_S, C_T, C_P, g_\pi^{(0)}, g_\pi^{(1)}, d_n^{sr}\}$

11 experiments / 7-8 parameters

Hadronic-level global analysis of EDMs

arxiv:2504.13030

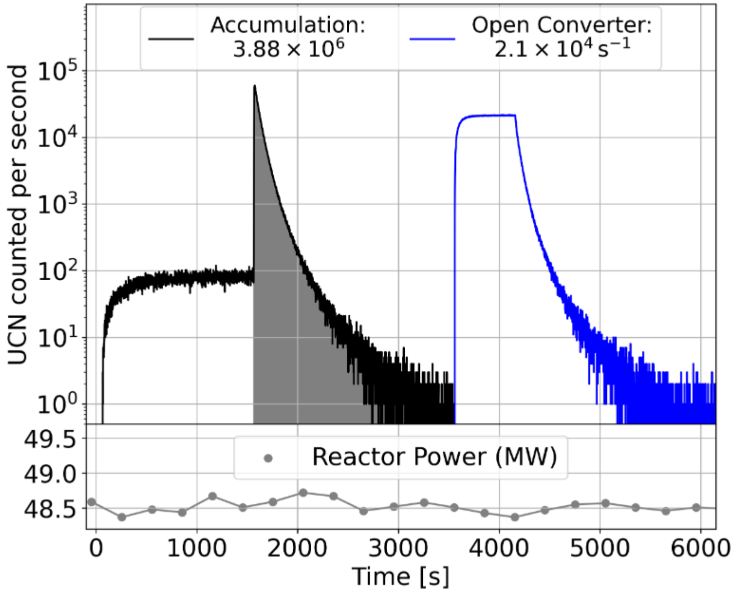

SuperSUN: ultracold neutrons for PanEDM

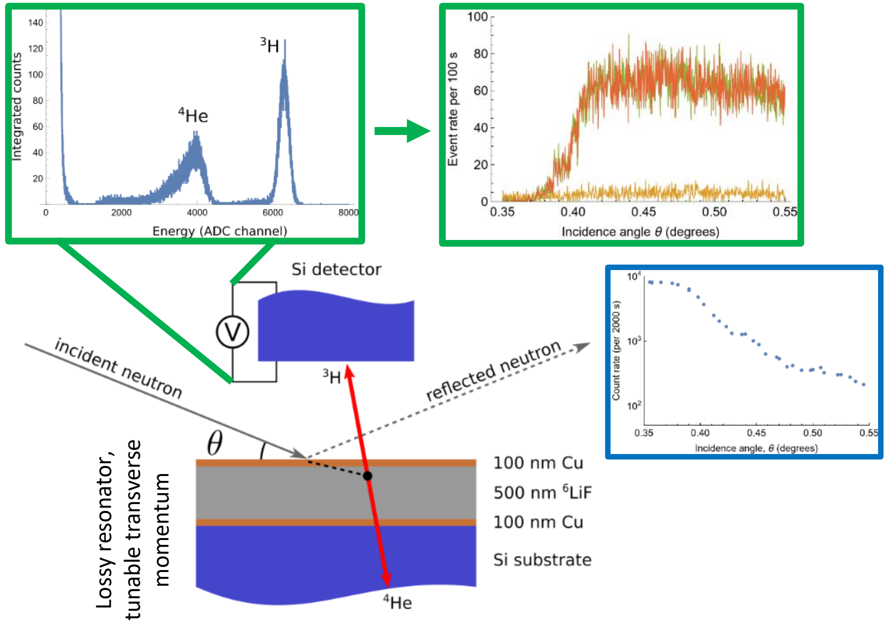

New methods: quantum sensing, QC

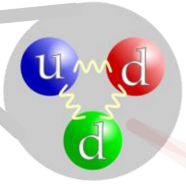

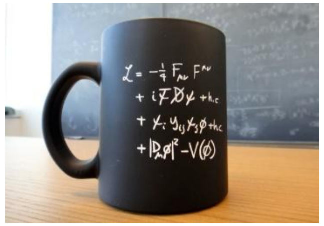

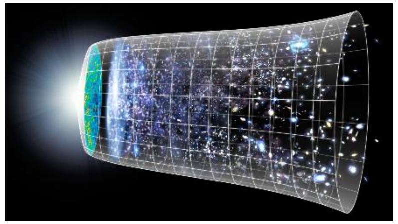

Observed photon density (CMB):

- $n_\gamma \approx 411\ \mathrm{cm}^{-3}$

Baryon density and asymmetry:

- $n_B \approx 6\times10^{-10}\, n_\gamma$

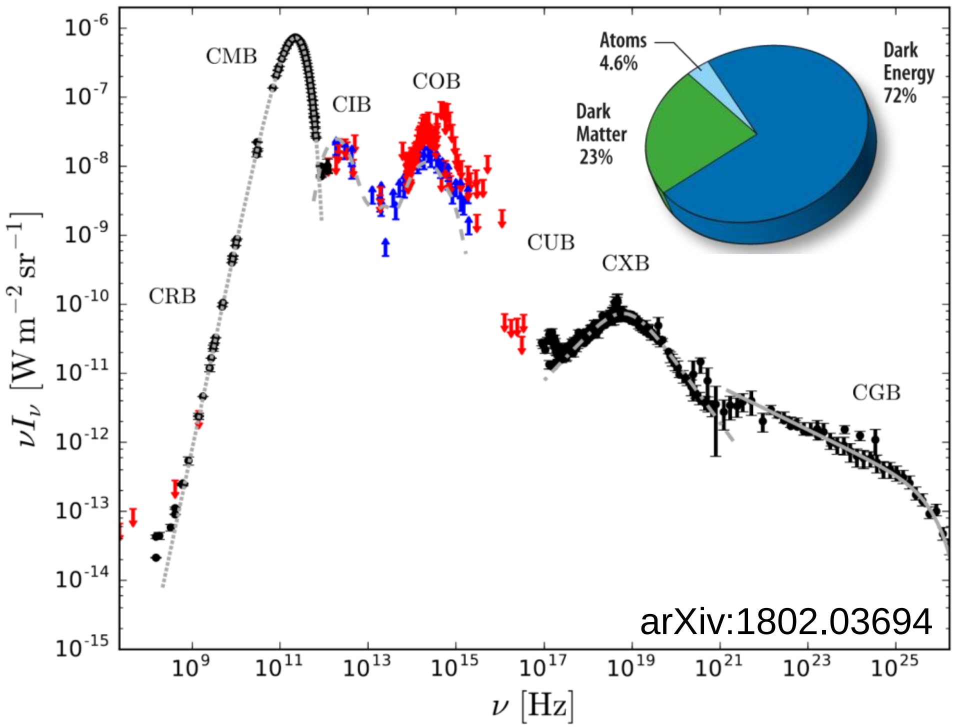

Sakharov criteria for Baryogenesis:

1. B non-conservation
2. **C and CP violation**
3. Far from thermal equilibrium

$$\mathscr{L}_{\text{fermion}} = -\frac{\mu}{2}\bar{\psi}\sigma^{\mu\nu}F_{\mu\nu}\psi - i\frac{d}{2}\bar{\psi}\sigma^{\mu\nu}\gamma^5 F_{\mu\nu}\psi$$

MDM **EDM**

Strong CP problem:

- $|d_n| < 10^{-26}\ e\cdot$cm (measured)
- implies $|\theta_{\mathrm{QCD}}| < 10^{-10}$ (too small)

$$H_{spin} = -\boldsymbol{\mu}\cdot\mathbf{B} - \mathbf{d}\cdot\mathbf{E}$$

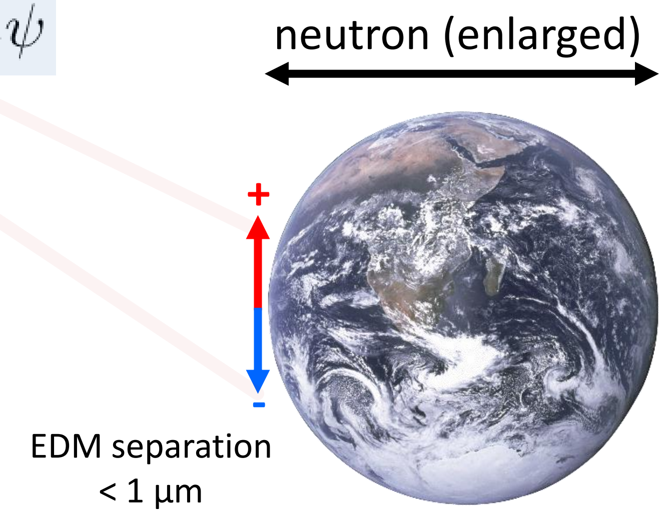

(European) Neutrons in the global context

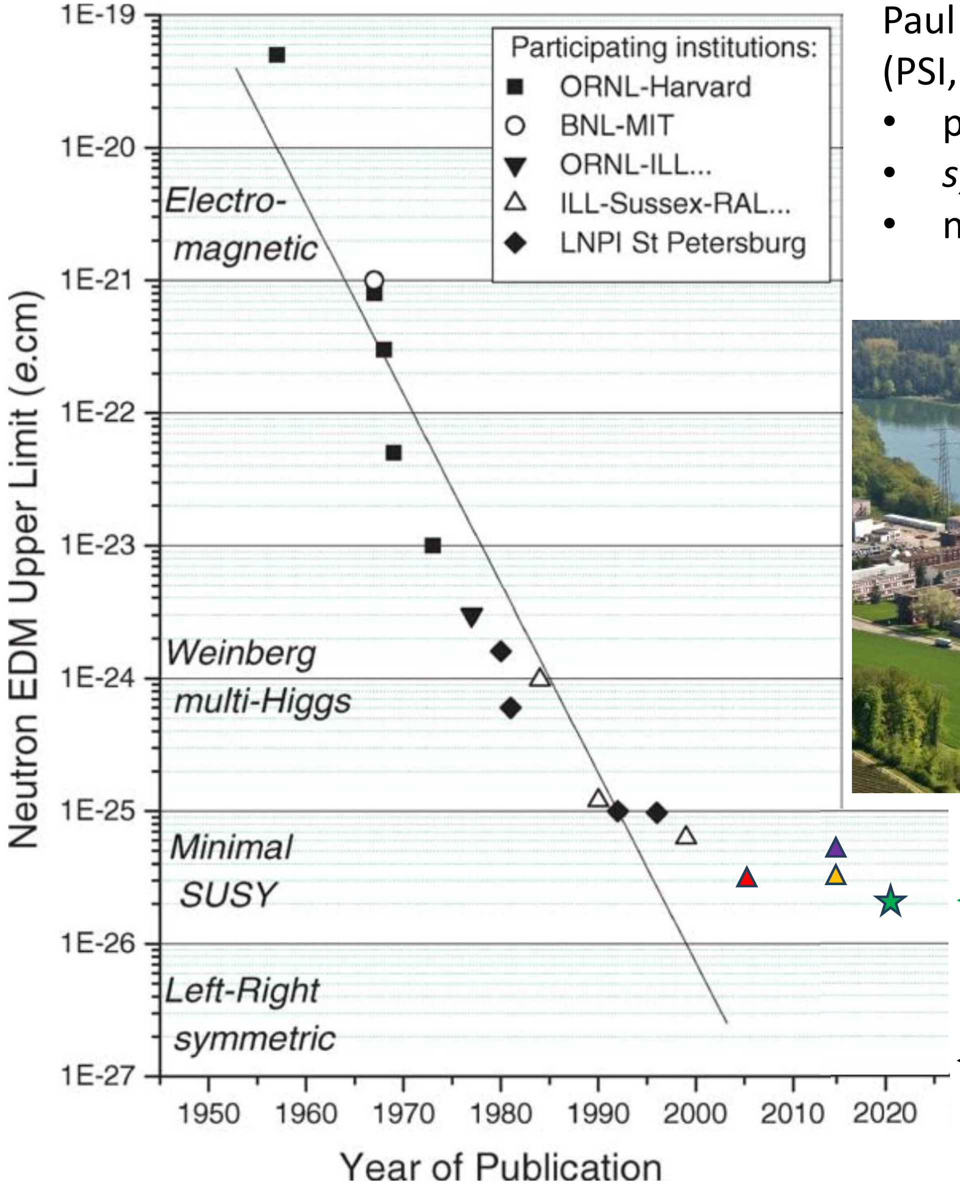

Paul Scherrer Institut
(PSI, Villigen)

- present limit
- *systematics*
- n2EDM

Institut Laue- Langevin
(ILL, Grenoble)

- previous limit
- *statistics*
- PanEDM

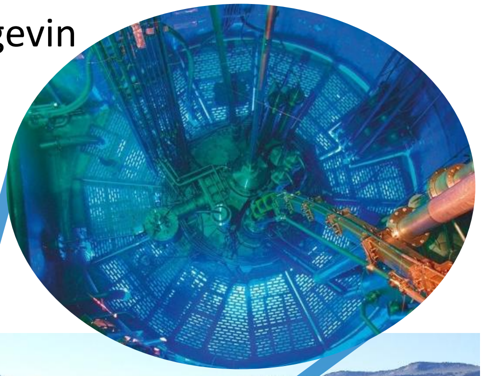

Now strongly limited by available neutrons

Sensitivity target for experiments now commissioning

(European) neutrons in the global context

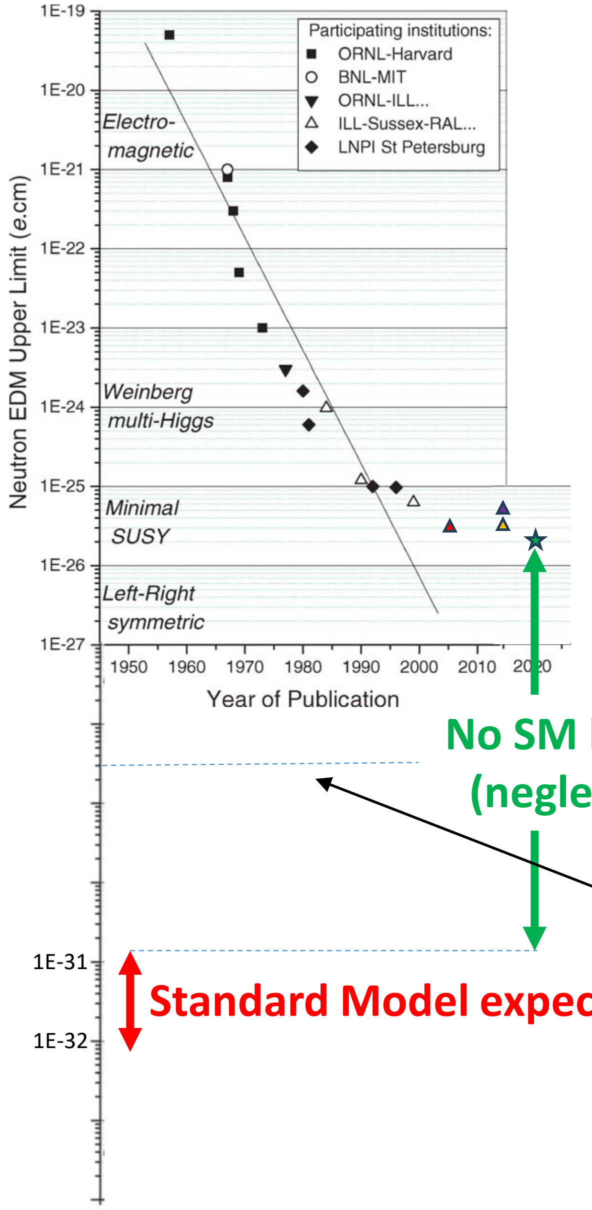

No SM background (neglecting θ_{QCD})

Standard Model expectation

JNR (2022) **24**(2), 123-143
potential reach with today's technology
(statistics only)

Paul Scherrer Institut (PSI, Villigen)

- present limit
- *systematics*
- n2EDM

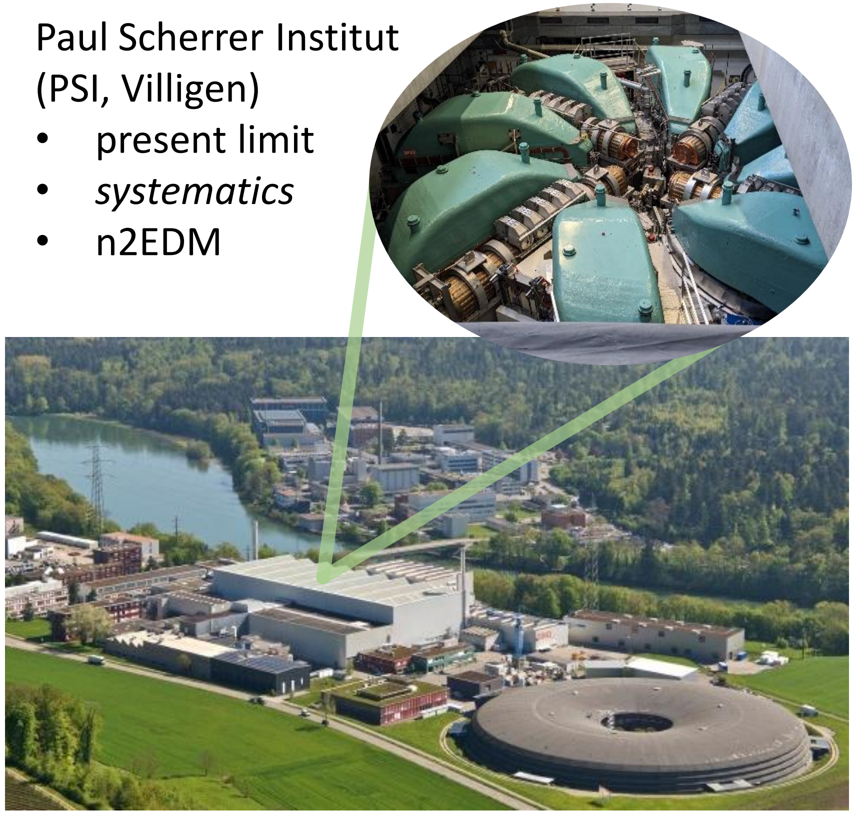

Institut Laue- Langevin (ILL, Grenoble)

- previous limit
- *statistics*
- PanEDM

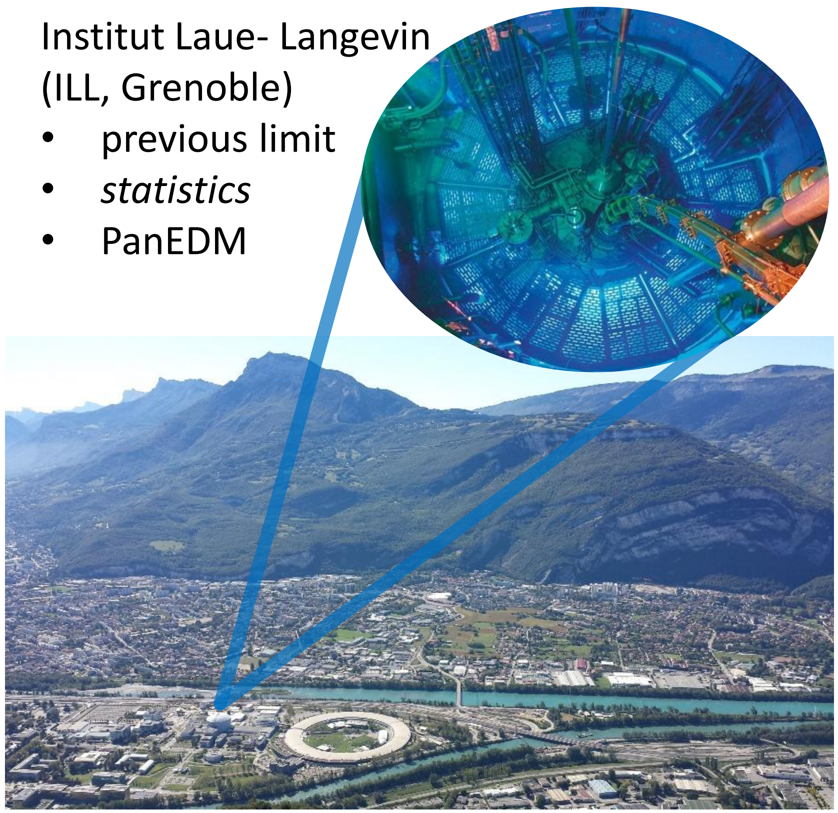

Very rough factors separating today's experiments and SM predictions:

10^8 (*) *10^7* *10^5-10^6*

How do electron and atomic/molecular EDMs compare to neutron?

$$\{d_e, C_S\} \quad \{C_T, C_P\} \quad \{g_\pi^{(0)}, g_\pi^{(1)}, d_n^{sr}\}$$

(*) or less… cf. PhysRevLett.129.231801

2020 European Strategy Update (2026: ongoing)

Other essential scientific activities for particle physics

A. The quest for dark matter and the exploration of flavour and fundamental symmetries are crucial components of the search for new physics. This search can be done in many ways, for example through precision measurements of flavour physics and electric or magnetic dipole moments, and searches for axions, dark sector candidates and feebly interacting particles. There are many options to address such physics topics including energy-frontier colliders, accelerator and non-accelerator experiments. A diverse programme that is complementary to the energy frontier is an essential part of the European particle physics Strategy. ***Experiments in such diverse areas that offer potential high-impact particle physics programmes at laboratories in Europe should be supported, as well as participation in such experiments in other regions of the world.***

Broad categories / sensitivity

<u>Open-shell</u> atoms and molecules

- "paramagnetic"
- Cs, Tl, YbF, ThO, HfF^+

Main sensitivities:

- electron EDM

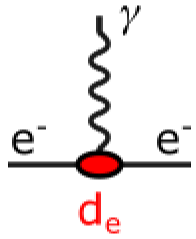

- semileptonic (nuclear spin *independent*)

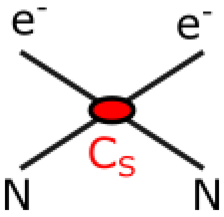

- others strongly suppressed

<u>Closed-shell</u> atoms and molecules

- "diamagnetic"
- Yb, Xe, Hg, Ra, TlF

Main sensitivities:

- nucleon EDMs

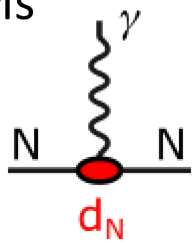

- nuclear forces

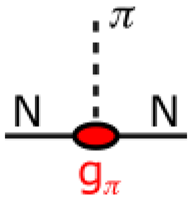

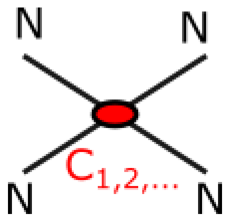

- semileptonic (nuclear spin-dependent)

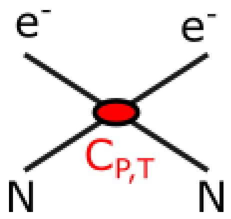

<u>Particles</u> and other…

- various properties
- *n*, (*p*), μ, τ, Λ, …

Main sensitivities:

- system dependent
- *n* constrains $\bar{\theta}$
- May need to look at higher scale for consistent interpretation

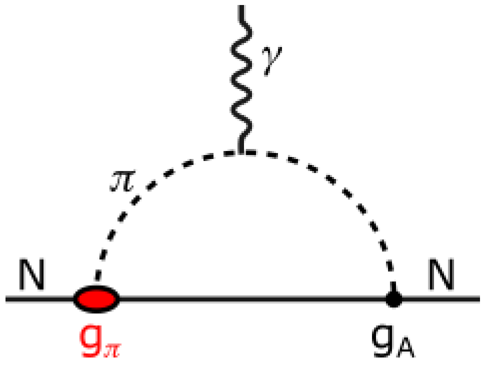

Precision Frontier: $d_n|\boldsymbol{E}| \leq 10^{-22}$ eV

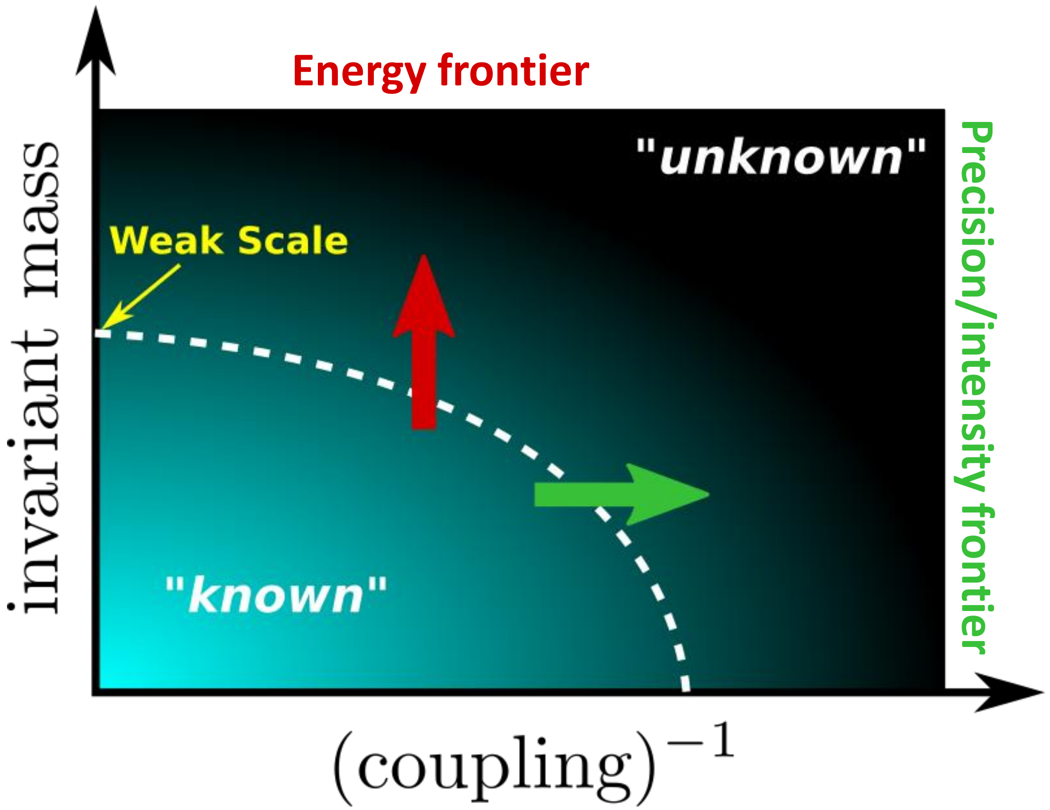

Statistical sensitivity:

$$\sigma(d_n) \gtrsim \frac{\hbar}{2\alpha\,|\boldsymbol{E}|\,T\sqrt{N}}$$

Current limit (PSI):
2.2×10^{-26} e cm, 95% C.L.

Polarization contrast ≈ 0.8

11 kV/cm

180 s

(54×10^{3})×(10^{4}/shot)

Naïve estimate for generic new physics:

$$d_n \propto \frac{m_q}{\Lambda^2} \cdot e \cdot \phi_{\mathrm{CPV}}$$

Λ ≈ 30 TeV

What would a finite neutron EDM mean?

- CP violation from BSM and three SM sources (if we ignore neutrinos):

$$\mathcal{L}_{\mathrm{CPV}} = \mathcal{L}_{\mathrm{BSM}} + \mathcal{L}_{\mathrm{CKM}} + \mathcal{L}_{\bar{\theta}}$$

- CKM CP-violation (Standard Model):

$$\mathcal{L}_{\mathrm{CKM}} = -\frac{ig_2}{\sqrt{2}} \sum_{p,q} V_{pq} \bar{U}_L^p \not{W}^+ D_L^q + \mathrm{H.c.}$$

- Strong CP-violation (Standard Model):

$$\mathcal{L}_{\bar{\theta}} = \frac{g_3^2}{32\pi^2} \bar{\theta}\, \mathrm{Tr}(G^{\mu\nu} \tilde{G}_{\mu\nu})$$

details: arXiv:2403.02052 *and earlier:*
Rev. Mod. Phys. ***91****, 015001 (2019)*
Phys. Rev. C ***91****, 035502 (2015)*
Prog. Part. Nucl. Phys. ***71****, 21 (2013)*

Reality: many parameters, many experiments

System i	Measured d_i [e cm]	Upper limit on $\|d_i\|$ [e cm]	Reference
n	$(0.0 \pm 1.1_{stat} \pm 0.2_{syst}) \cdot 10^{-26}$	$2.2 \cdot 10^{-26}$	[47]
^{205}Tl	$(-4.0 \pm 4.3) \cdot 10^{-25}$	$1.1 \cdot 10^{-24}$	[48]
^{133}Cs	$(-1.8 \pm 6.7_{stat} \pm 1.8_{syst}) \cdot 10^{-24}$	$1.4 \cdot 10^{-23}$	[49]
HfF^+	$(-1.3 \pm 2.0_{stat} \pm 0.6_{syst}) \cdot 10^{-30}$	$4.8 \cdot 10^{-30}$	[50]
ThO	$(4.3 \pm 3.1_{stat} \pm 2.6_{syst}) \cdot 10^{-30}$	$1.1 \cdot 10^{-29}$	[51]
YbF	$(-2.4 \pm 5.7_{stat} \pm 1.5_{syst}) \cdot 10^{-28}$	$1.2 \cdot 10^{-27}$	[52]
^{199}Hg	$(2.20 \pm 2.75_{stat} \pm 1.48_{syst}) \cdot 10^{-30}$	$7.4 \cdot 10^{-30}$	[53, 54]
^{129}Xe	$(-1.76 \pm 1.82) \cdot 10^{-28}$	$4.8 \cdot 10^{-28}$	[55, 56]
^{171}Yb	$(-6.8 \pm 5.1_{stat} \pm 1.2_{syst}) \cdot 10^{-27}$	$1.5 \cdot 10^{-26}$	[57]
^{225}Ra	$(4 \pm 6_{stat} \pm 0.2_{syst}) \cdot 10^{-24}$	$1.4 \cdot 10^{-23}$	[58]
TlF	$(-1.7 \pm 2.9) \cdot 10^{-23}$	$6.5 \cdot 10^{-23}$	[59]
	Measured ω_i [mrad/s]	Rescaling factor x_i for d_i	Reference
HfF^+	$(-0.0459 \pm 0.0716_{stat} \pm 0.0217_{syst})^*$	0.999	[50]
ThO	$(-0.510 \pm 0.373_{stat} \pm 0.310_{syst})$	0.982	[51]
YbF	$(5.30 \pm 12.60_{stat} \pm 3.30_{syst})$	1.12	[52]

Table 1: Measured EDM values and 95% C.L. ranges used in our global analysis. For ^{129}Xe we combine two independent results with similar precision, using inverse-variance weighting. For the paramagnetic molecules, we also provide the measured angular frequencies and the rescaling factor which allows us to use $x_i d_i$ for each experimentally reported d_i. *The frequency for HfF^+ is scaled by a factor of 2 relative to Ref. [50], to consistently use Eq.(27) for all systems.

arXiv:2403.02052

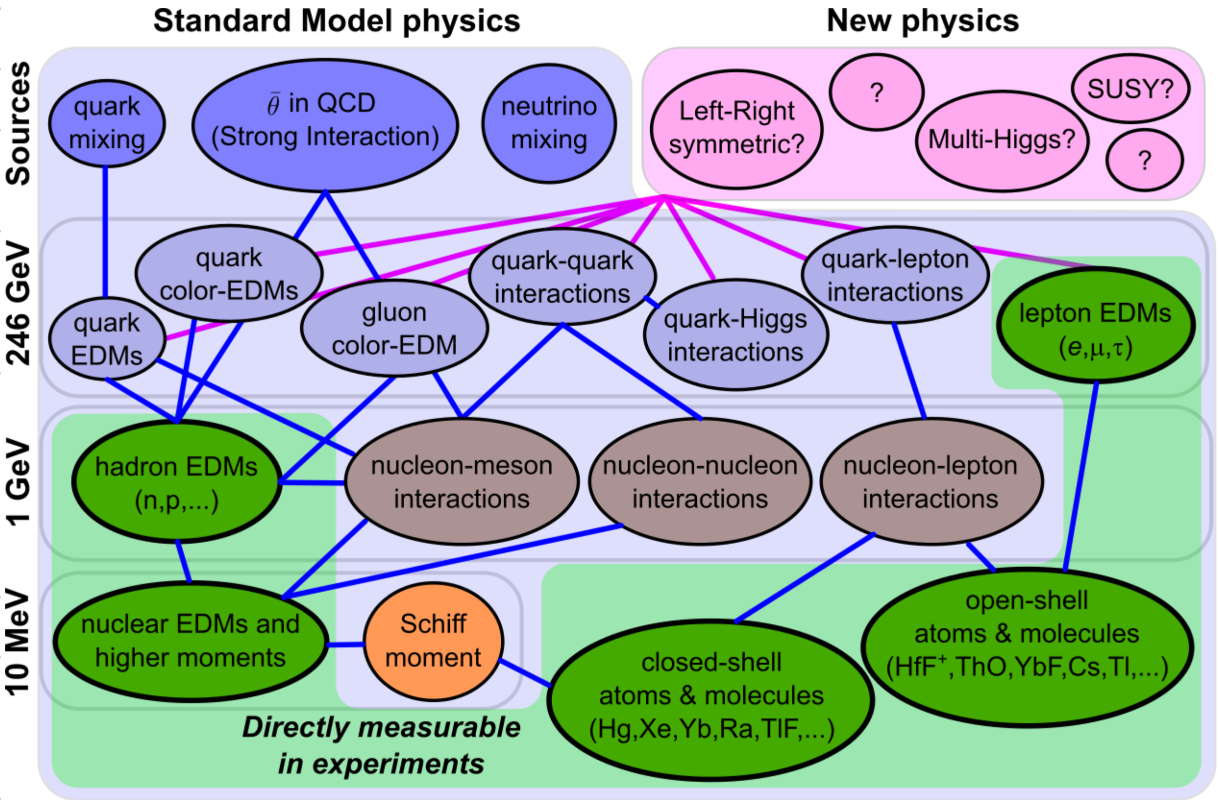

EDMs as a "lightning rod" for new physics – without assumptions about the underlying model

Clear prediction that ***there is a signal to detect***

Global analysis: 11 experiments / 7 parameters

System i	Measured d_i [e cm]	Upper limit on $\lvert d_i \rvert$ [e cm]	Reference
n	$(0.0 \pm 1.1_{\mathrm{stat}} \pm 0.2_{\mathrm{syst}}) \cdot 10^{-26}$	$2.2 \cdot 10^{-26}$	[47]
^{205}Tl	$(-4.0 \pm 4.3) \cdot 10^{-25}$	$1.1 \cdot 10^{-24}$	[48]
^{133}Cs	$(-1.8 \pm 6.7_{\mathrm{stat}} \pm 1.8_{\mathrm{syst}}) \cdot 10^{-24}$	$1.4 \cdot 10^{-23}$	[49]
HfF^+	$(-1.3 \pm 2.0_{\mathrm{stat}} \pm 0.6_{\mathrm{syst}}) \cdot 10^{-30}$	$4.8 \cdot 10^{-30}$	[50]
ThO	$(4.3 \pm 3.1_{\mathrm{stat}} \pm 2.6_{\mathrm{syst}}) \cdot 10^{-30}$	$1.1 \cdot 10^{-29}$	[51]
YbF	$(-2.4 \pm 5.7_{\mathrm{stat}} \pm 1.5_{\mathrm{syst}}) \cdot 10^{-28}$	$1.2 \cdot 10^{-27}$	[52]
^{199}Hg	$(2.20 \pm 2.75_{\mathrm{stat}} \pm 1.48_{\mathrm{syst}}) \cdot 10^{-30}$	$7.4 \cdot 10^{-30}$	[53, 54]
^{129}Xe	$(-1.76 \pm 1.82) \cdot 10^{-28}$	$4.8 \cdot 10^{-28}$	[55, 56]
^{171}Yb	$(-6.8 \pm 5.1_{\mathrm{stat}} \pm 1.2_{\mathrm{syst}}) \cdot 10^{-27}$	$1.5 \cdot 10^{-26}$	[57]
^{225}Ra	$(4 \pm 6_{\mathrm{stat}} \pm 0.2_{\mathrm{syst}}) \cdot 10^{-24}$	$1.4 \cdot 10^{-23}$	[58]
TlF	$(-1.7 \pm 2.9) \cdot 10^{-23}$	$6.5 \cdot 10^{-23}$	[59]

	Measured ω_i [mrad/s]	Rescaling factor x_i for d_i	Reference
HfF^+	$(-0.0459 \pm 0.0716_{\mathrm{stat}} \pm 0.0217_{\mathrm{syst}})^*$	0.999	[50]
ThO	$(-0.510 \pm 0.373_{\mathrm{stat}} \pm 0.310_{\mathrm{syst}})$	0.982	[51]
YbF	$(5.30 \pm 12.60_{\mathrm{stat}} \pm 3.30_{\mathrm{syst}})$	1.12	[52]

Table 1: Measured EDM values and 95% C.L. ranges used in our global analysis. For ^{129}Xe we combine two independent results with similar precision, using inverse-variance weighting. For the paramagnetic molecules, we also provide the measured angular frequencies and the rescaling factor which allows us to use $x_i d_i$ for each experimentally reported d_i. *The frequency for HfF^+ is scaled by a factor of 2 relative to Ref. [50], to consistently use Eq.(27) for all systems.

arXiv:2403.02052

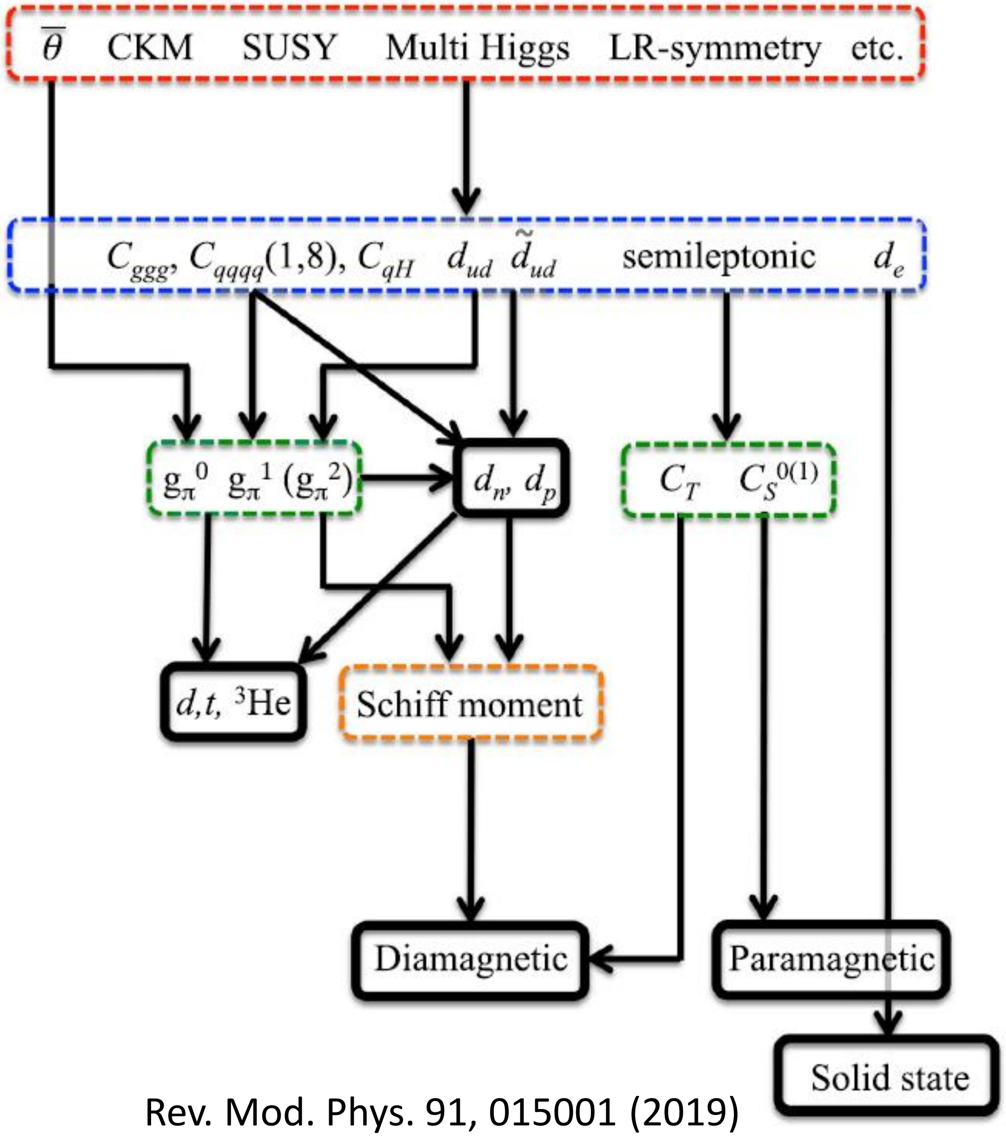

Rev. Mod. Phys. 91, 015001 (2019)

Open-shell systems constrain d_e and C_S

arXiv:2403.02052

Global result:

cf. arXiv:2212.11841

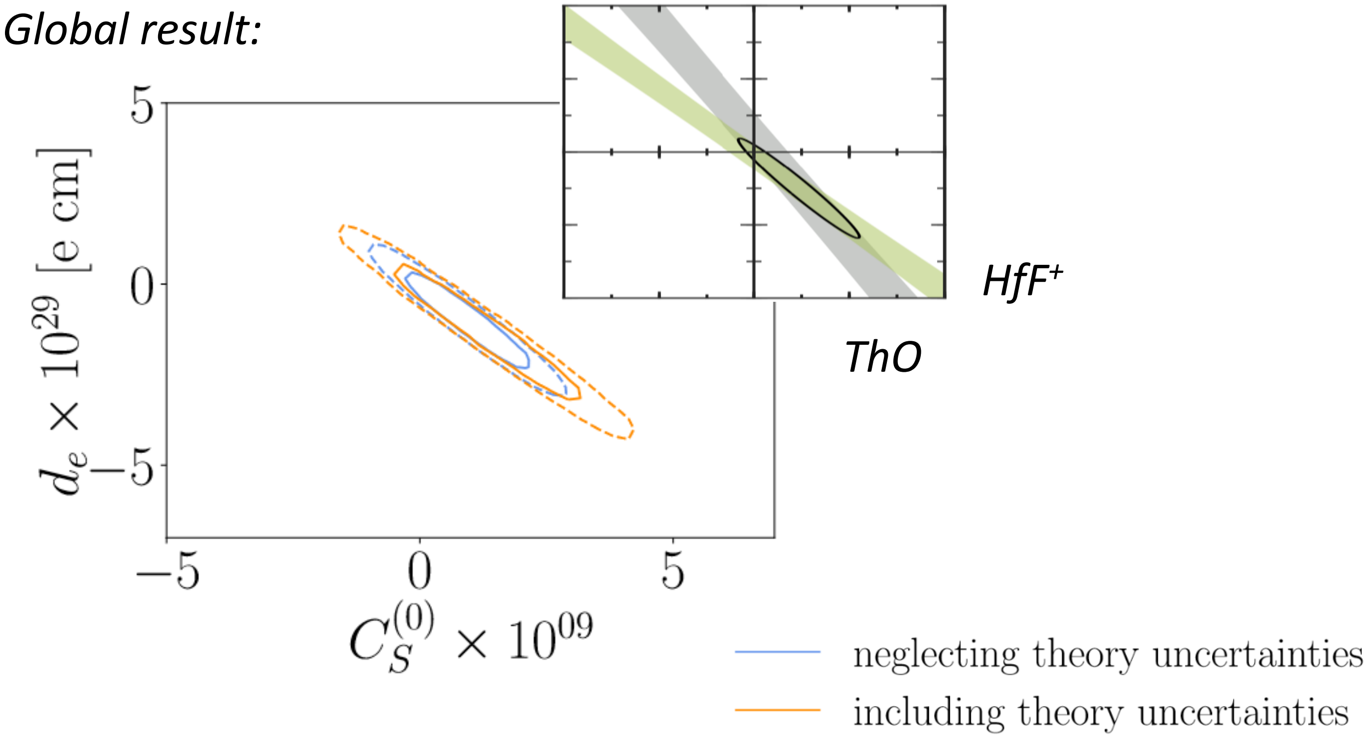

^{205}Tl	$(-4.0 \pm 4.3) \cdot 10^{-25}$	$1.1 \cdot 10^{-24}$	[48]
^{133}Cs	$(-1.8 \pm 6.7_{\text{stat}} \pm 1.8_{\text{syst}}) \cdot 10^{-24}$	$1.4 \cdot 10^{-23}$	[49]
HfF^+	$(-1.3 \pm 2.0_{\text{stat}} \pm 0.6_{\text{syst}}) \cdot 10^{-30}$	$4.8 \cdot 10^{-30}$	[50]
ThO	$(4.3 \pm 3.1_{\text{stat}} \pm 2.6_{\text{syst}}) \cdot 10^{-30}$	$1.1 \cdot 10^{-29}$	[51]
YbF	$(-2.4 \pm 5.7_{\text{stat}} \pm 1.5_{\text{syst}}) \cdot 10^{-28}$	$1.2 \cdot 10^{-27}$	[52]

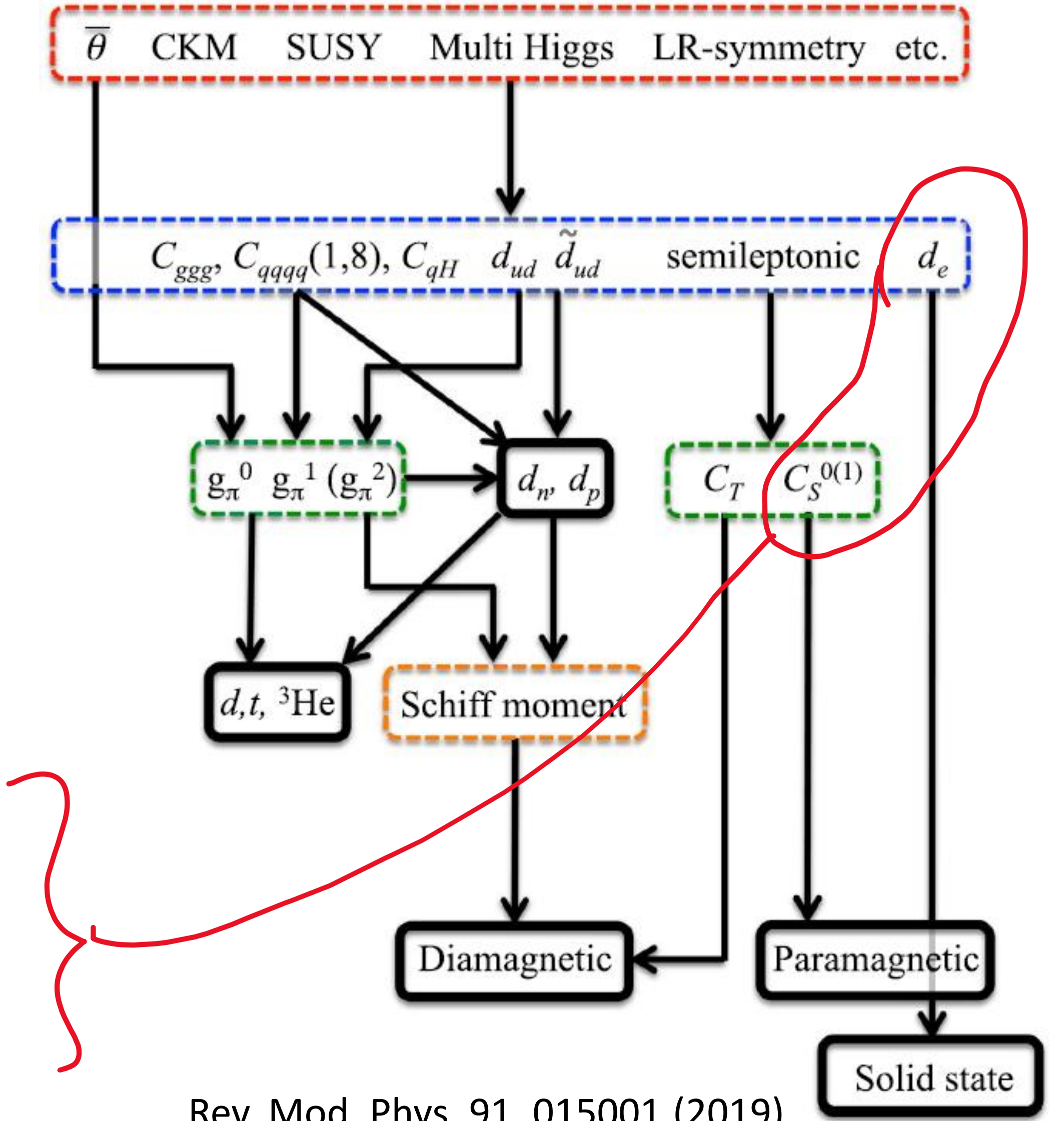

Rev. Mod. Phys. 91, 015001 (2019)

Global analysis: 11 experiments / 7 parameters

System i	Measured d_i [e cm]	Upper limit on $\|d_i\|$ [e cm]	Reference
n	$(0.0 \pm 1.1_{\rm stat} \pm 0.2_{\rm syst}) \cdot 10^{-26}$	$2.2 \cdot 10^{-26}$	[47]
^{205}Tl	$(-4.0 \pm 4.3) \cdot 10^{-25}$	$1.1 \cdot 10^{-24}$	[48]
^{133}Cs	$(-1.8 \pm 6.7_{\rm stat} \pm 1.8_{\rm syst}) \cdot 10^{-24}$	$1.4 \cdot 10^{-23}$	[49]
HfF$^+$	$(-1.3 \pm 2.0_{\rm stat} \pm 0.6_{\rm syst}) \cdot 10^{-30}$	$4.8 \cdot 10^{-30}$	[50]
ThO	$(4.3 \pm 3.1_{\rm stat} \pm 2.6_{\rm syst}) \cdot 10^{-30}$	$1.1 \cdot 10^{-29}$	[51]
YbF	$(-2.4 \pm 5.7_{\rm stat} \pm 1.5_{\rm syst}) \cdot 10^{-28}$	$1.2 \cdot 10^{-27}$	[52]
^{199}Hg	$(2.20 \pm 2.75_{\rm stat} \pm 1.48_{\rm syst}) \cdot 10^{-30}$	$7.4 \cdot 10^{-30}$	[53, 54]
^{129}Xe	$(-1.76 \pm 1.82) \cdot 10^{-28}$	$4.8 \cdot 10^{-28}$	[55, 56]
^{171}Yb	$(-6.8 \pm 5.1_{\rm stat} \pm 1.2_{\rm syst}) \cdot 10^{-27}$	$1.5 \cdot 10^{-26}$	[57]
^{225}Ra	$(4 \pm 6_{\rm stat} \pm 0.2_{\rm syst}) \cdot 10^{-24}$	$1.4 \cdot 10^{-23}$	[58]
TlF	$(-1.7 \pm 2.9) \cdot 10^{-23}$	$6.5 \cdot 10^{-23}$	[59]
	Measured ω_i [mrad/s]	Rescaling factor x_i for d_i	Reference
HfF$^+$	$(-0.0459 \pm 0.0716_{\rm stat} \pm 0.0217_{\rm syst})^*$	0.999	[50]
ThO	$(-0.510 \pm 0.373_{\rm stat} \pm 0.310_{\rm syst})$	0.982	[51]
YbF	$(5.30 \pm 12.60_{\rm stat} \pm 3.30_{\rm syst})$	1.12	[52]

Table 1: Measured EDM values and 95% C.L. ranges used in our global analysis. For ^{129}Xe we combine two independent results with similar precision, using inverse-variance weighting. For the paramagnetic molecules, we also provide the measured angular frequencies and the rescaling factor which allows us to use $x_i d_i$ for each experimentally reported d_i. *The frequency for HfF$^+$ is scaled by a factor of 2 relative to Ref. [50], to consistently use Eq.(27) for all systems.

Hadronic scale global analysis: arXiv:2403.02052

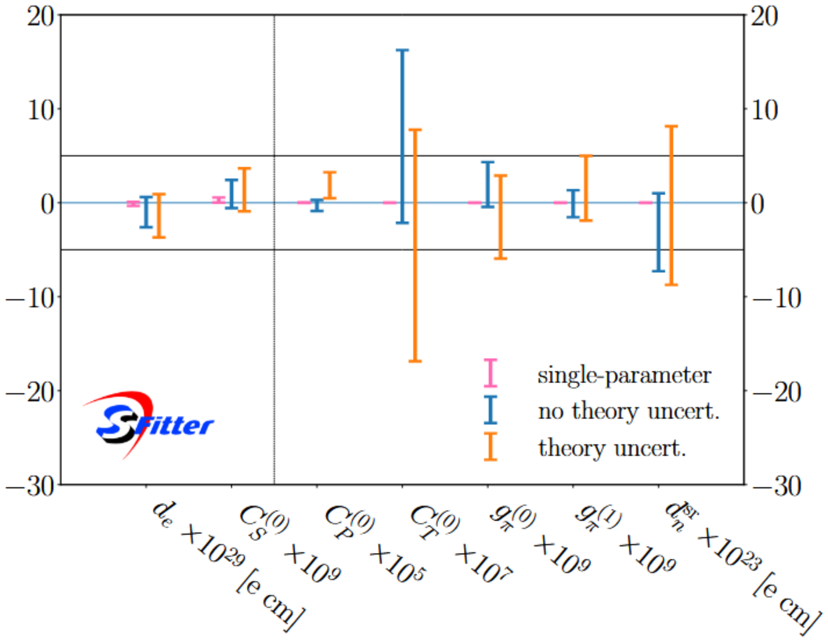

"A Global View of the EDM Landscape"

SMD, Nina Elmer, Tanmoy Modak,
Margarete Mühlleitner, Tilman Plehn

Global analysis: 11 experiments / 7 parameters

Theory uncertainties mostly lack a statistical interpretation
- Assume flat likelihood
- Coefficients compatibly with zero do not constrain

Correlations are automatically built into the analysis
- Comagnetometer measurements neglect a sub-dominant EDM by construction
- Deliberately-correlated EDM experiments could offer complementary constraining power

Flat directions appear already with 4 or 5 parameters
- Depends on treatment of neutron/proton, and pion loops

Formally: 7 parameters are overconstrained by 11 experiments
Reality: the experiments are insufficiently complementary!
- Well-constrained subspace (2 parameters: d_e, C_S)
- Poorly-constrained subspace (5 parameters / 5 measurements)
- Other parameters should really be included as well…

Hadronic scale global analysis: arXiv:2403.02052

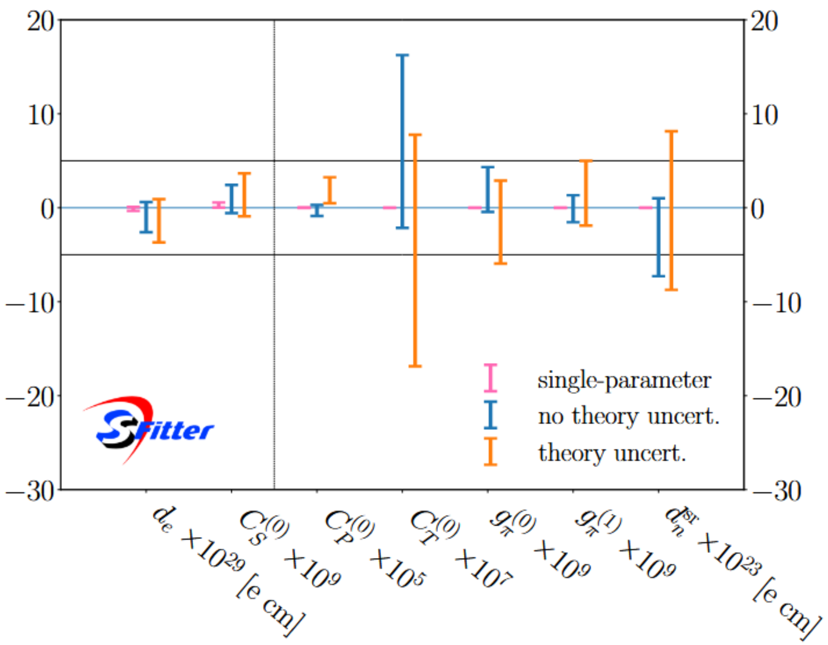

"A Global View of the EDM Landscape"

SMD, Nina Elmer, Tanmoy Modak, Margarete Mühlleitner, Tilman Plehn

Constructing, and deconstructing, an EDM

$$d_i = \sum_{c_j} \alpha_{i,c_j} c_j = \alpha_{i,d_e} d_e + \alpha_{i,C_S} C_S + \ldots$$

$$c_j \in \left\{ d_e, C_S^{(0)}, C_T^{(0)}, C_P^{(0)}, g_\pi^{(0)}, g_\pi^{(1)}, d_n \right\}$$

Schiff Moment parameterization:

$$k_{i,S} S_i = \sum_{c_j \in \{d_{n,p}, g_\pi^{(0,1,2)}\}} \alpha_{i,c_j} c_j$$

$$\approx k_{i,S} \left[s_{i,n} d_n + s_{i,p} d_p + \frac{m_N g_A}{F_\pi} \left(a_{i,0} g_\pi^{(0)} + a_{i,1} g_\pi^{(1)} + a_{i,2} g_\pi^{(2)} \right) \right]$$

$$= k_{i,S} \left[s_{i,n} d_n^{\mathrm{sr}} + s_{i,p} d_p^{\mathrm{sr}} + \frac{m_N g_A}{F_\pi} \left(\tilde{a}_{i,0} g_\pi^{(0)} + \tilde{a}_{i,1} g_\pi^{(1)} + \tilde{a}_{i,2} g_\pi^{(2)} \right) \right]$$

Contours, correlations, <u>likelihoods</u>:

$$\chi^2(C_j) = \sum_i \left(\frac{d_i^{\mathrm{measured}} - d_i^{\mathrm{calculated}}(C_j)}{\sigma_i^{\mathrm{measured}}} \right)^2$$

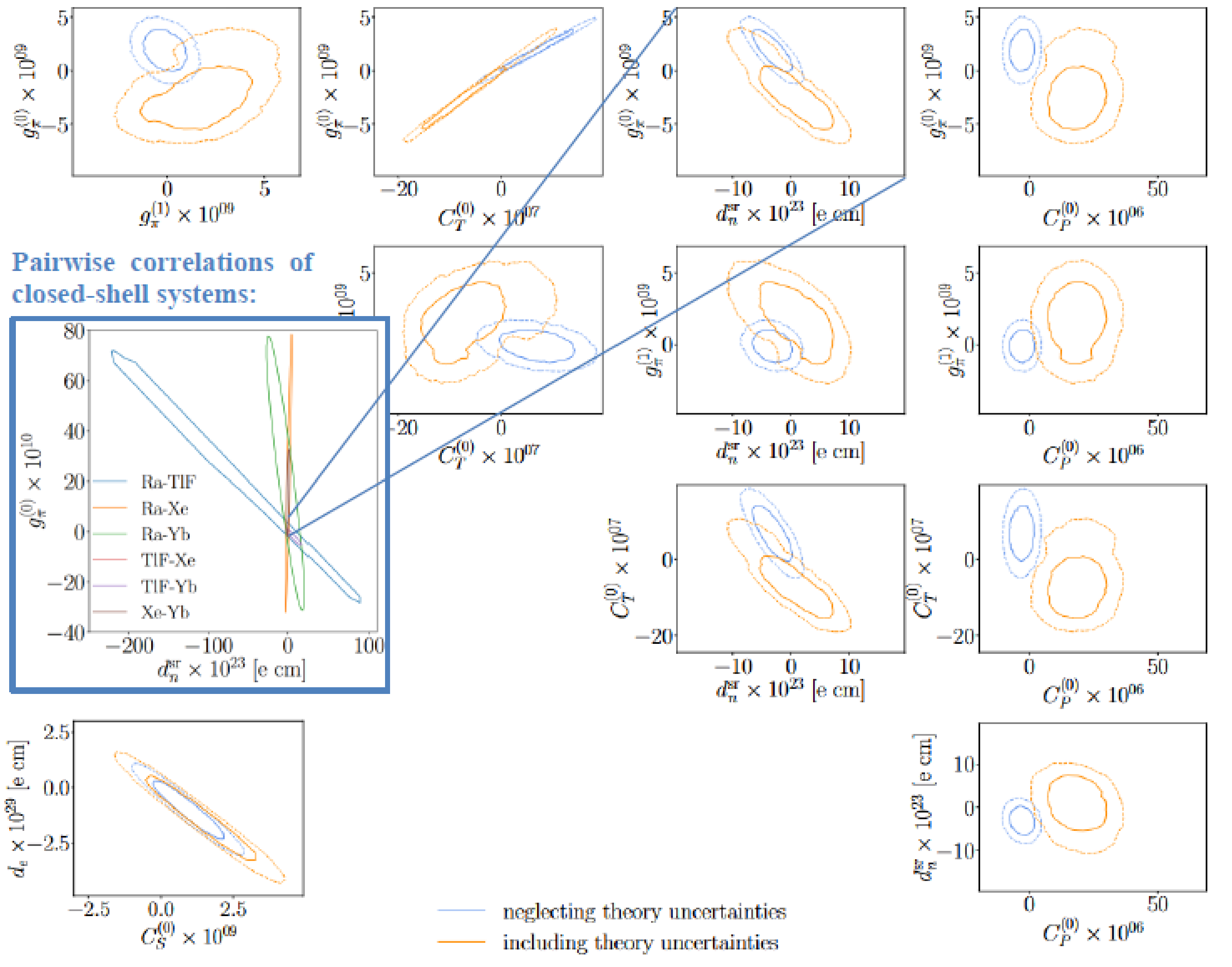

Effective Hadronic-Scale Lagrangian

- Semileptonic interactions at the weak scale:

$$\mathscr{L}_{\mathrm{EFT}} \supset C_{\ell e q d} \left(\bar{L}^j e_R\right)\left(\bar{d}_R Q_j\right) + C^{(1)}_{\ell e q u}\left(\bar{L}^j e_R\right)\epsilon_{jk}\left(\bar{Q}^k u_R\right) + C^{(3)}_{\ell e q u}\left(\bar{L}^j \sigma_{\mu\nu} e_R\right)\epsilon_{jk}\left(\bar{Q}^k \sigma_{\mu\nu} u_R\right)$$
$$+ C^{(1)}_{quqd}\left(\bar{Q}^j u_R\right)\epsilon_{jk}\left(\bar{Q}^k d_R\right) + C^{(8)}_{quqd}\left(\bar{Q}^j T^a u_R\right)\epsilon_{jk}\left(\bar{Q}^k T^a d_R\right) + \mathrm{h.c.}$$

- Low-energy constants at GeV energies, from weak-scale Wilson coefficients:

$$C_S^{(0)} = -g_S^{(0)}\frac{v^2}{\Lambda^2}\,\mathrm{Im}\left(C_{\ell e d q} - C^{(1)}_{\ell e q u}\right) \qquad C_S^{(1)} = g_S^{(1)}\frac{v^2}{\Lambda^2}\,\mathrm{Im}\left(C_{\ell e d q} + C^{(1)}_{\ell e q u}\right)$$
$$C_T^{(0)} = -g_T^{(0)}\frac{v^2}{\Lambda^2}\,\mathrm{Im}\left(C^{(3)}_{\ell e q u}\right) \qquad C_T^{(1)} = -g_T^{(1)}\frac{v^2}{\Lambda^2}\,\mathrm{Im}\left(C^{(3)}_{\ell e q u}\right)$$
$$C_P^{(0)} = g_P^{(0)}\frac{v^2}{\Lambda^2}\,\mathrm{Im}\left(C_{\ell e d q} + C^{(1)}_{\ell e q u}\right) \qquad C_P^{(1)} = -g_P^{(1)}\frac{v^2}{\Lambda^2}\,\mathrm{Im}\left(C_{\ell e d q} - C^{(1)}_{\ell e q u}\right)$$

Effective Hadronic-Scale Lagrangian

- Semileptonic interactions at the **hadronic** scale (w/ nonrelativistic nucleons):

$$\mathcal{L}_{eN} = -\frac{G_F}{\sqrt{2}}\,(\bar{e}i\gamma_5 e)\,\bar{N}\left(C_S^{(0)} + C_S^{(1)}\tau_3\right)N + \frac{8G_F}{\sqrt{2}}\,v_\nu\,(\bar{e}\sigma^{\mu\nu}e)\,\bar{N}\left(C_T^{(0)} + C_T^{(1)}\tau_3\right)S_\mu N$$

$$-\frac{G_F}{\sqrt{2}}\,(\bar{e}e)\,\frac{\partial^\mu}{m_N}\left[\bar{N}\left(C_P^{(0)} + C_P^{(1)}\tau_3\right)S_\mu N\right]$$

- Low-energy constants also depend on hadronic matrix elements:

$$g_S^{(0)}\,\bar{\psi}_N\psi_N = \frac{1}{2}\langle N\,|\bar{u}u + \bar{d}d|\,N\rangle \qquad g_T^{(0)}\,\bar{\psi}_N\sigma_{\mu\nu}\psi_N = \frac{1}{2}\langle N\,|\bar{u}\sigma_{\mu\nu}u + \bar{d}\sigma_{\mu\nu}d|\,N\rangle$$

$$g_S^{(1)}\,\bar{\psi}_N\tau_3\psi_N = \frac{1}{2}\langle N\,|\bar{u}u - \bar{d}d|\,N\rangle \qquad g_T^{(1)}\,\bar{\psi}_N\sigma_{\mu\nu}\tau_3\psi_N = \frac{1}{2}\langle N\,|\bar{u}\sigma_{\mu\nu}u - \bar{d}\sigma_{\mu\nu}d|\,N\rangle$$

$$g_P^{(0)}\,\bar{\psi}_N\gamma_5\psi_N = \frac{1}{2}\langle N\,|\bar{u}\gamma_5 u + \bar{d}\gamma_5 d|\,N\rangle$$

$$g_P^{(1)}\,\bar{\psi}_N\gamma_5\tau_3\psi_N = \frac{1}{2}\langle N\,|\bar{u}\gamma_5 u - \bar{d}\gamma_5 d|\,N\rangle$$

Effective Hadronic-Scale Lagrangian

- Semileptonic interactions at the **hadronic** scale:

$$\mathscr{L}_{eN} = -\frac{G_F}{\sqrt{2}}\,(\bar{e} i\gamma_5 e)\,\bar{N}\left(C_S^{(0)} + C_S^{(1)}\tau_3\right)N + \frac{8G_F}{\sqrt{2}}\,v_\nu\,(\bar{e}\sigma^{\mu\nu}e)\,\bar{N}\left(C_T^{(0)} + C_T^{(1)}\tau_3\right)S_\mu N$$

$$-\frac{G_F}{\sqrt{2}}\,(\bar{e}e)\,\frac{\partial^\mu}{m_N}\left[\bar{N}\left(C_P^{(0)} + C_P^{(1)}\tau_3\right)S_\mu N\right]$$

$$g_P^{(0)}\,\bar{\psi}_N\gamma_5\psi_N = \frac{1}{2}\langle N|\bar{u}\gamma_5 u + \bar{d}\gamma_5 d|N\rangle$$

$$g_P^{(1)}\,\bar{\psi}_N\gamma_5\tau_3\psi_N = \frac{1}{2}\langle N|\bar{u}\gamma_5 u - \bar{d}\gamma_5 d|N\rangle$$

η replaces π ; factor $m_{ud}/m_s \approx 1/20$

$$C_P^{(0)} = \quad g_P^{(0)}\frac{v^2}{\Lambda^2}\,\mathrm{Im}\left(C_{\ell edq} + C_{\ell equ}^{(1)}\right)$$

$$C_P^{(1)} = -g_P^{(1)}\frac{v^2}{\Lambda^2}\,\mathrm{Im}\left(C_{\ell edq} - C_{\ell equ}^{(1)}\right)$$

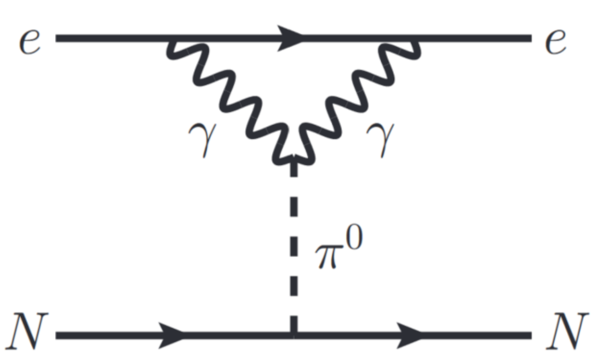

$$\langle N|\bar{q}i\gamma_5 q|N\rangle \propto g_{\pi NN}\frac{1}{m_\pi^2}\langle 0|\bar{q}i\gamma_5 q|\pi\rangle$$

$$\sim g_{\pi NN}\frac{1}{f_\pi m_\pi^2}\langle 0|\bar{q}q|0\rangle$$

$$\sim O(100)$$

Effective Hadronic-Scale Lagrangian

- "Long-range" nuclear forces, involving pion-nucleon couplings:

$$\mathscr{L}_{\pi N} = \bar{N}\Big[g_\pi^{(0)}\vec{\tau}\cdot\vec{\pi} + g_\pi^{(1)}\pi^0 + g_\pi^{(2)}\left(3\tau_3\pi^0 - \vec{\tau}\cdot\vec{\pi}\right)\Big]N$$
$$+ C_1\,\left(\bar{N}N\right)\,\partial_\mu\left(\bar{N}S^\mu\bar{N}\right) + C_2\,\left(\bar{N}\vec{\tau}N\right)\cdot\partial_\mu\left(\bar{N}S^\mu\bar{N}\vec{\tau}\right) + \cdots$$

- "Short-range" leftovers (can be absorbed differently):

$$\mathscr{L}_{N,\mathrm{sr}} = -2\bar{N}\left[d_p^{\mathrm{sr}}\frac{1+\tau_3}{2} + d_n^{\mathrm{sr}}\frac{1-\tau_3}{2}\right]S_\mu N v_\nu F^{\mu\nu} \;-\frac{i}{2}F^{\mu\nu}\sum_\ell d_\ell\,\left(\bar{\ell}\sigma_{\mu\nu}\gamma_5\ell\right)$$

- Nuclear Schiff moment (and MQM for I>1/2):

$$k_{i,S}S_i = k_{i,S}\left[s_{i,n}d_n + s_{i,p}d_p + \frac{m_N g_A}{F_\pi}\left(a_{i,0}g_\pi^{(0)} + a_{i,1}g_\pi^{(1)} + a_{i,2}g_\pi^{(2)}\right)\right]$$

Effective Hadronic-Scale Lagrangian

- “Long-range” nuclear forces, involving pion-nucleon couplings:

$$\mathcal{L}_{\pi N} = \bar{N}\Big[g_\pi^{(0)}\vec{\tau}\cdot\vec{\pi} + g_\pi^{(1)}\pi^0 + g_\pi^{(2)}\left(3\tau_3\pi^0 - \vec{\tau}\cdot\vec{\pi}\right)\Big]N$$
$$+ C_1\,(\bar{N}N)\,\partial_\mu\left(\bar{N}S^\mu\bar{N}\right) + C_2\,(\bar{N}\vec{\tau}N)\cdot\partial_\mu\left(\bar{N}S^\mu\bar{N}\vec{\tau}\right) + \cdots$$

- “Short-range” leftovers (can be absorbed differently):

$$\mathcal{L}_{N,\mathrm{sr}} = -2\bar{N}\left[d_p^{\mathrm{sr}}\frac{1+\tau_3}{2} + d_n^{\mathrm{sr}}\frac{1-\tau_3}{2}\right]S_\mu N v_\nu F^{\mu\nu} - \frac{i}{2}F^{\mu\nu}\sum_\ell d_\ell\,\left(\bar{\ell}\sigma_{\mu\nu}\gamma_5\ell\right)$$

Assume:

$$d_p^{\mathrm{sr}} \approx -d_n^{\mathrm{sr}}$$

- Nuclear Schiff moment (and MQM for I>1/2):

$$k_{i,S}S_i = k_{i,S}\left[s_{i,n}d_n + s_{i,p}d_p + \frac{m_N g_A}{F_\pi}\left(a_{i,0}g_\pi^{(0)} + a_{i,1}g_\pi^{(1)} + a_{i,2}g_\pi^{(2)}\right)\right]$$

Complementary atoms/nuclei

$$S = s_N d_N + \frac{m_N g_A}{F_\pi}[a_0 \bar{g}_\pi^{(0)} + a_1 \bar{g}_\pi^{(1)} + a_2 \bar{g}_\pi^{(2)}]$$

We do *not* expect large Schiff moments in ^{129}Xe/ ^{199}Hg (suppressed by the screening effect)

$$\longrightarrow d_A(\text{dia}) = \kappa_S S - [k_{C_T}^{(0)} C_T^{(0)} + k_{C_T}^{(1)} C_T^{(1)}]$$

But deformed nuclei can actually have **enhanced** EDMs:

$$\longrightarrow d_A(\text{dia}) = \kappa_S S - [k_{C_T}^{(0)} C_T^{(0)} + k_{C_T}^{(1)} C_T^{(1)}]$$

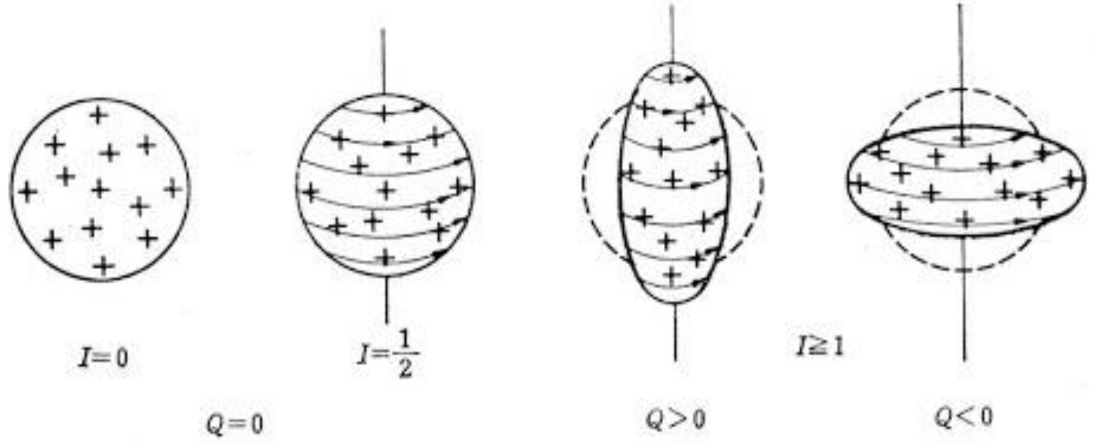

Complementary atoms/nuclei

$$S = s_N d_N + \frac{m_N g_A}{F_\pi}[a_0 \bar{g}_\pi^{(0)} + a_1 \bar{g}_\pi^{(1)} + \cancel{a_2 \bar{g}_\pi^{(2)}}]$$

We do *not* expect large Schiff moments in ^{129}Xe/ ^{199}Hg (suppressed by the screening effect)

$$\longrightarrow d_A(\text{dia}) = \kappa_S S - \underline{[k_{C_T}^{(0)} C_T^{(0)} + k_{C_T}^{(1)} C_T^{(1)}]}$$

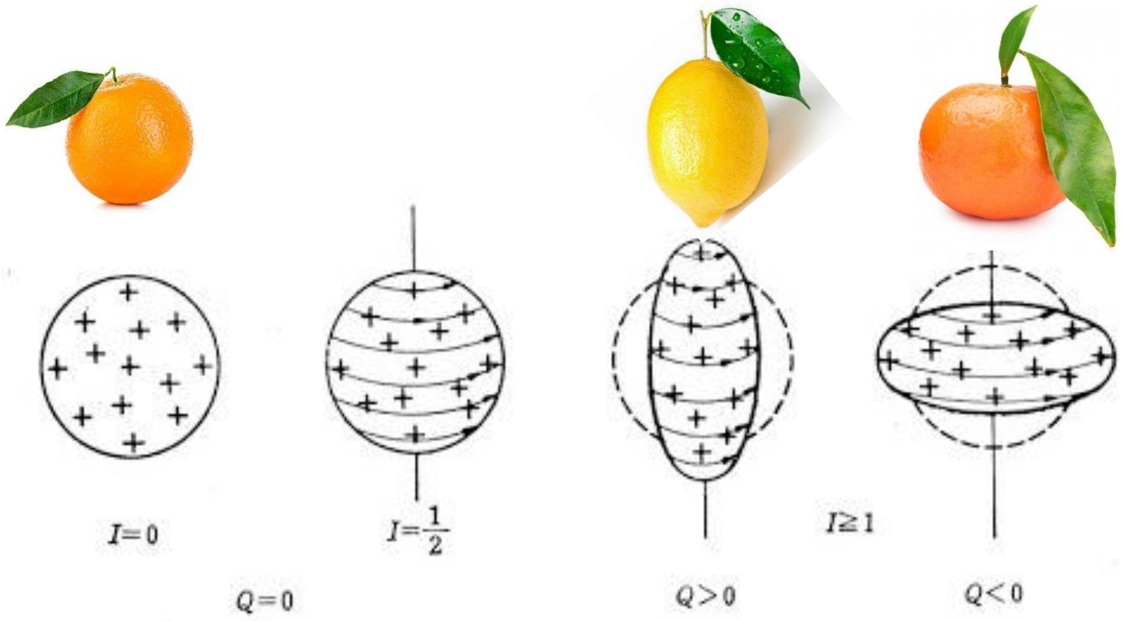

But deformed nuclei can actually have **enhanced** EDMs:

$$\longrightarrow d_A(\text{dia}) = \underline{\kappa_S} S - [k_{C_T}^{(0)} C_T^{(0)} + k_{C_T}^{(1)} C_T^{(1)}]$$

Complementary atoms/nuclei

$$S = s_N d_N + \frac{m_N g_A}{F_\pi}\left[a_0 \bar{g}_\pi^{(0)} + a_1 \bar{g}_\pi^{(1)} + a_2 \bar{g}_\pi^{(2)}\right]$$

We do *not* expect large Schiff moments in ^{129}Xe/ ^{199}Hg (suppressed by the screening effect)

$$\longrightarrow \; d_A(\text{dia}) = \kappa_S S - [k_{C_T}^{(0)} C_T^{(0)} + k_{C_T}^{(1)} C_T^{(1)}]$$

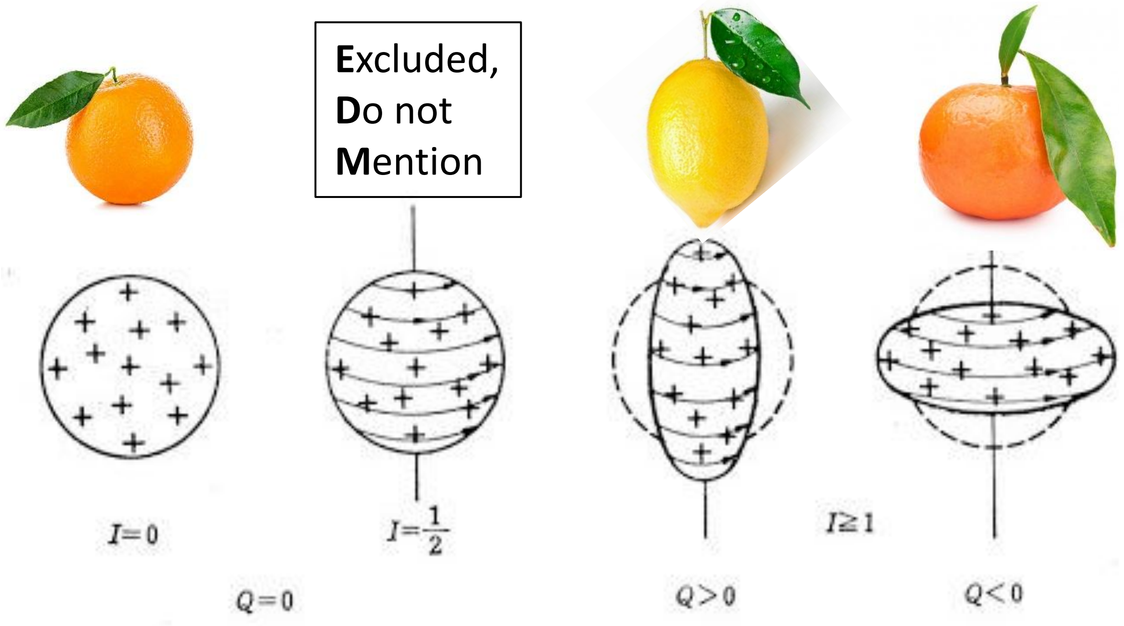

But deformed nuclei can actually have **enhanced** EDMs:

$$\longrightarrow \; d_A(\text{dia}) = \kappa_S S - [k_{C_T}^{(0)} C_T^{(0)} + k_{C_T}^{(1)} C_T^{(1)}]$$

Reflection asymmetry

Complementary atoms/nuclei

$$S = s_N d_N + \frac{m_N g_A}{F_\pi}[a_0 \bar{g}_\pi^{(0)} + a_1 \bar{g}_\pi^{(1)} + a_2 \bar{g}_\pi^{(2)}]$$

We do *not* expect large Schiff moments in ^{129}Xe/ ^{199}Hg (suppressed by the screening effect)

$$\longrightarrow d_A(\text{dia}) = \kappa_S S - [k_{C_T}^{(0)} C_T^{(0)} + k_{C_T}^{(1)} C_T^{(1)}]$$

Excluded, **D**o not **M**ention

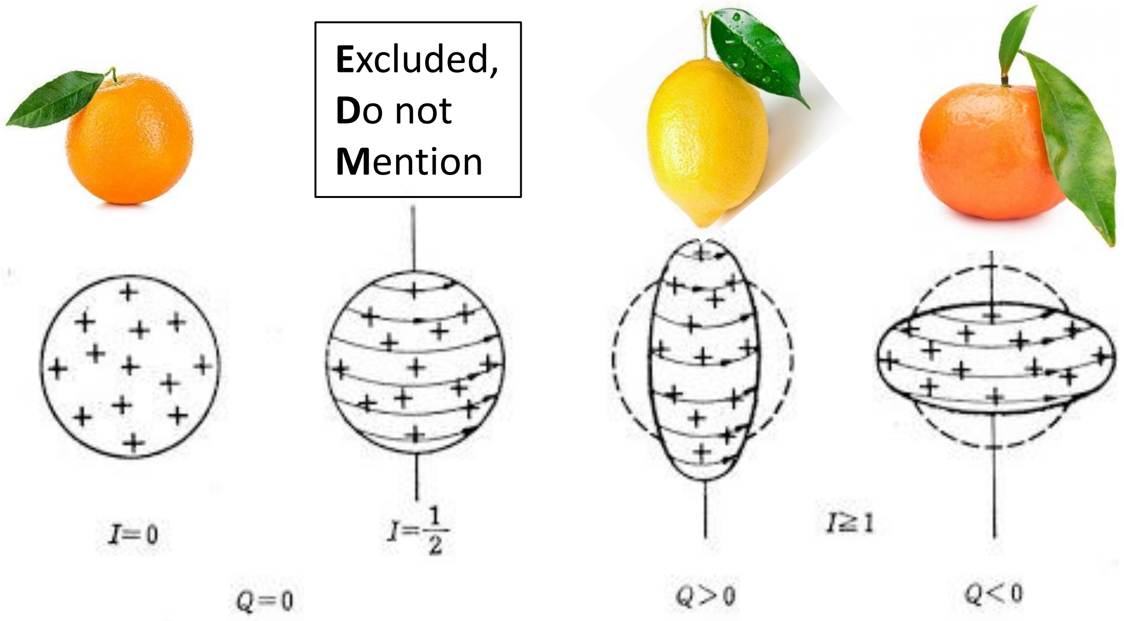

But deformed nuclei can actually have **enhanced** EDMs:

$$\longrightarrow d_A(\text{dia}) = \kappa_S S - [k_{C_T}^{(0)} C_T^{(0)} + k_{C_T}^{(1)} C_T^{(1)}]$$

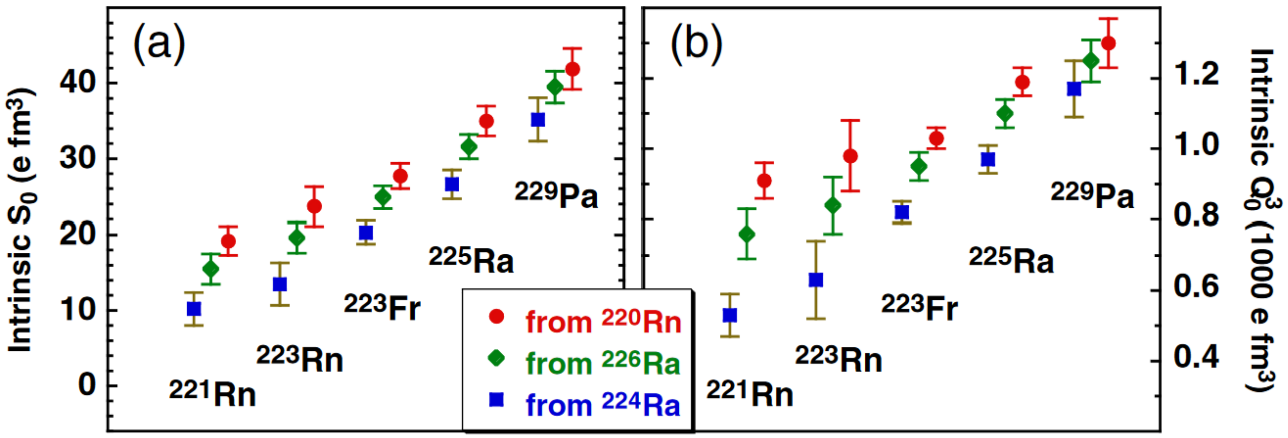

Phy. Rev. Lett. **121**, 232501 (2018)

Complementary atoms/nuclei

VOLUME 60, NUMBER 21 PHYSICAL REVIEW LETTERS 23 MAY 1988

Nuclear Orientation of Radon Isotopes by Spin-Exchange Optical Pumping

M. Kitano,[a] F. P. Calaprice, M. L. Pitt, J. Clayhold, W. Happer, M. Kadar-Kallen, and M. Musolf
Department of Physics, Princeton University, Princeton, New Jersey 08544

G. Ulm[b] and K. Wendt[c]
ISOLDE, CERN, Geneva Switzerland

T. Chupp
Harvard University, Cambridge, Massachusetts 02138

J. Bonn, R. Neugart, and E. Otten
Universität Mainz, Mainz, Germany

and

H. T. Duong
Laboratoire Aimè Cotton, Orsay, France
(Received 22 June 1987)

This paper reports the first demonstration of nuclear orientation of radon atoms. The method employed was spin exchange with potassium atoms polarized by optical pumping. The radon isotopes were produced at the ISOLDE isotope separator of CERN. The nuclear alignment of ^{209}Rn and ^{223}Rn has been measured by observation of γ-ray anisotropies and the magnetic dipole moment for ^{209}Rn has been measured by the nuclear-magnetic-resonance method to be $|\mu| = 0.83881(39)\mu_N$.

PHYSICAL REVIEW C **77**, 052501(R) (2008)

Polarization and relaxation rates of radon

E. R. Tardiff,[1] J. A. Behr,[3] T. E. Chupp,[1] K. Gulyuz,[4] R. S. Lefferts,[4] W. Lorenzon,[2] S. R. Nuss-Warren,[1] M. R. Pearson,[3] N. Pietralla,[4] G. Rainovski,[4] J. F. Sell,[4] and G. D. Sprouse[4]
[1]*FOCUS Center, University of Michigan Physics Department, 450 Church Street, Ann Arbor, Michigan 48109-1040, USA*
[2]*University of Michigan Physics Department, 450 Church Street, Ann Arbor, Michigan 48109-1040, USA*
[3]*TRIUMF, 4004 Westbrook Mall, Vancouver V6T 2A3, Canada*
[4]*SUNY Stony Brook Department of Physics and Astronomy, Stony Brook, New York 11794-3800, USA*
(Received 10 January 2008; published 23 May 2008)

Polarization and relaxation of radon isotopes by spin exchange with laser optically pumped rubidium were studied in preparation for electric dipole moment measurements with octupole deformed ^{223}Rn. γ-ray anisotropies provided a measure of nuclear polarization produced by spin exchange with laser polarized rubidium vapor, and the temperature dependence over the range 130 to 220°C was measured to parametrize the spin exchange polarization and the quadrupole-dominated wall relaxation rate. These results provide quantitative data for developing electric dipole moment measurements of octupole-deformed ^{223}Rn and other radon isotopes.

DOI: 10.1103/PhysRevC.77.052501 PACS number(s): 32.10.Dk, 11.30.−j, 23.20.En, 23.20.Gq

Complementary closed-shell atoms: ^{211}Rn/^{129}Xe

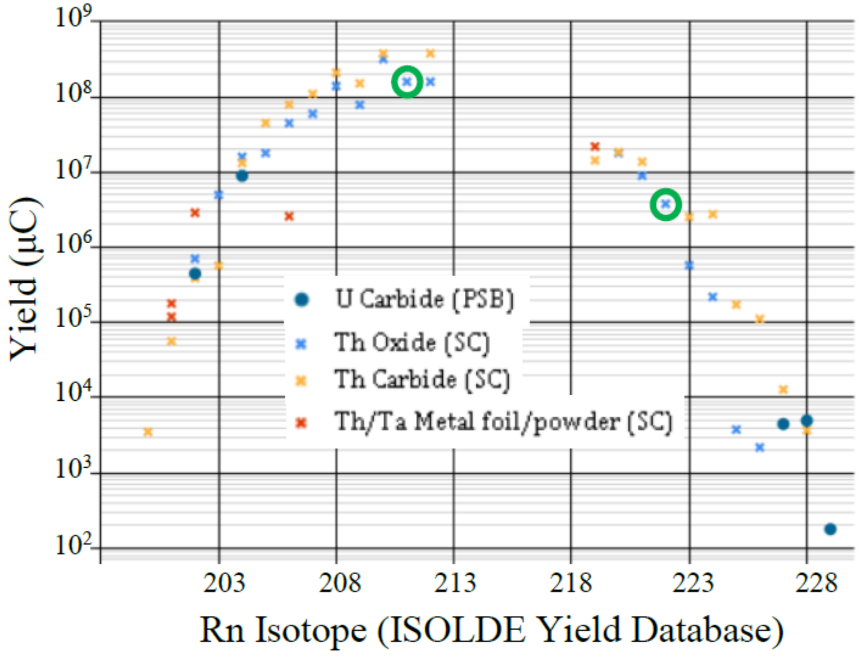

Figure 5: Radon production yields from the CERN-ISOLDE facility, with the relevant isotopes ^{211}Rn and ^{222}Rn circled. Extraction of ^{220}Rn was already demonstrated at REXTRAP, with 1.25×10^7 ions/s arriving at the experiment [Gaf13]. The yield now may be even higher with protons, and in any case the finally desired isotope ^{211}Rn lies near the peak of the yield curve.

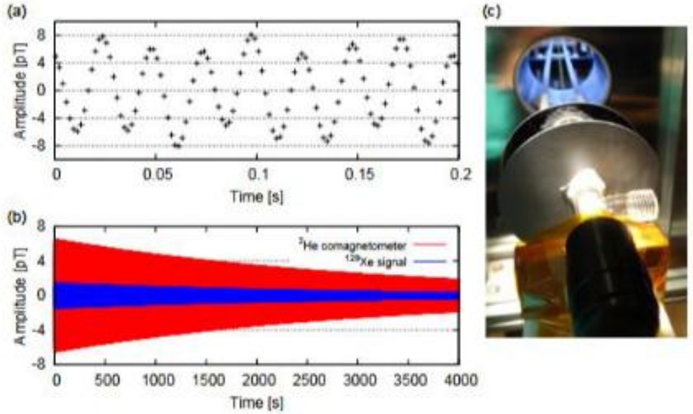

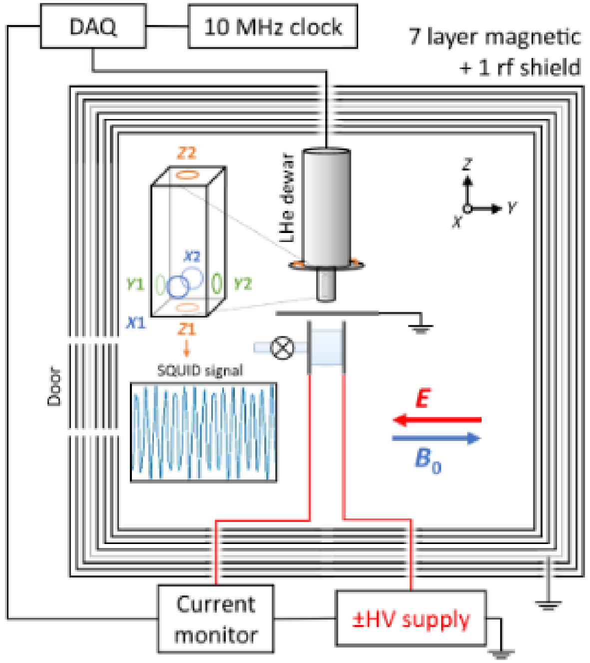

PRL **123** 143003 (2019)

^{211}Rn/^{129}Xe comagnetometry
…with laser readout

$$\chi^2(C_j) = \sum_i \left(\frac{d_i^{\text{measured}} - d_i^{\text{calculated}}(C_j)}{\sigma_i^{\text{measured}}} \right)^2$$

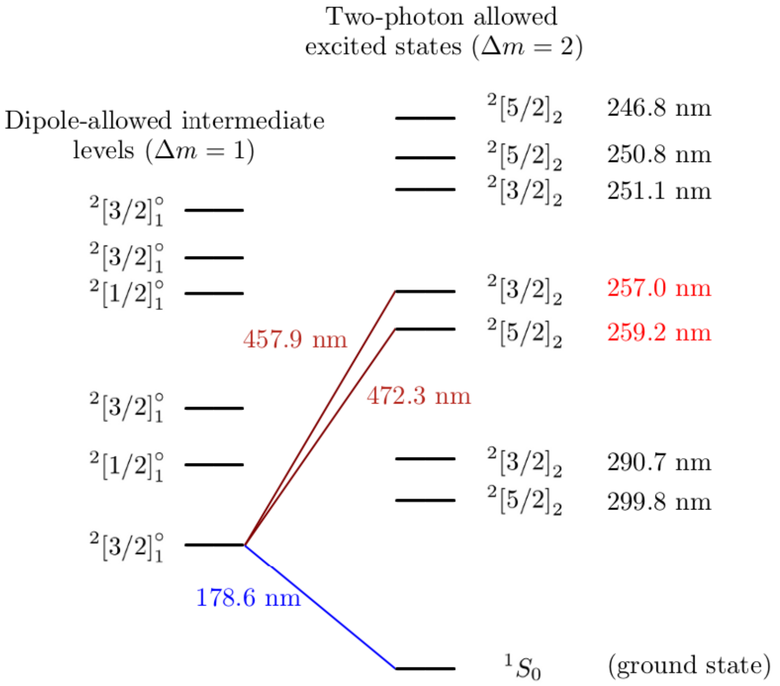

Return to the overview

Constraints on … come mainly from …

d_e	open shell molecules
C_S	open shell molecules
C_T	closed-shell atoms (Hg, Xe)
C_P	closed-shell atoms (Hg, Xe)
$g_\pi^{(0)}$	neutron, Hg
$g_\pi^{(1)}$	neutron, Hg, other closed-shell
d_n^{sr}	neutron, Hg

…i.e., from 5 dominating measurements

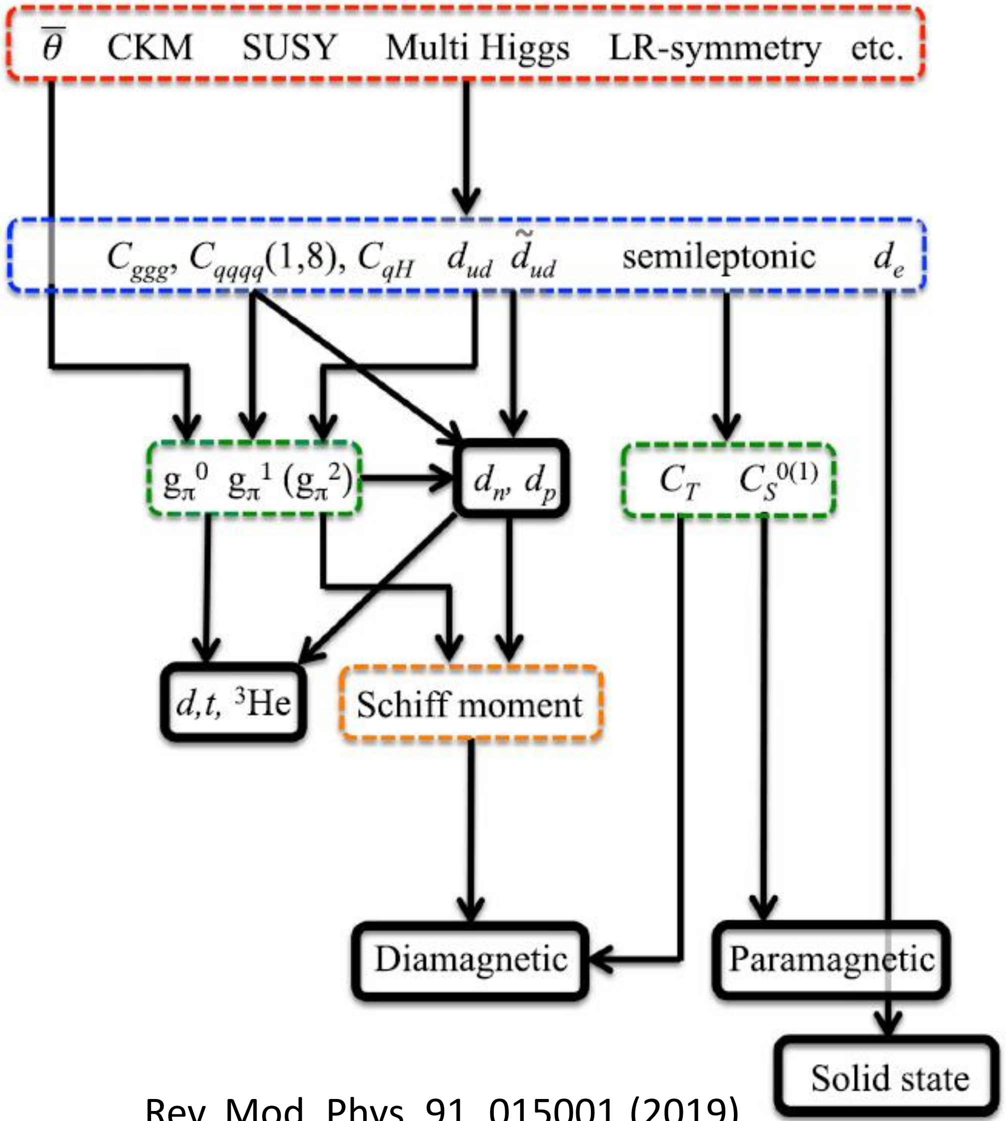

Rev. Mod. Phys. 91, 015001 (2019)

Closed-shell systems constrain $g_\pi, d_{n,p}$, *and* $C_{T,P}$

arXiv:2403.02052

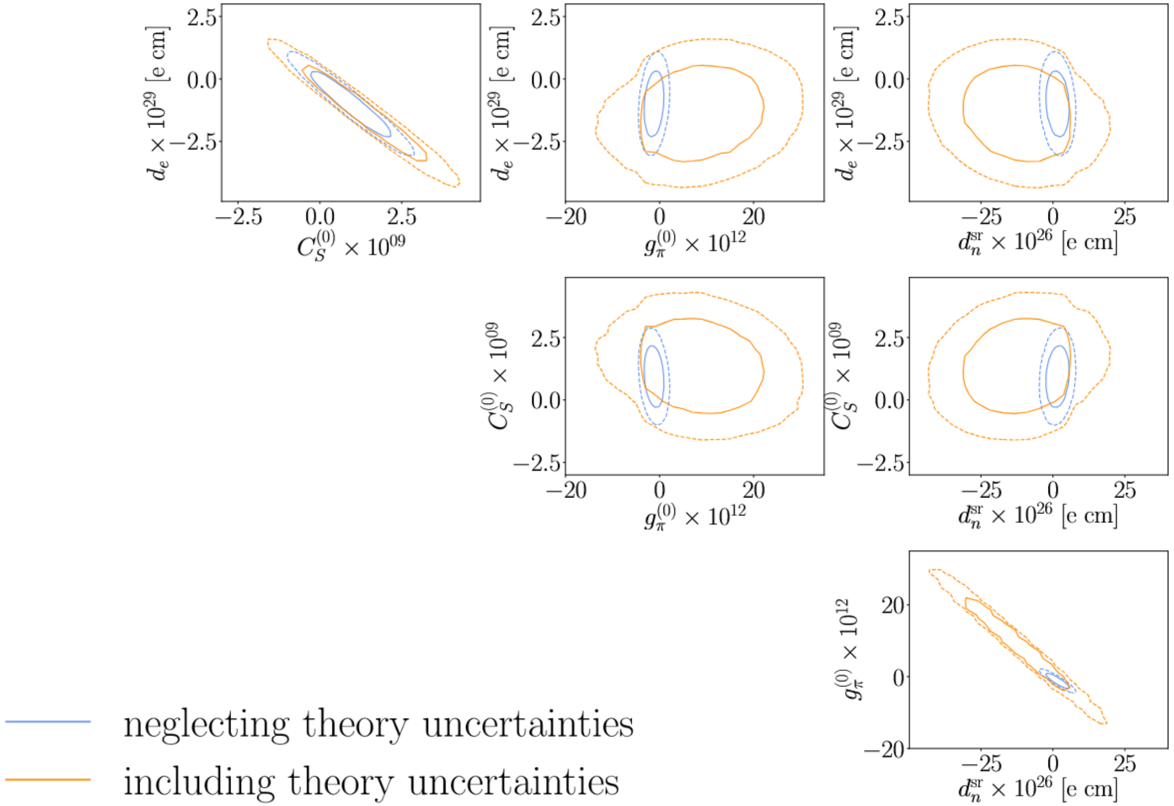

n	$(0.0 \pm 1.1_{stat} \pm 0.2_{syst}) \cdot 10^{-26}$	$2.2 \cdot 10^{-26}$
^{199}Hg	$(2.20 \pm 2.75_{stat} \pm 1.48_{syst}) \cdot 10^{-30}$	$7.4 \cdot 10^{-30}$
^{129}Xe	$(-1.76 \pm 1.82) \cdot 10^{-28}$	$4.8 \cdot 10^{-28}$
^{171}Yb	$(-6.8 \pm 5.1_{stat} \pm 1.2_{syst}) \cdot 10^{-27}$	$1.5 \cdot 10^{-26}$
^{225}Ra	$(4 \pm 6_{stat} \pm 0.2_{syst}) \cdot 10^{-24}$	$1.4 \cdot 10^{-23}$
TlF	$(-1.7 \pm 2.9) \cdot 10^{-23}$	$6.5 \cdot 10^{-23}$

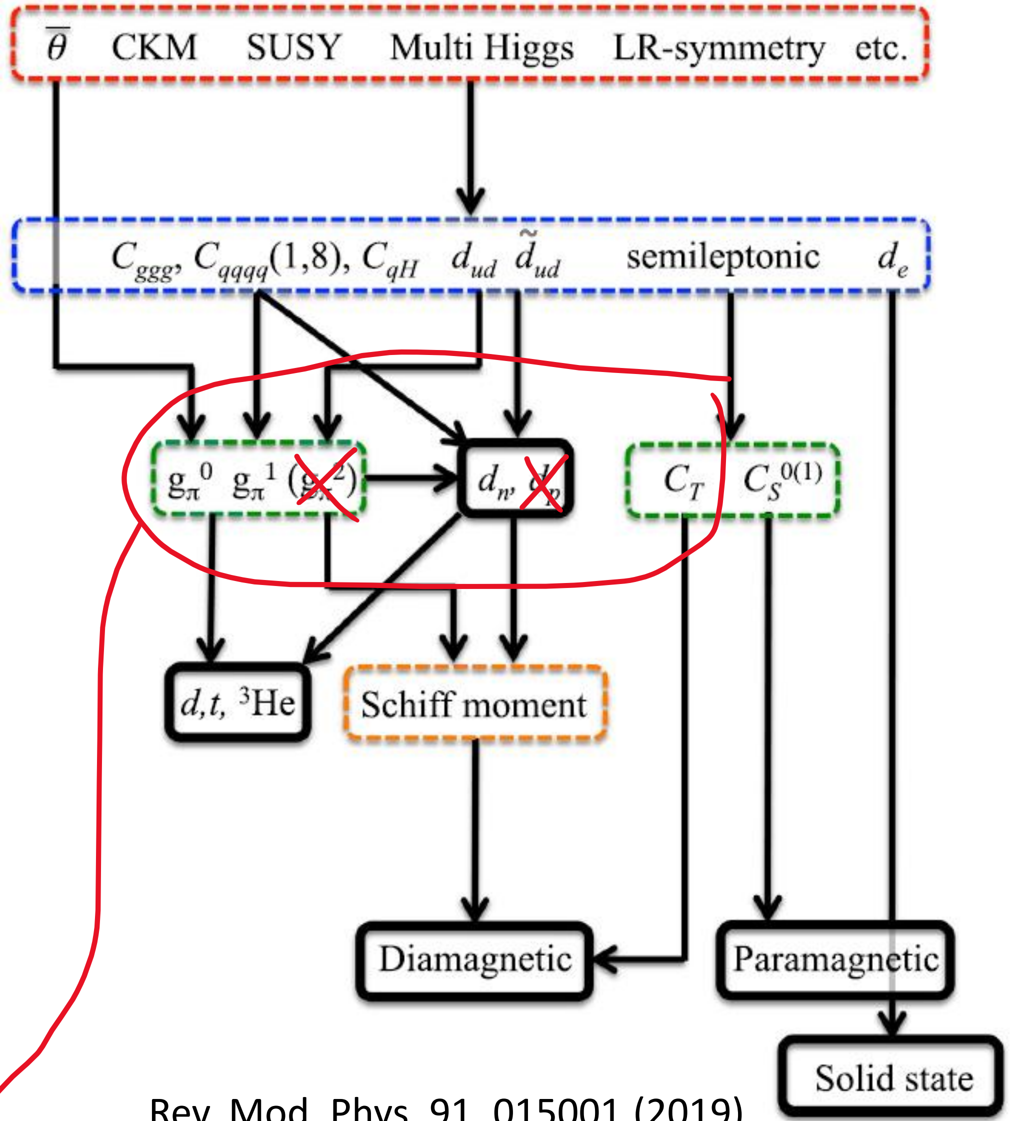

Rev. Mod. Phys. 91, 015001 (2019)

Closed-shell systems constrain $g_\pi, d_{n,p}$, *and* $C_{T,P}$

arXiv:2403.02052

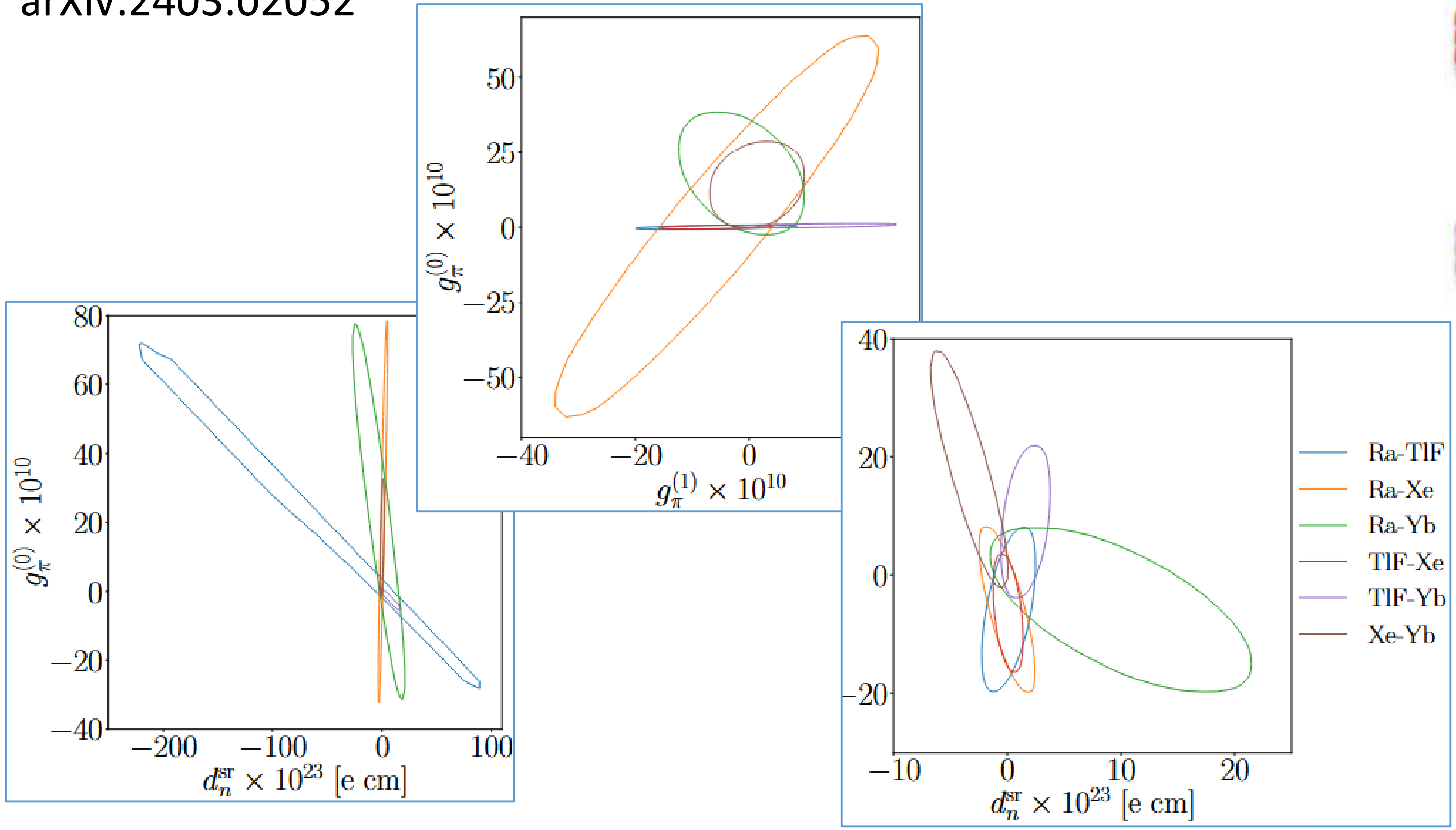

n	$(0.0 \pm 1.1_{stat} \pm 0.2_{syst}) \cdot 10^{-26}$	$2.2 \cdot 10^{-26}$
^{199}Hg	$(2.20 \pm 2.75_{stat} \pm 1.48_{syst}) \cdot 10^{-30}$	$7.4 \cdot 10^{-30}$
^{129}Xe	$(-1.76 \pm 1.82) \cdot 10^{-28}$	$4.8 \cdot 10^{-28}$
^{171}Yb	$(-6.8 \pm 5.1_{stat} \pm 1.2_{syst}) \cdot 10^{-27}$	$1.5 \cdot 10^{-26}$
^{225}Ra	$(4 \pm 6_{stat} \pm 0.2_{syst}) \cdot 10^{-24}$	$1.4 \cdot 10^{-23}$
TlF	$(-1.7 \pm 2.9) \cdot 10^{-23}$	$6.5 \cdot 10^{-23}$

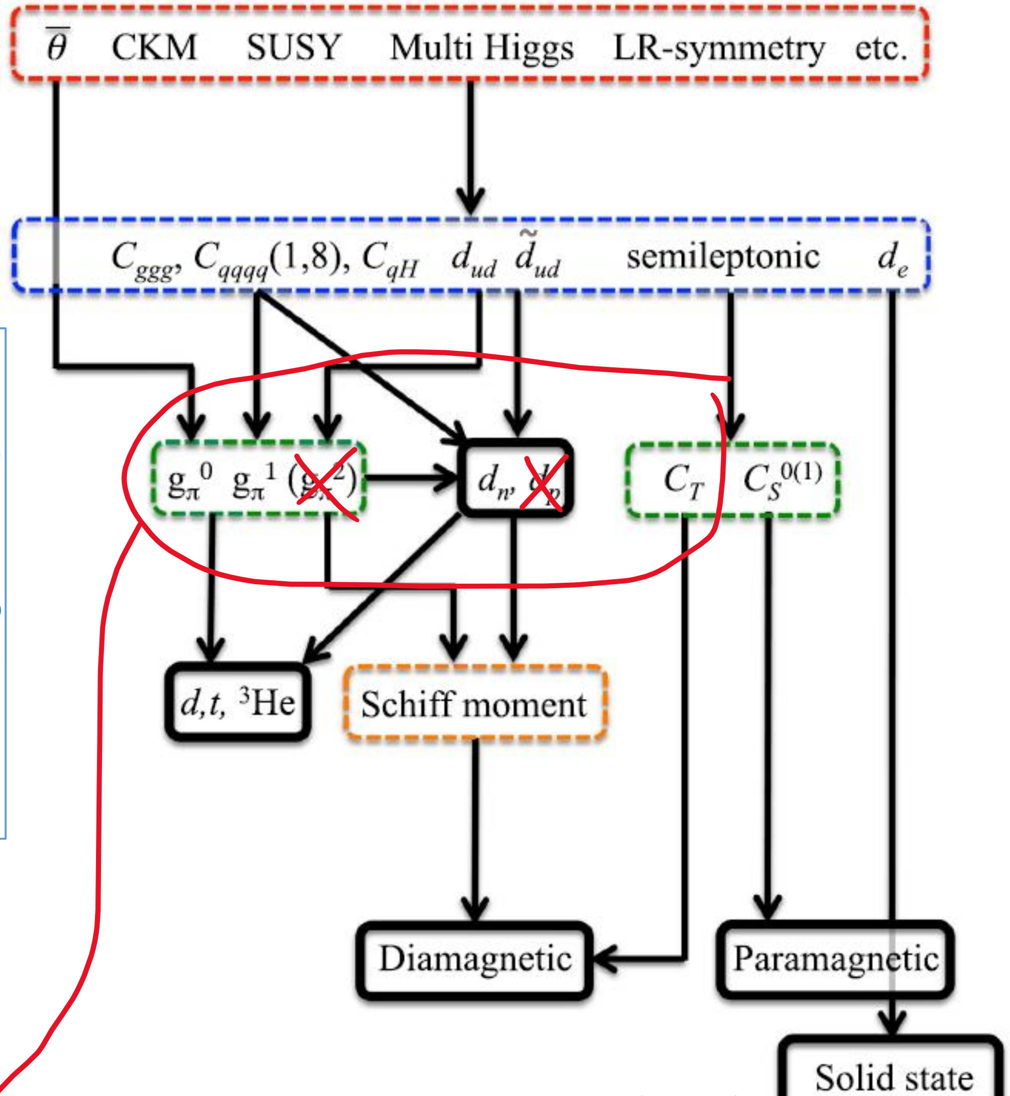

Rev. Mod. Phys. 91, 015001 (2019)

Closed-shell systems constrain $g_\pi, d_{n,p}$, *and* $C_{T,P}$

arXiv:2403.02052

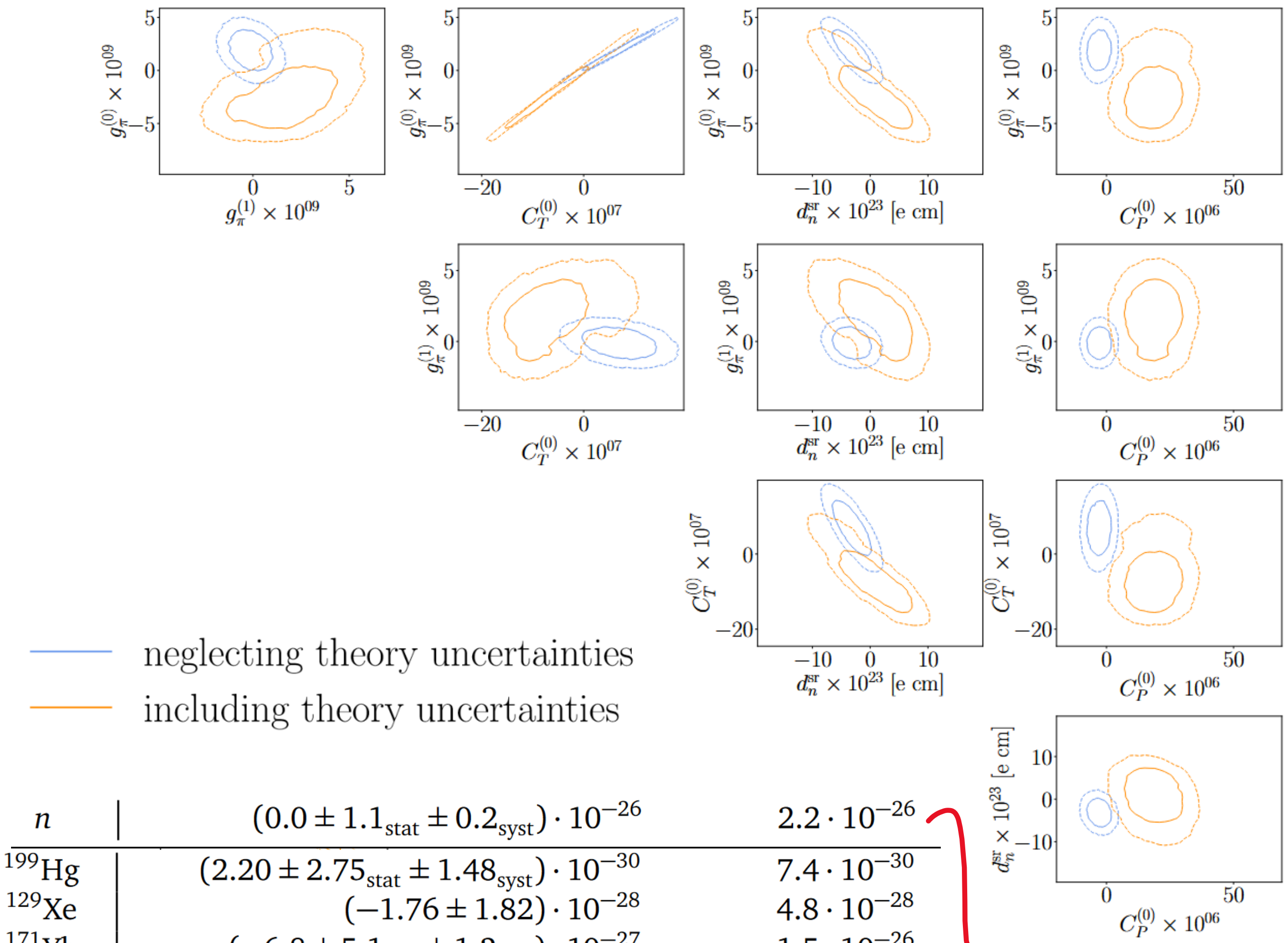

n	$(0.0 \pm 1.1_{\text{stat}} \pm 0.2_{\text{syst}}) \cdot 10^{-26}$	$2.2 \cdot 10^{-26}$
^{199}Hg	$(2.20 \pm 2.75_{\text{stat}} \pm 1.48_{\text{syst}}) \cdot 10^{-30}$	$7.4 \cdot 10^{-30}$
^{129}Xe	$(-1.76 \pm 1.82) \cdot 10^{-28}$	$4.8 \cdot 10^{-28}$
^{171}Yb	$(-6.8 \pm 5.1_{\text{stat}} \pm 1.2_{\text{syst}}) \cdot 10^{-27}$	$1.5 \cdot 10^{-26}$
^{225}Ra	$(4 \pm 6_{\text{stat}} \pm 0.2_{\text{syst}}) \cdot 10^{-24}$	$1.4 \cdot 10^{-23}$
TlF	$(-1.7 \pm 2.9) \cdot 10^{-23}$	$6.5 \cdot 10^{-23}$

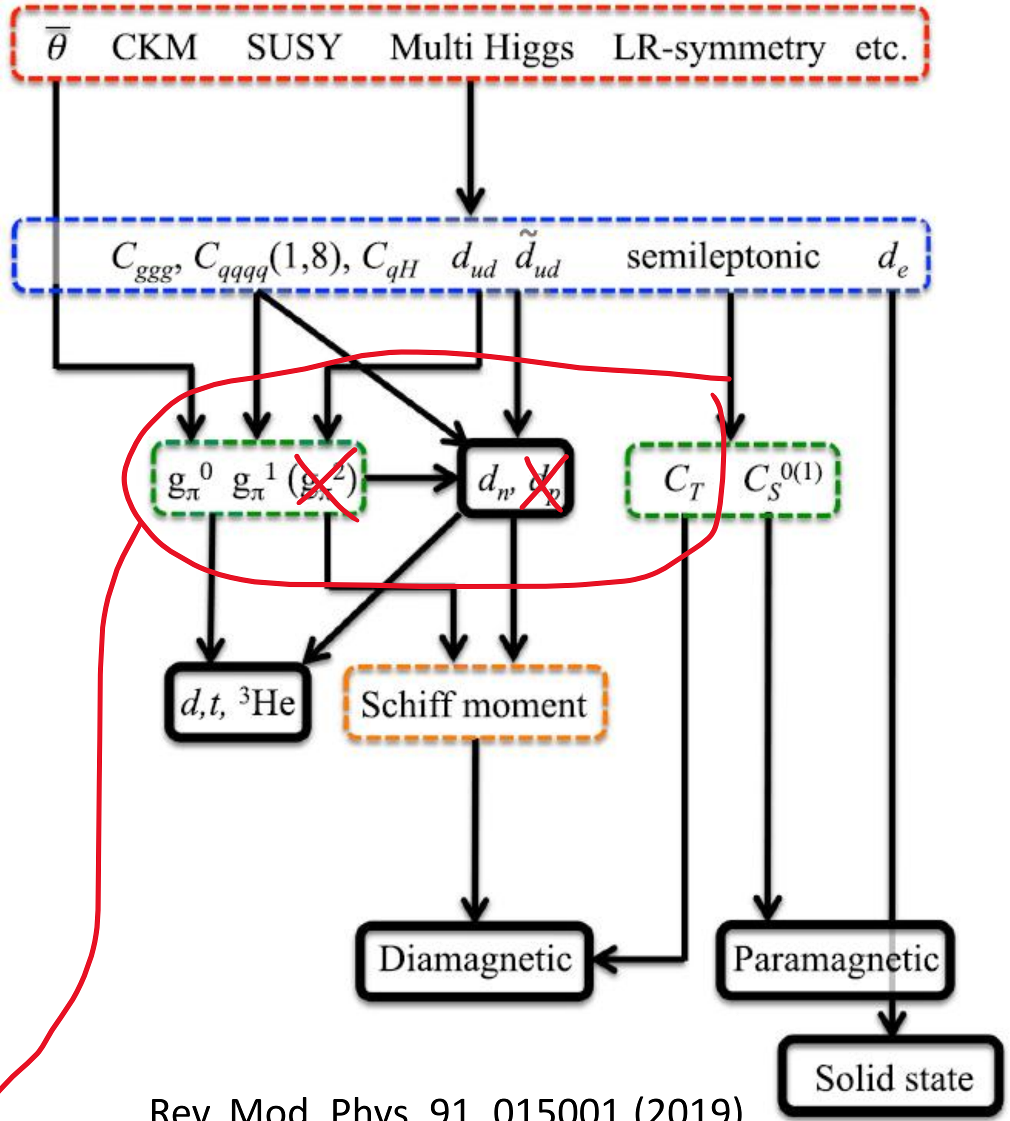

Rev. Mod. Phys. 91, 015001 (2019)

Caveats

System i	$\langle\sigma_n\rangle$	$\langle\sigma_p\rangle$	$\langle\sigma_z\rangle^{(0)}$
Tl	0.274	0.726	1
Cs	−0.206	−0.572	−0.778
^{199}Hg	−0.302	−0.032	−0.334
^{129}Xe	0.73	0.27	1
^{171}Yb	−0.3	−0.034	−0.334
^{225}Ra	0.72	0.28	1
TlF	0.274	0.726	1

Shell-model estimates
for deformed nuclei…
Residual inconsistencies…

System i	$k_{i,S}$ [cm/fm^3]	$s_{i,n}$ [fm^2]	$s_{i,p}$ [fm^2]
Tl	$-4.2^{+2.1}_{-1.8} \cdot 10^{-18}$ [35]	$0.14^{\pm 0.03}$	$-0.38^{+1.38}_{-0.45}$
Cs	$-9.99^{+2.9}_{-4.1} \cdot 10^{-18}$ [35]		$0.1^{\pm 0.1}$
^{199}Hg	$-2.26^{\pm 0.23} \cdot 10^{-17}$ [115]	$0.6^{+1.33}_{-0.12}$	$0.06^{+0.20}_{-0.01}$
^{129}Xe	$3.62^{\pm 0.25} \cdot 10^{-18}$ [115]	$0.63^{+0.16}_{-0.12}$	$0.14^{\pm 0.03}$
^{171}Yb	$-2.10^{+0.22}_{-0.0} \cdot 10^{-17}$ [66, 116]	$0.54^{+0.13}_{-0.11}$	$0.054^{+0.016}_{-0.014}$
^{225}Ra	$-8.5^{+0.25}_{-0.3} \cdot 10^{-17}$ [18, 66, 116]	$0.63^{+0.16}_{-0.12}$	$0.14^{+0.04}_{-0.03}$
TlF	$-4.59^{\pm 0.41} \cdot 10^{-13}$ [115]	$0.14^{\pm 0.03}$	$-0.38^{+1.38}_{-0.45}$

Still missing/challenging:

- Some nuclear structure
  - Valence nucleon EDMs
  - Sign of some pion couplings
  - Short-range forces
- Hadronic matrix elements
- Sub-leading coefficients for open-shell molecules

So what can we do/attempt now?

- Work upwards in energy
- Add new experiments
- Include more parameters, and effects
  - MQM (beyond Cs…)
  - Muon and tau lepton (also indirect limits)
  - Short-range nuclear forces (hard…)
- Evaluate impact of improvements
  - Theory coefficients
  - Experimental bounds
  - Correlated experiments… new ideas?
- Constrain specific BSM scenarios

Still missing/challenging:

- Some nuclear structure
  - Valence nucleon EDMs
  - Sign of some pion couplings
  - Short-range forces
- Hadronic matrix elements
- Sub-leading coefficients for open-shell molecules

Thematic Recap

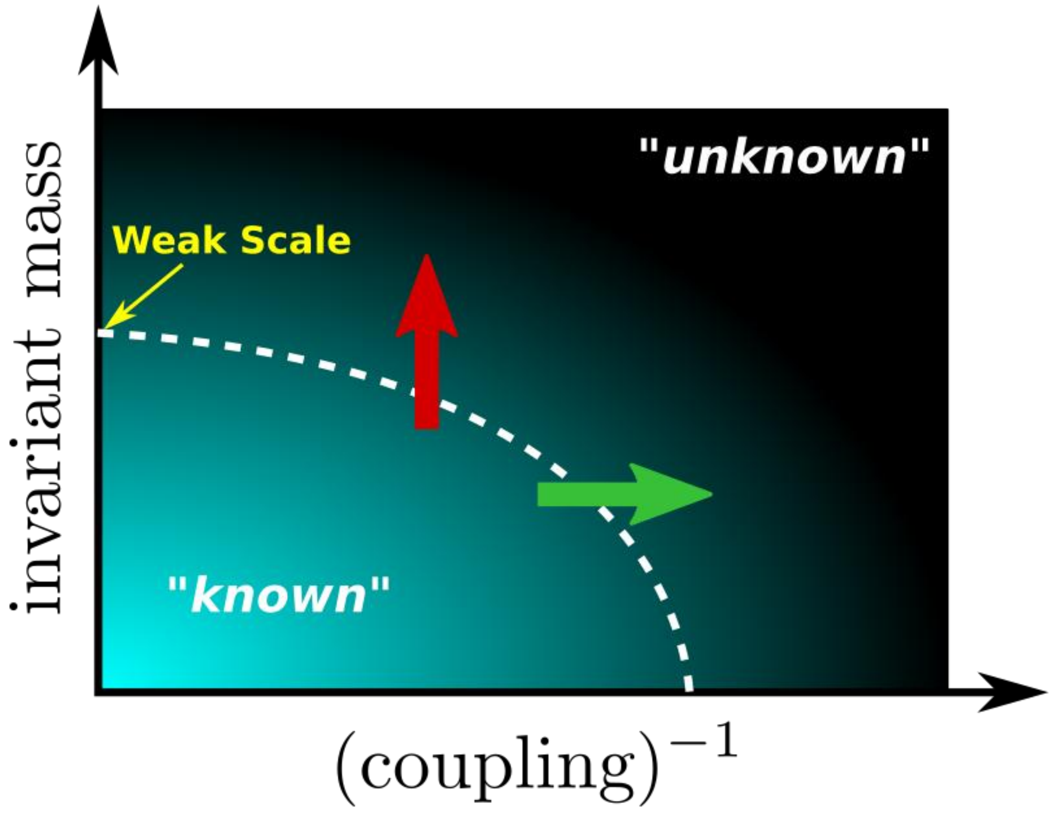

1. Write down the Lagrangian! (or Hamiltonian) and make the conventions clear…

2. More experiments is good; complementary is better

3. Theory <u>values</u>, and especially <u>uncertainties</u>, can also improve

Questions?

Seeking students and Post-Docs!

what-if.xkcd.com

Special thanks to:

N. Elmer, T. Plehn, T. Modak (HD)
M. Mühlleitner (KIT)

Many, *many* colleagues who helped answer questions and pinpoint errors (see acknowledgements in 2403.02052)

EDMs 2026 at Les Houches!

March 1-6, 2026

WE-Heraeus funding to cover participant room & board

Scientific program:

- Experiments targeting EDMs of the neutron, charged particles in storage rings, atoms, molecules...
- Theory for interpreting EDM, including hadronic, nuclear, atomic/molecular calculations…
- Phenomenological models and global analysis for CP-violating physics
- Connections between EDMs and other observables

Organizers: SMD, Stéphanie Roccia, Guillaume Pignol

Producing UCN with helium

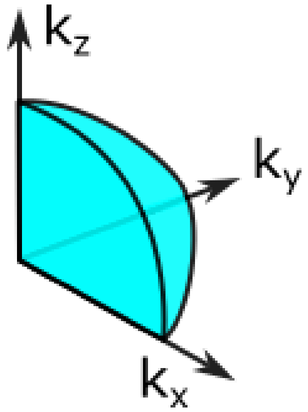

$$E = \frac{\hbar^2 |\boldsymbol{k}|^2}{2m} = \frac{1}{2} m v^2$$

$$V_k \sim \frac{4}{3} \pi |\boldsymbol{k}|^3 \propto E^{\frac{3}{2}}$$

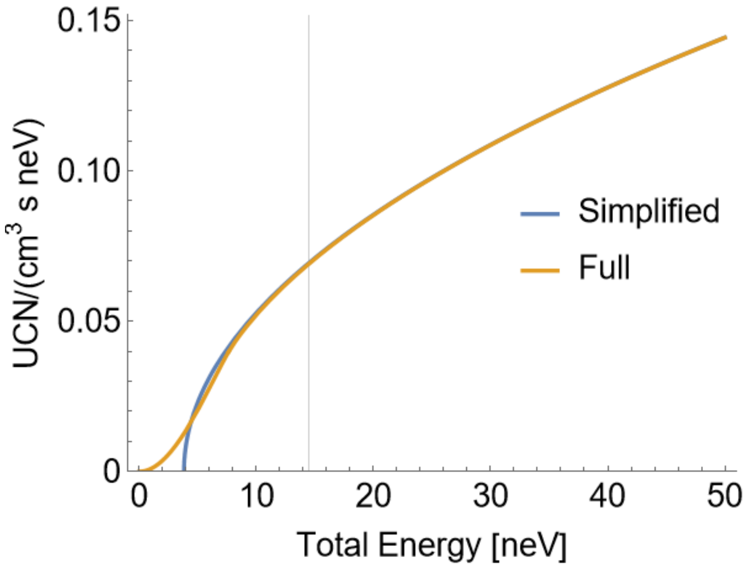

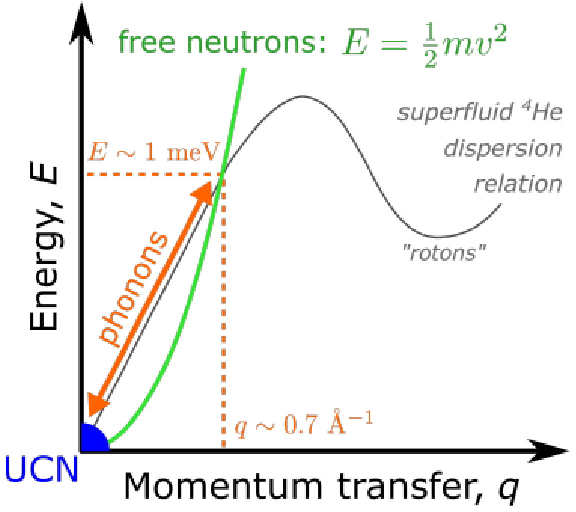

efficiency (cross-section)

cold neutron flux at "resonance"

UCN trap depth

$$R \sim \left(\frac{5 \times 10^{-8}}{\text{cm}^3 \text{ s}} \right) \times \left. \frac{d\Phi}{d\lambda} \right|_{8.9\text{Å}} \times \left(\frac{V_{\text{trap}}}{233 \text{ neV}} \right)^{\frac{3}{2}}$$

production rate density

$$\frac{1}{\tau} = \frac{1}{\tau_\beta} + \frac{1}{\tau_{\text{up}}} + \frac{1}{\tau_{\text{capture}}} + \frac{1}{\tau_{\text{wall}}} + \cdots$$

total loss (add partial rates)

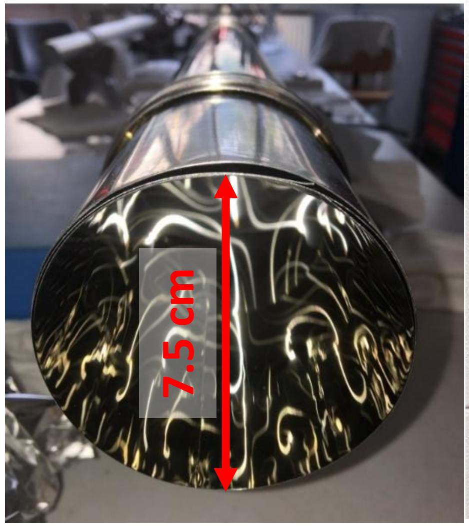

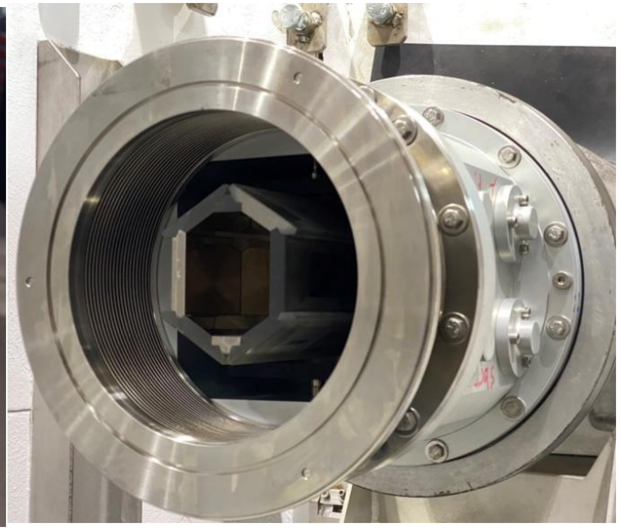

Producing UCN with helium

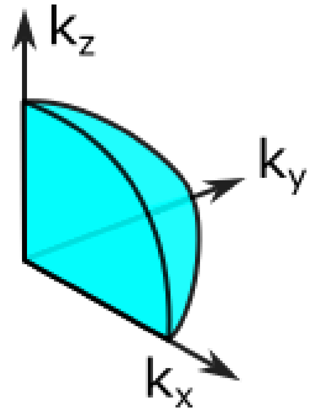

$$E = \frac{\hbar^2 |\boldsymbol{k}|^2}{2m} = \frac{1}{2}mv^2$$

$$V_k \sim \frac{4}{3}\pi |\boldsymbol{k}|^3 \propto E^{\frac{3}{2}}$$

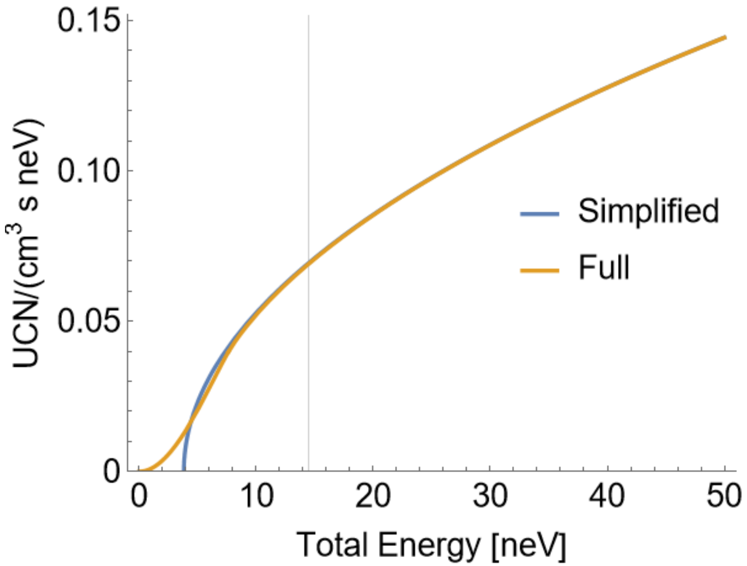

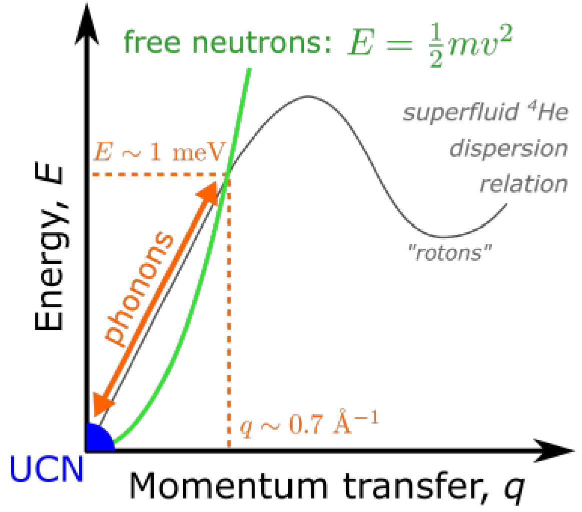

efficiency (cross-section)

cold neutron flux at "resonance"

UCN trap depth

$$R \sim \left(\frac{5 \times 10^{-8}}{\text{cm}^3\ \text{s}}\right) \times \left.\frac{d\Phi}{d\lambda}\right|_{8.9\text{Å}} \times \left(\frac{V_{\text{trap}}}{233\ \text{neV}}\right)^{\frac{3}{2}}$$

production rate density

$$\frac{1}{\tau} = \frac{1}{\tau_\beta} + \frac{1}{\tau_{\text{up}}} + \frac{1}{\tau_{\text{capture}}} + \frac{1}{\tau_{\text{wall}}} + \cdots$$

total loss (add partial rates)

trap volume

energy-dependent production/loss

mean survival time

$$N = \int d^3\boldsymbol{r} \int^{V_{\text{trap}}} dE \frac{dR}{dE}\tau(E) \sim \underbrace{\mathcal{V} \cdot R}\cdot \langle \tau(E) \rangle$$

total production rate

Delivering Cold Neutrons

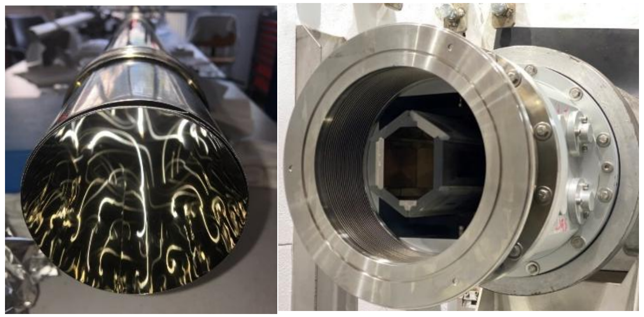

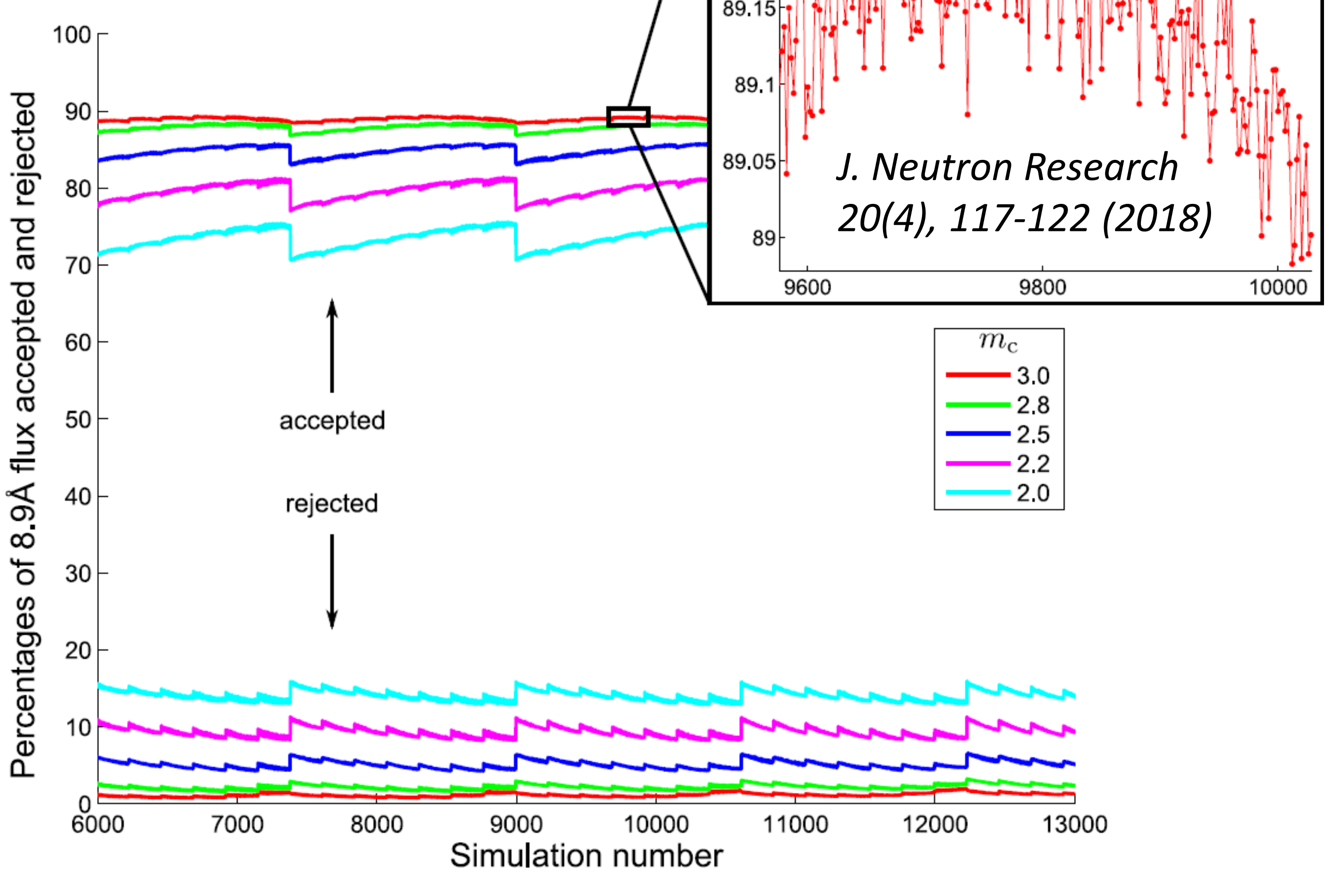

all wavelengths, capture-weighted

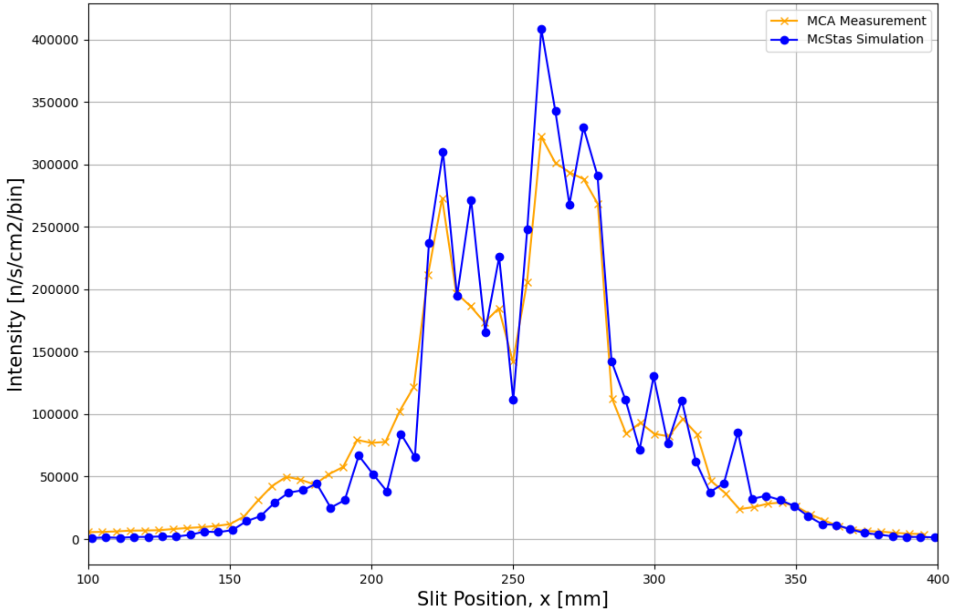

H. Manasawala

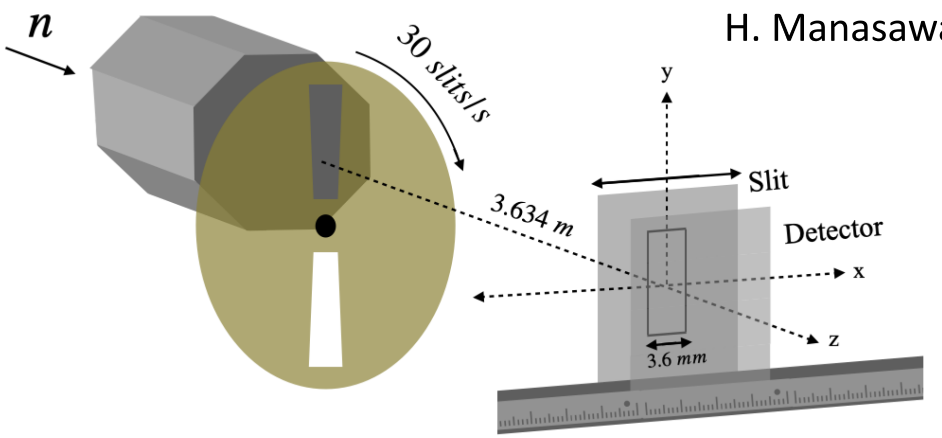

Delivering Cold Neutrons

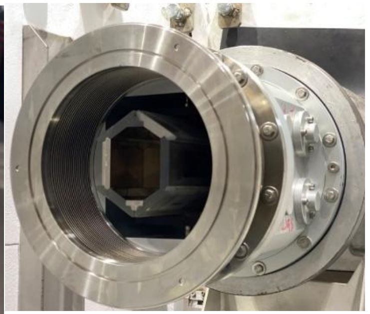

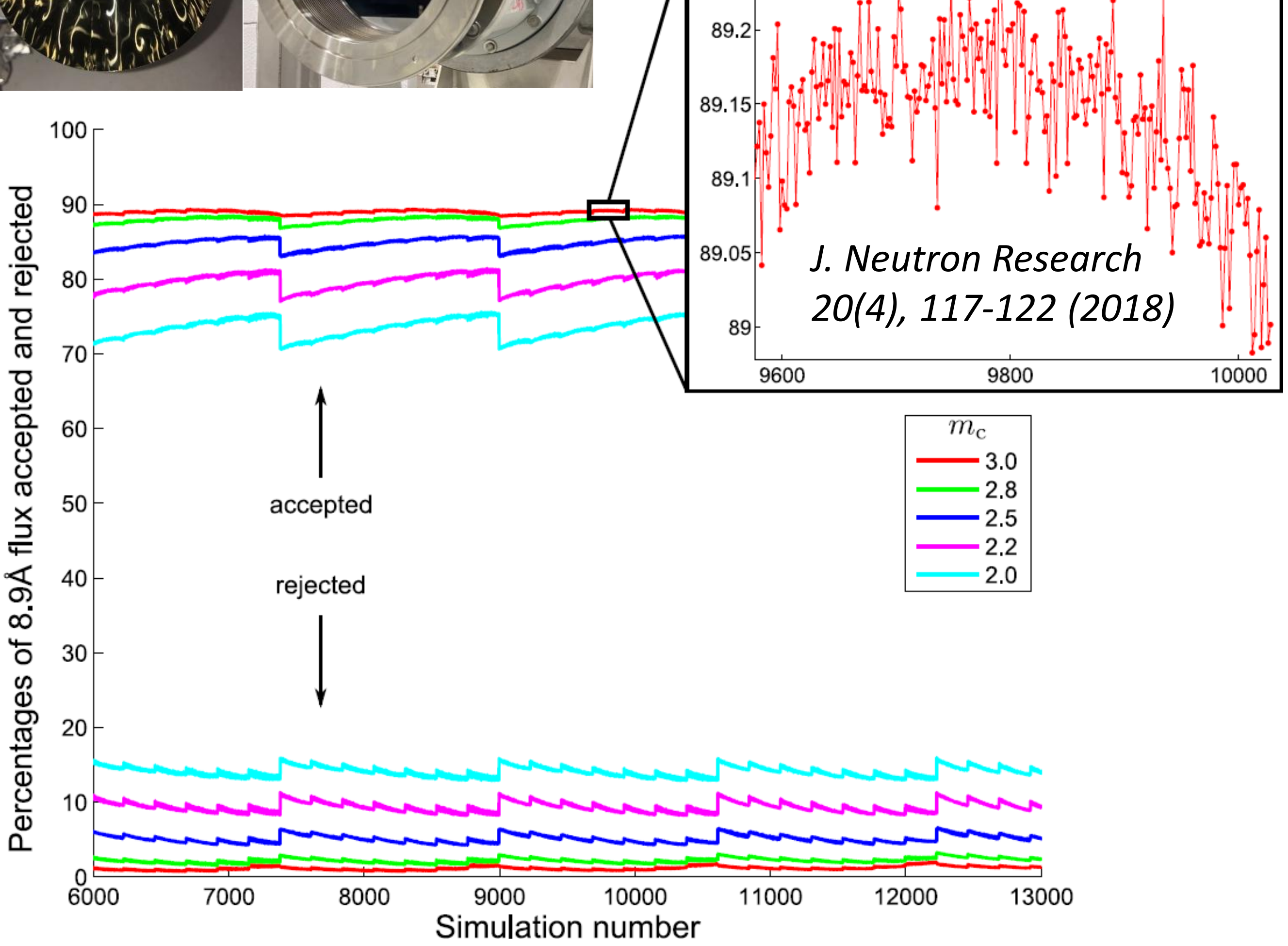

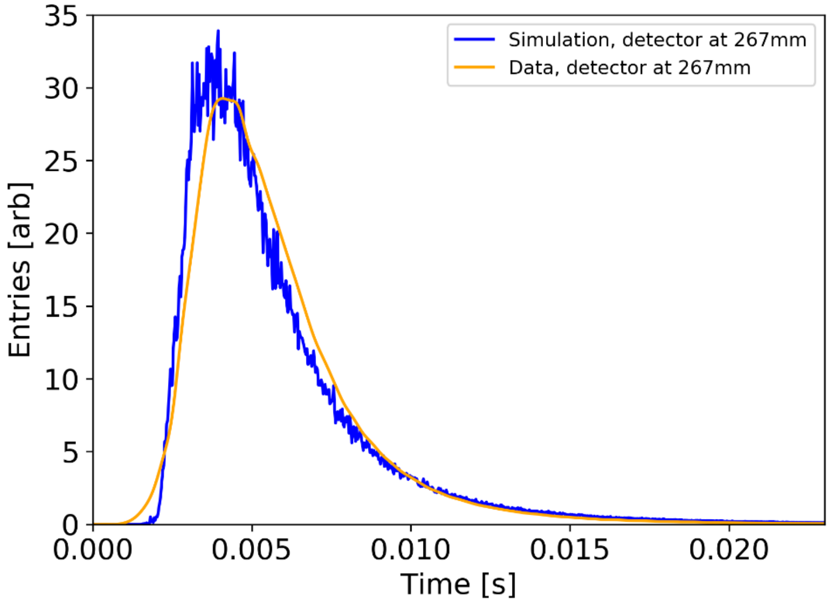

H. Manasawala

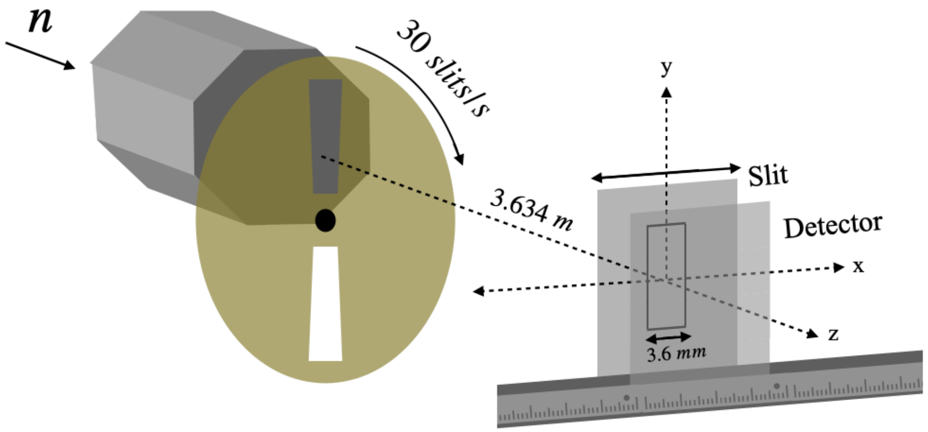

Delivering Cold Neutrons

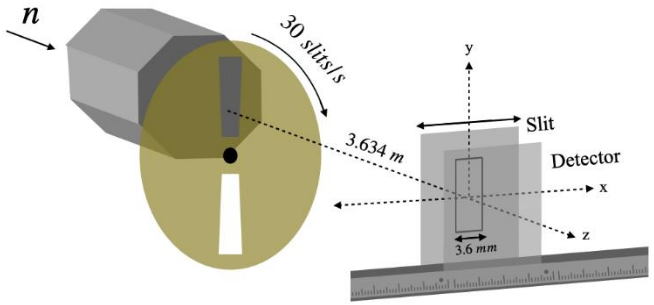

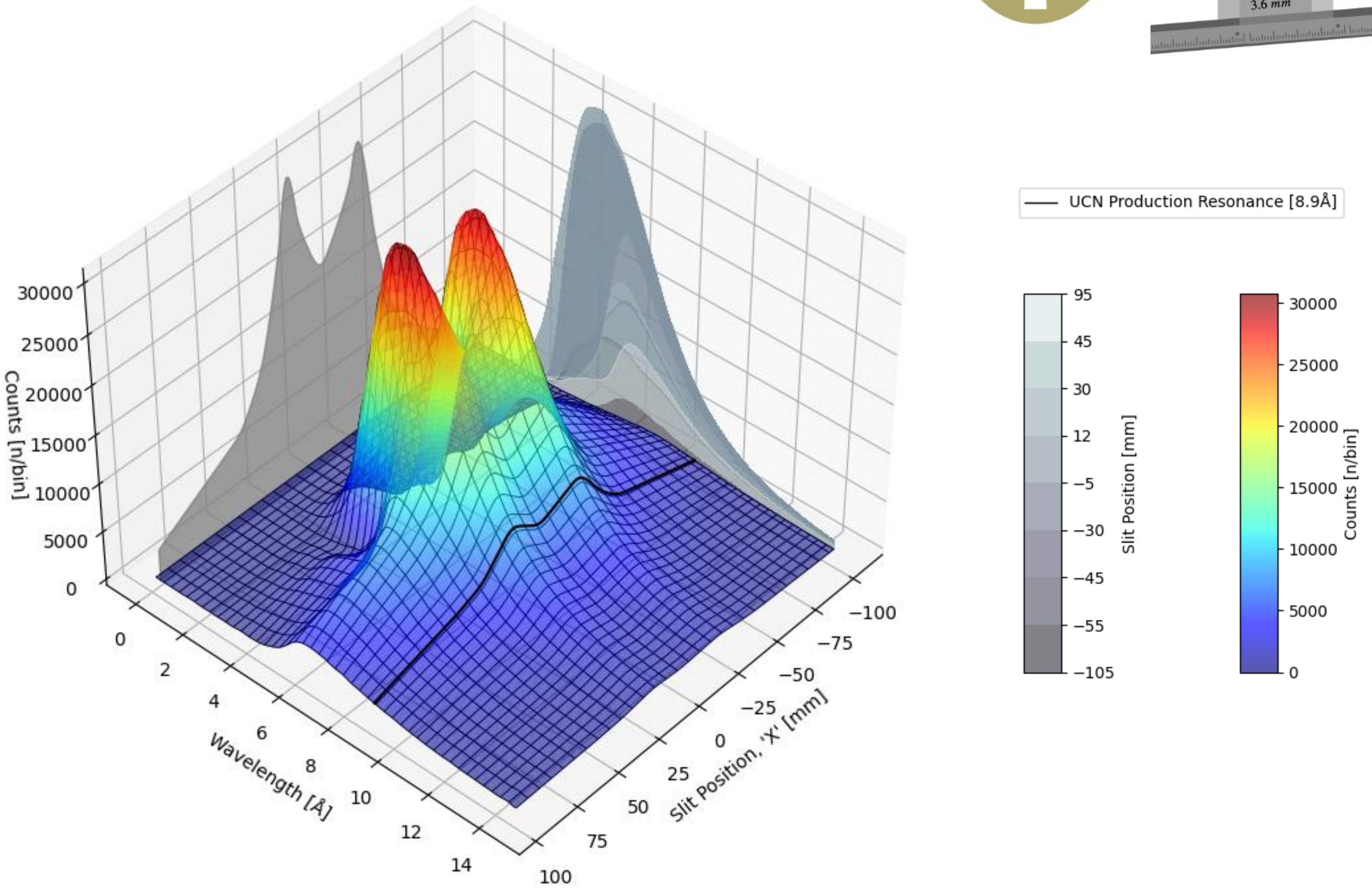

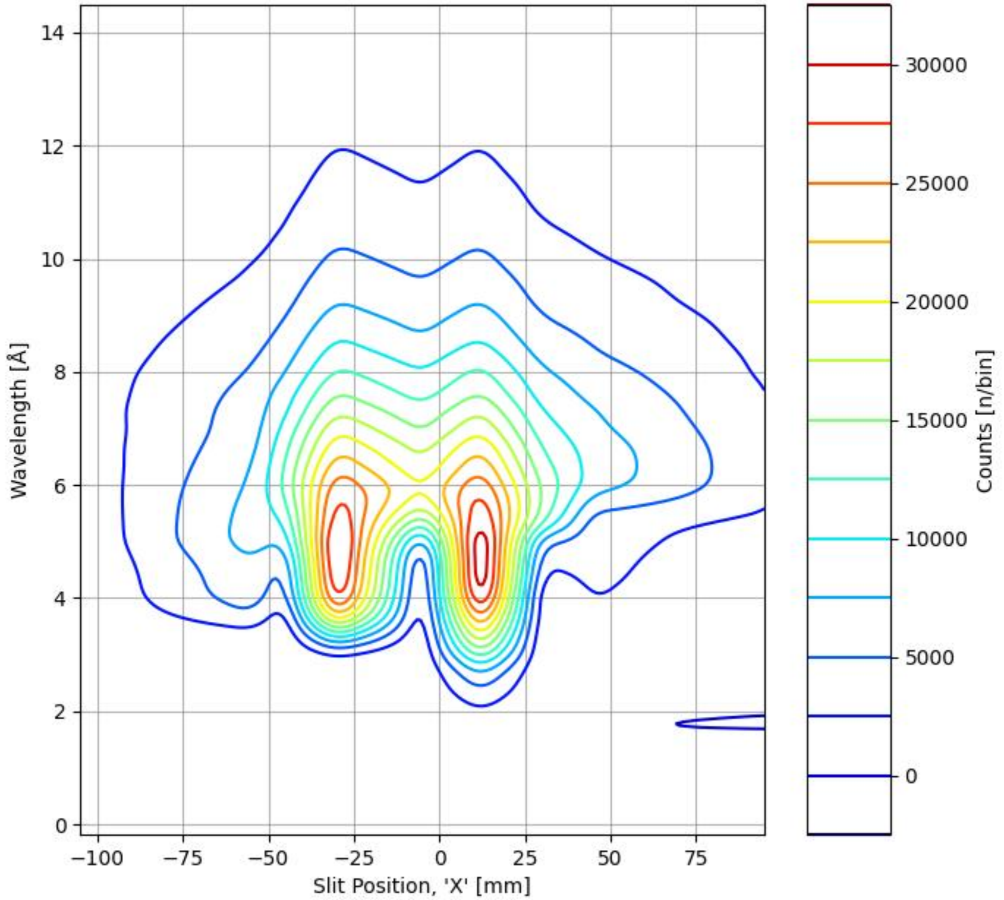

Wall loss in UCN storage

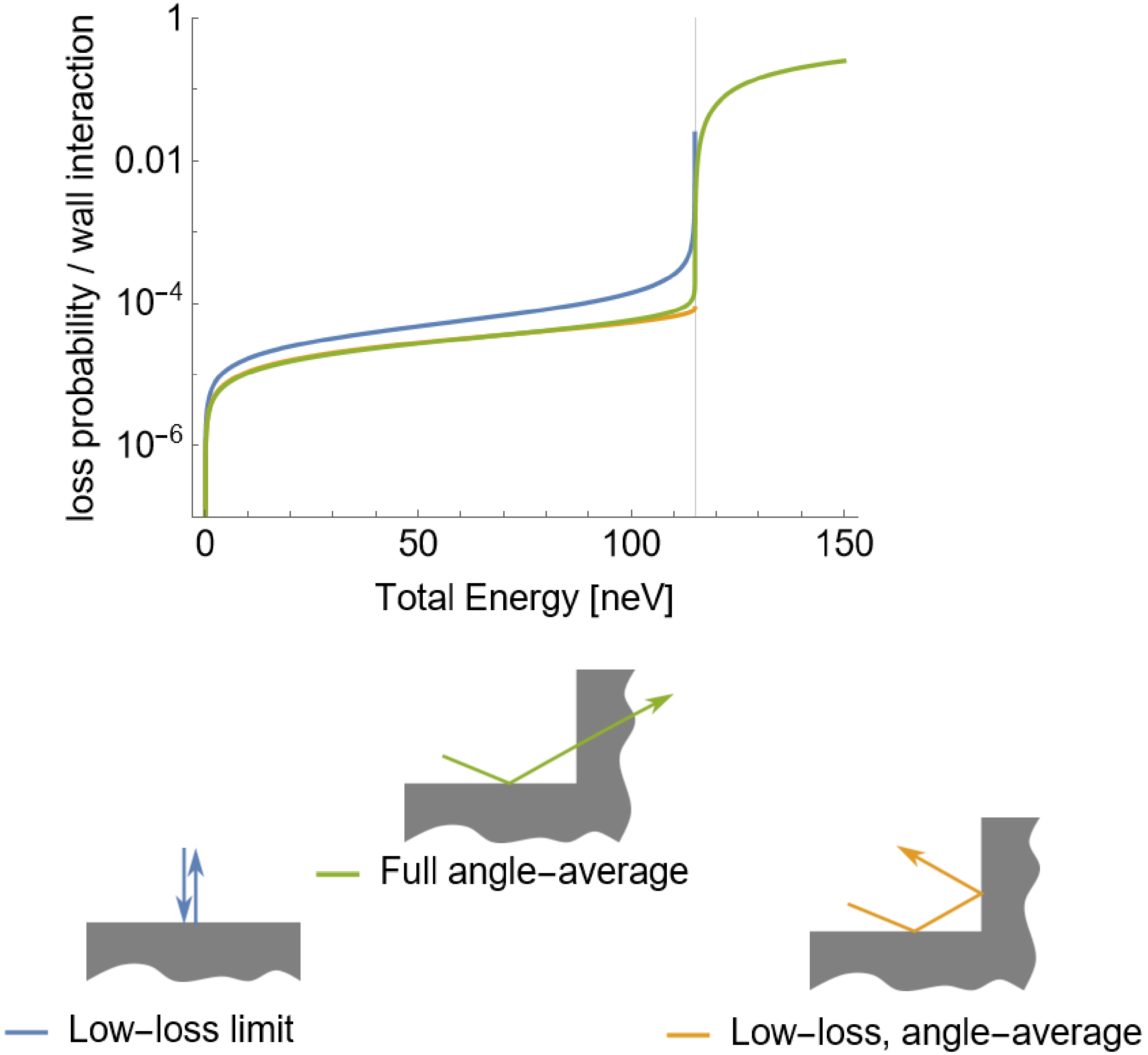

Wall loss in UCN storage

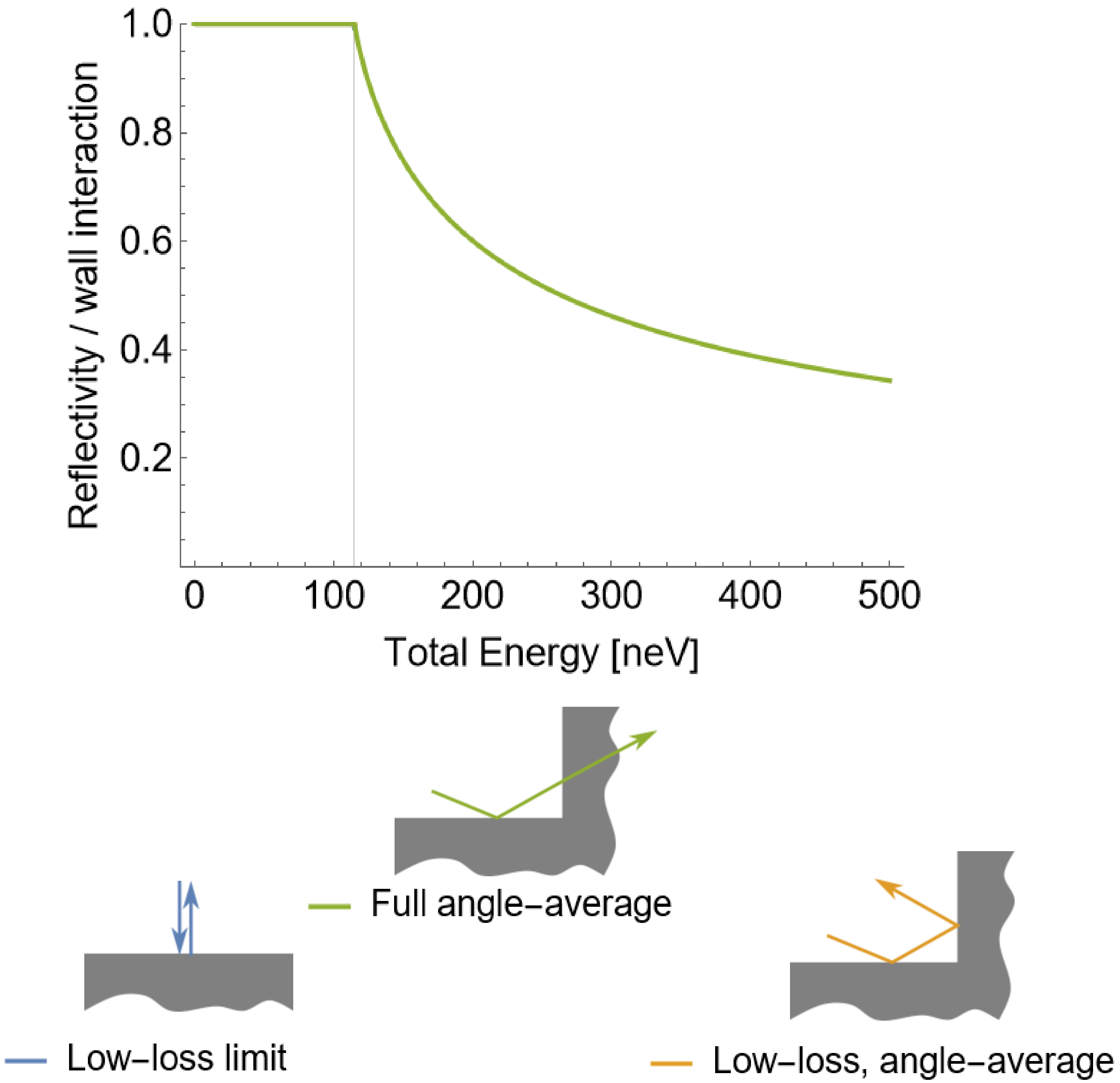

Wall loss in UCN storage

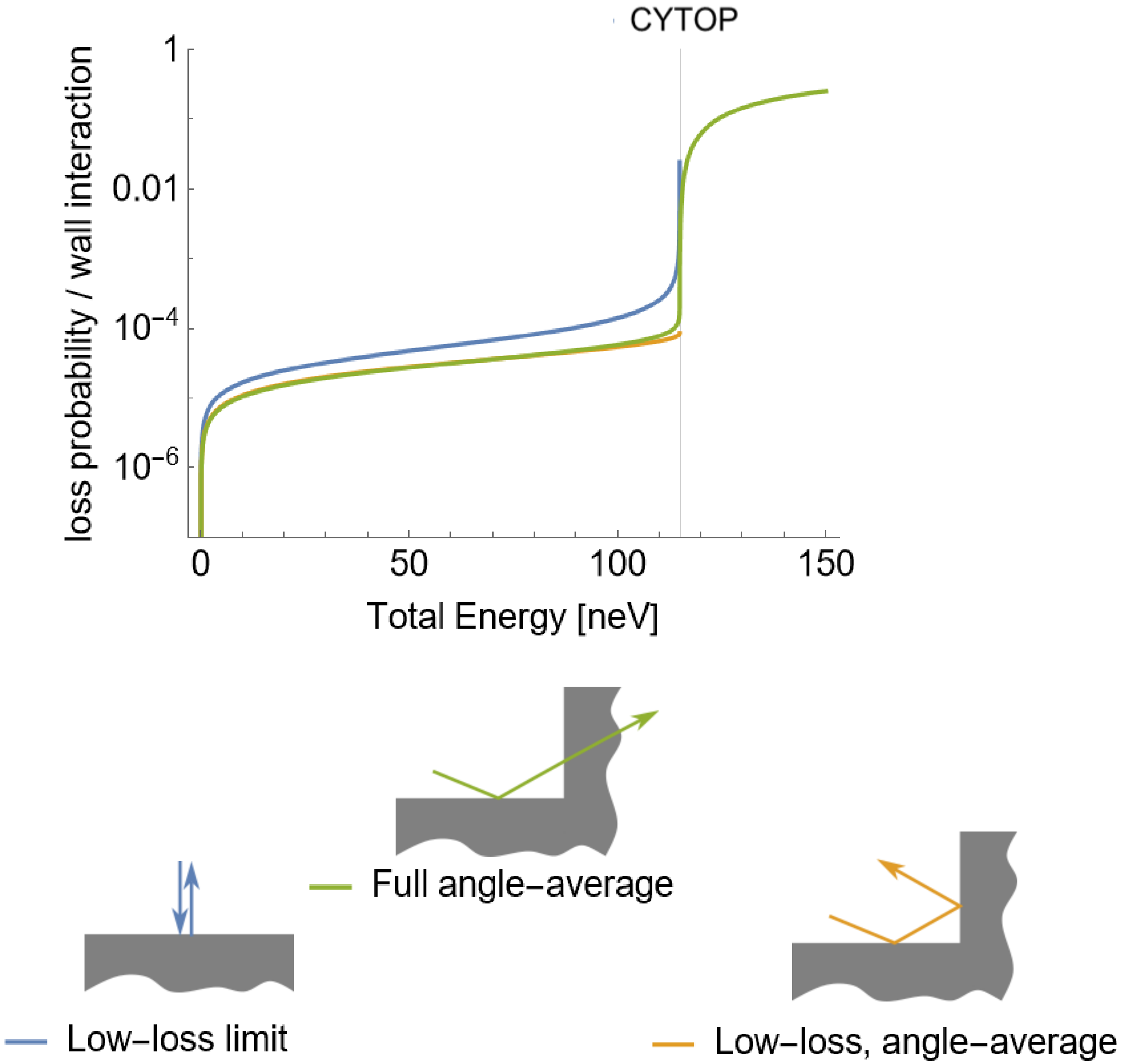

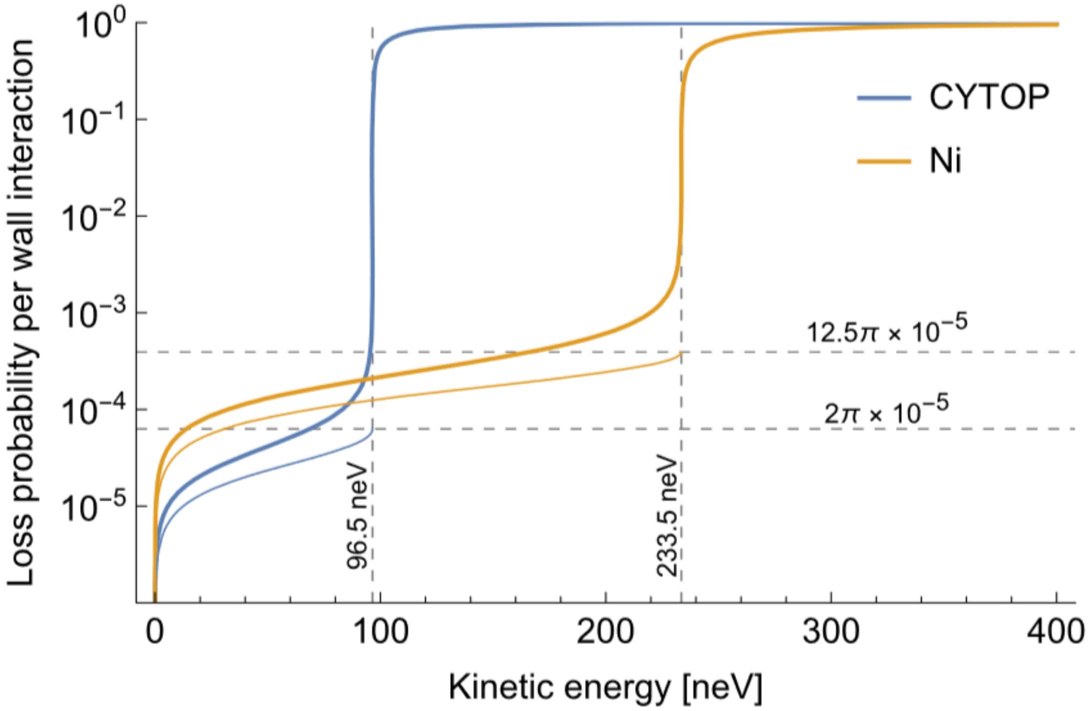

- Different materials
- Include effect of ambient medium

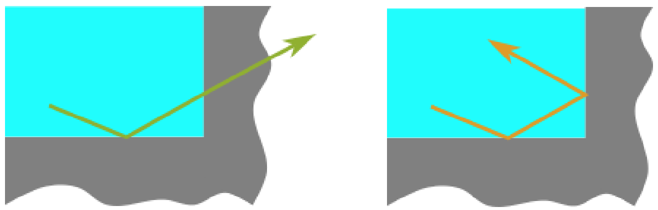

Wall loss in UCN storage

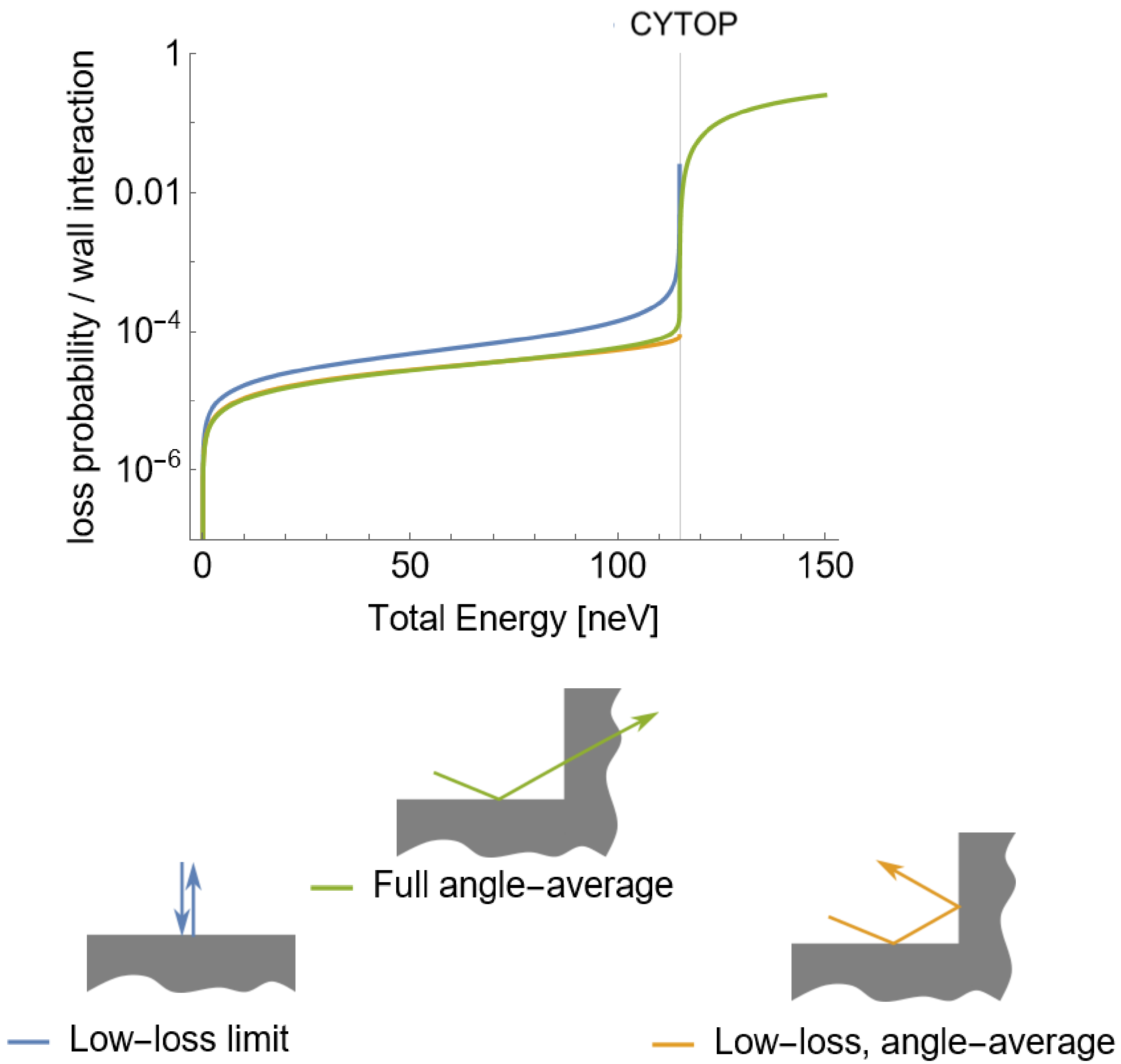

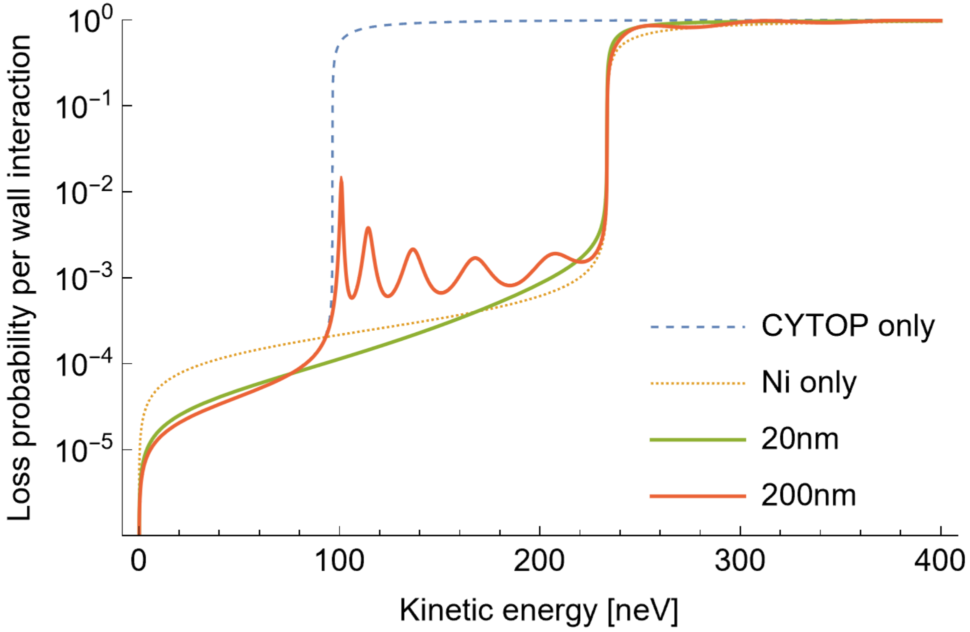

- Different materials
- Include effect of ambient medium
- Include surface layers

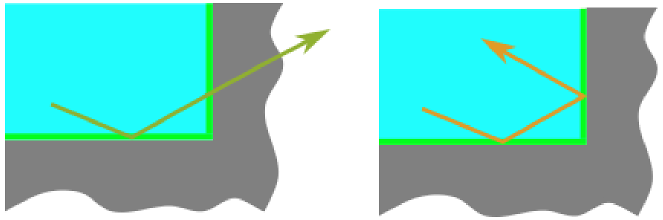

From wall loss to storage times

mean wall collision rate

beta decay

$$\tau^{-1} = \frac{A}{4V} v \bar{\mu}(E) + \tau_\beta^{-1}$$

wall loss

How long should we accumulate?

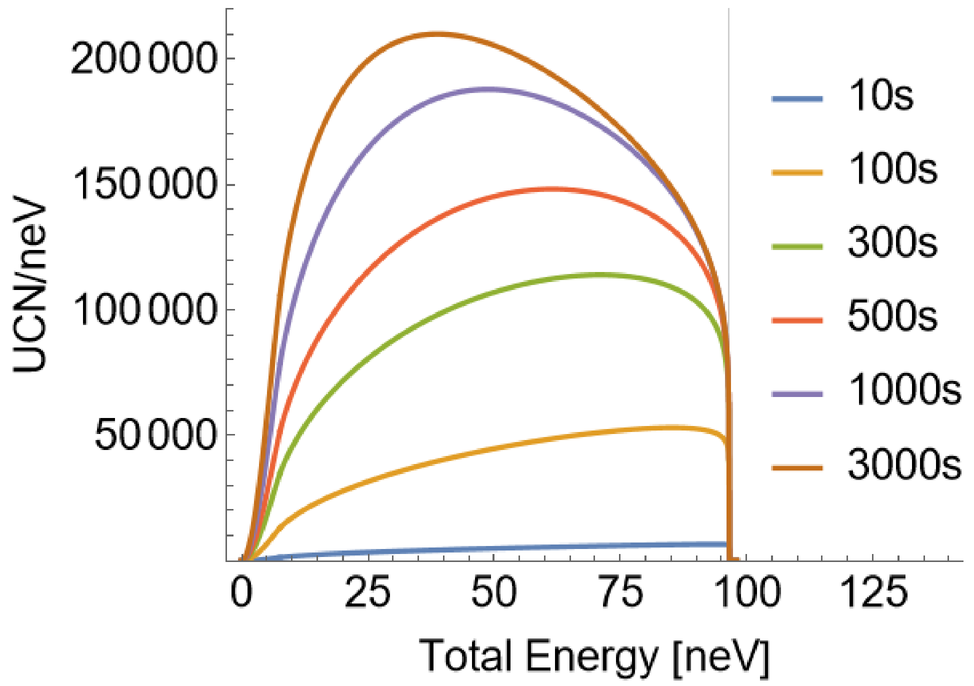

Get some idea of measured spectrum via time-of-flight

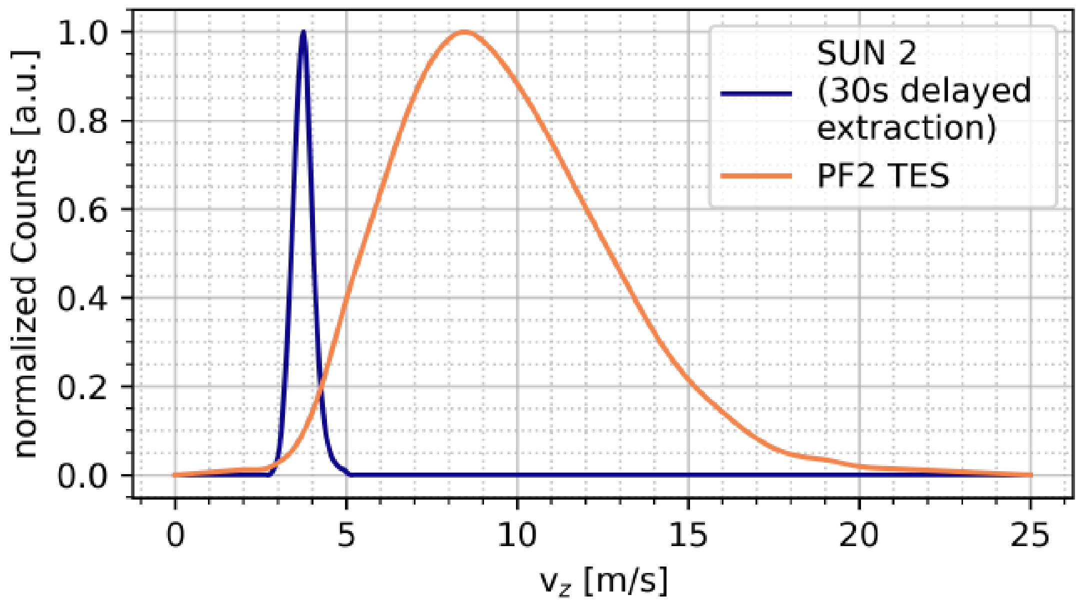

What if we extract after a holding delay?

$$\tau^{-1} = \frac{A}{4V} v \bar{\mu}(E) + \tau_\beta^{-1}$$

mean wall collision rate: $\frac{A}{4V}v$

wall loss: $\bar{\mu}(E)$

beta decay: τ_β^{-1}

(Fixed 100s accumulation time.)

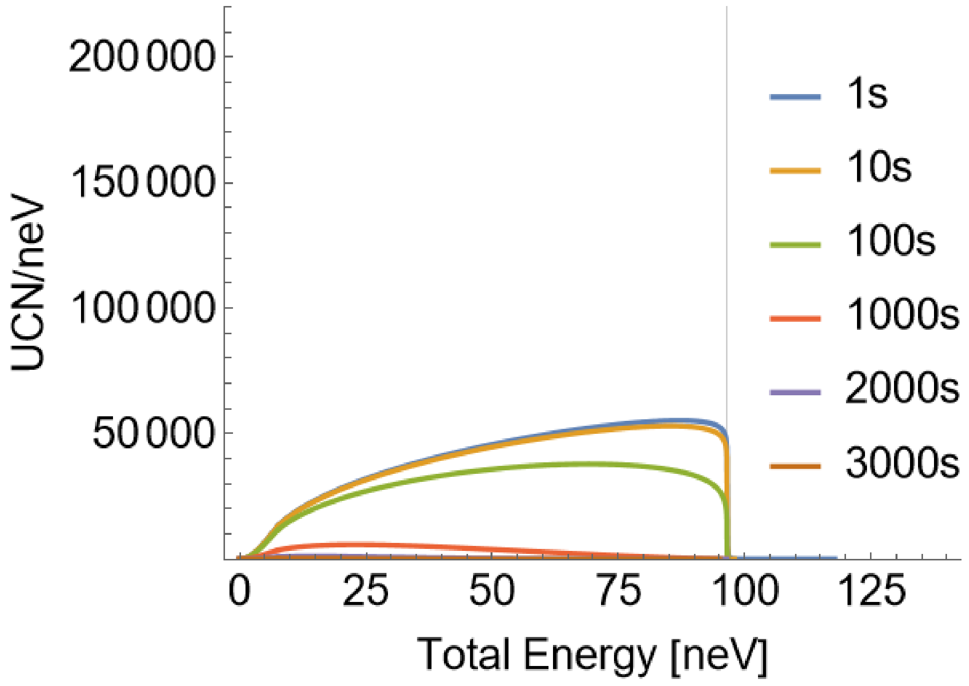

(Fixed 3000s accumulation time.)

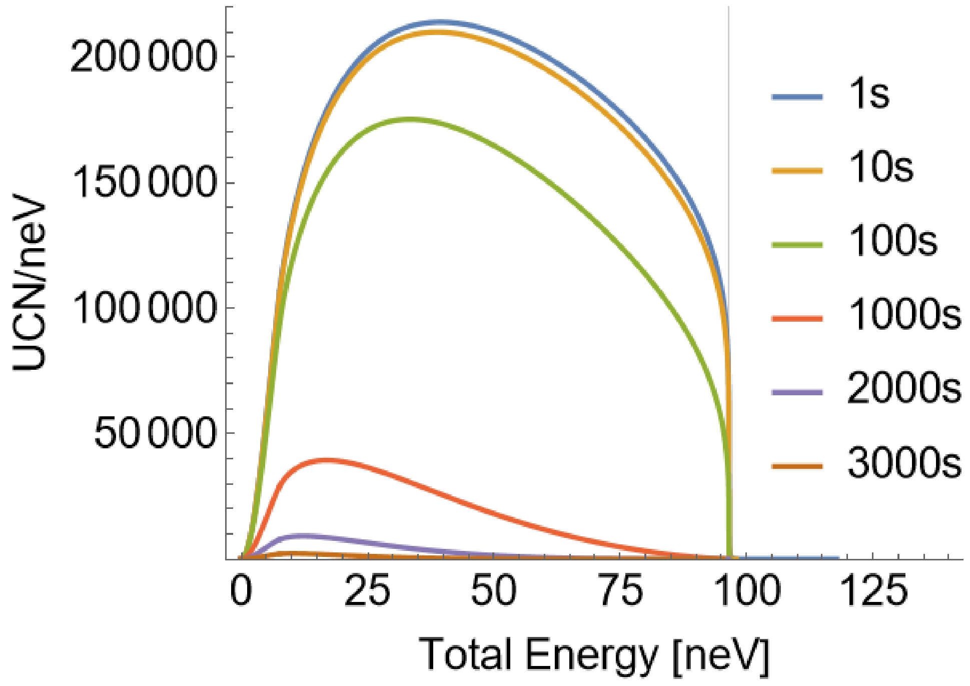

What about overcritical neutrons?

$$\tau^{-1} = \frac{A}{4V} v \bar{\mu}(E) + \tau_\beta^{-1}$$

mean wall collision rate

wall loss

beta decay

(Fixed 100s accumulation time.)

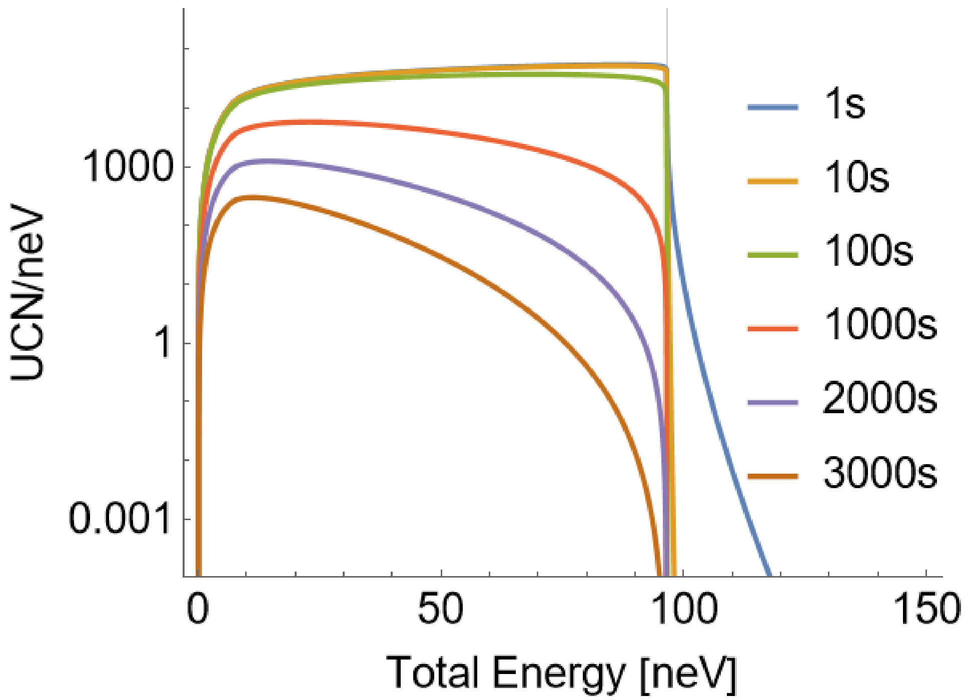

(Fixed 3000s accumulation time.)

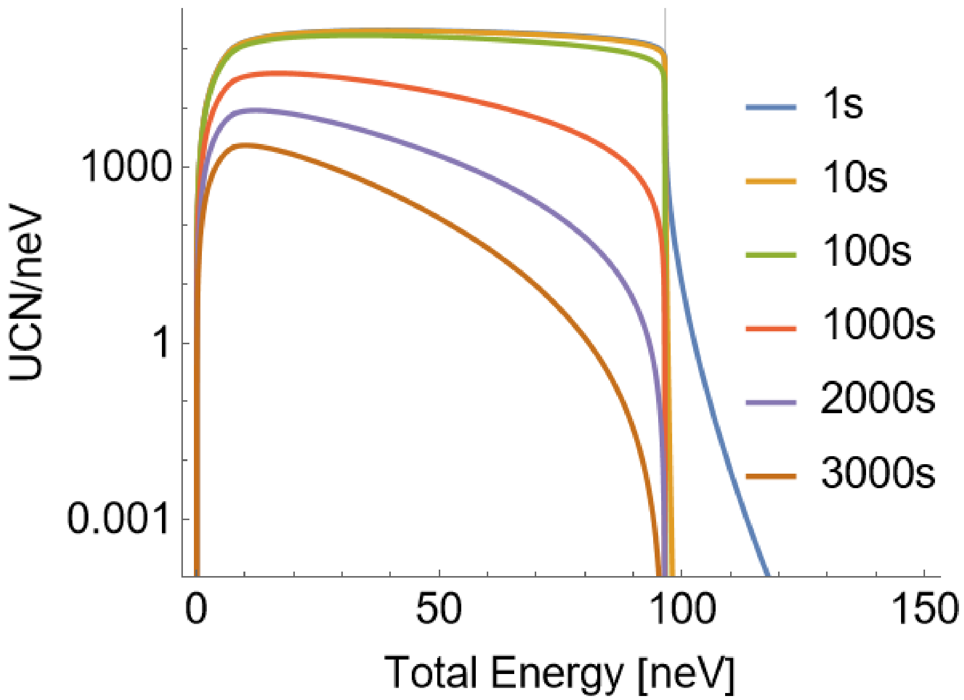

Overview of the SuperSUN UCN Source

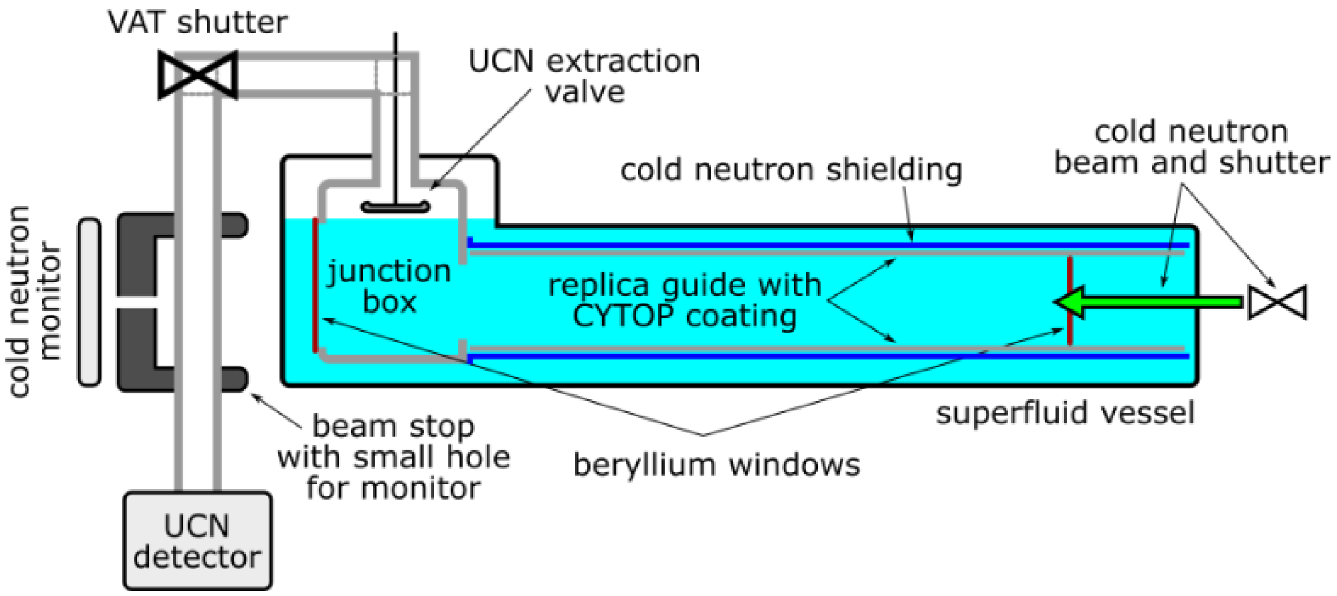

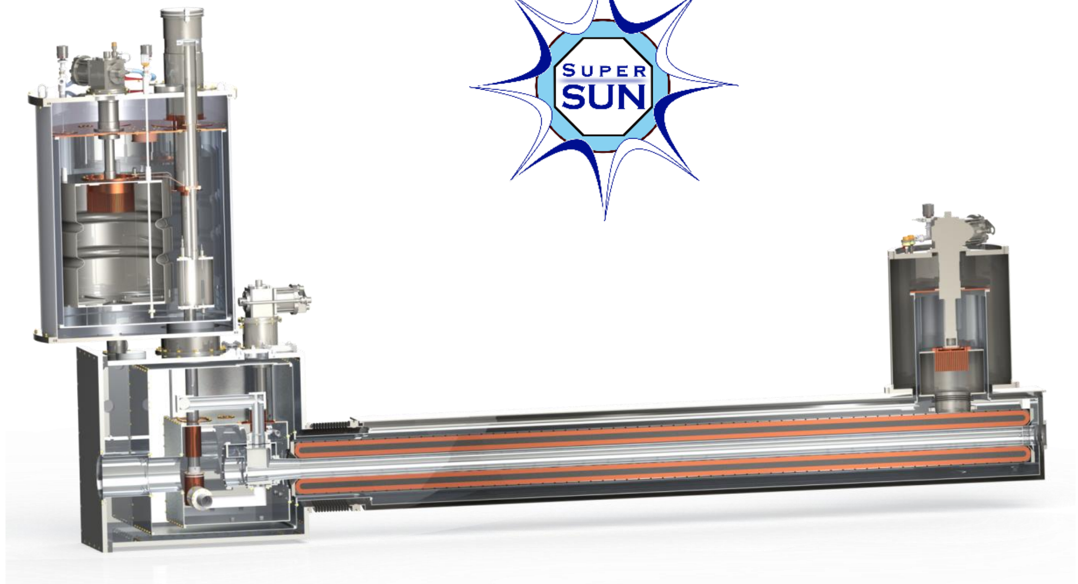

- Open converter / fill-and-empty
- Extraction / delivery efficiency

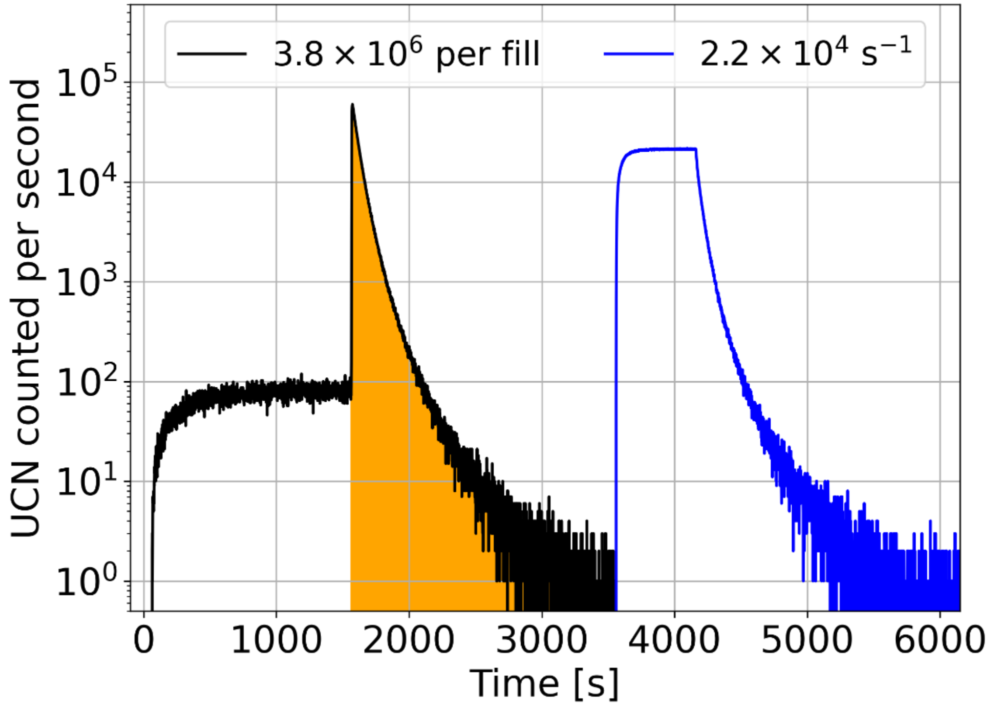

SuperSUN: High density UCN source

Phase I characterization

Measurement agrees with expectation (48 MW)

cf. EPJ Conf. 219, 02006 (2019)

Total UCN output: 3.8×10^6 (integral of blue peak)

Source density: 270 UCN/cm^3

Long storage times: 126000 UCN remaining after 20min

Expected density in PanEDM: 3.9 UCN/cm^3 (58 MW)

Source characterization, PanEDM commissioning ongoing

Phase II expectation

Peak field:	2.1 T
Source density:	1670 UCN/cm^3 (**x5 gain**)
Density in PanEDM:	40 UCN/cm^3 (**x10 gain**)

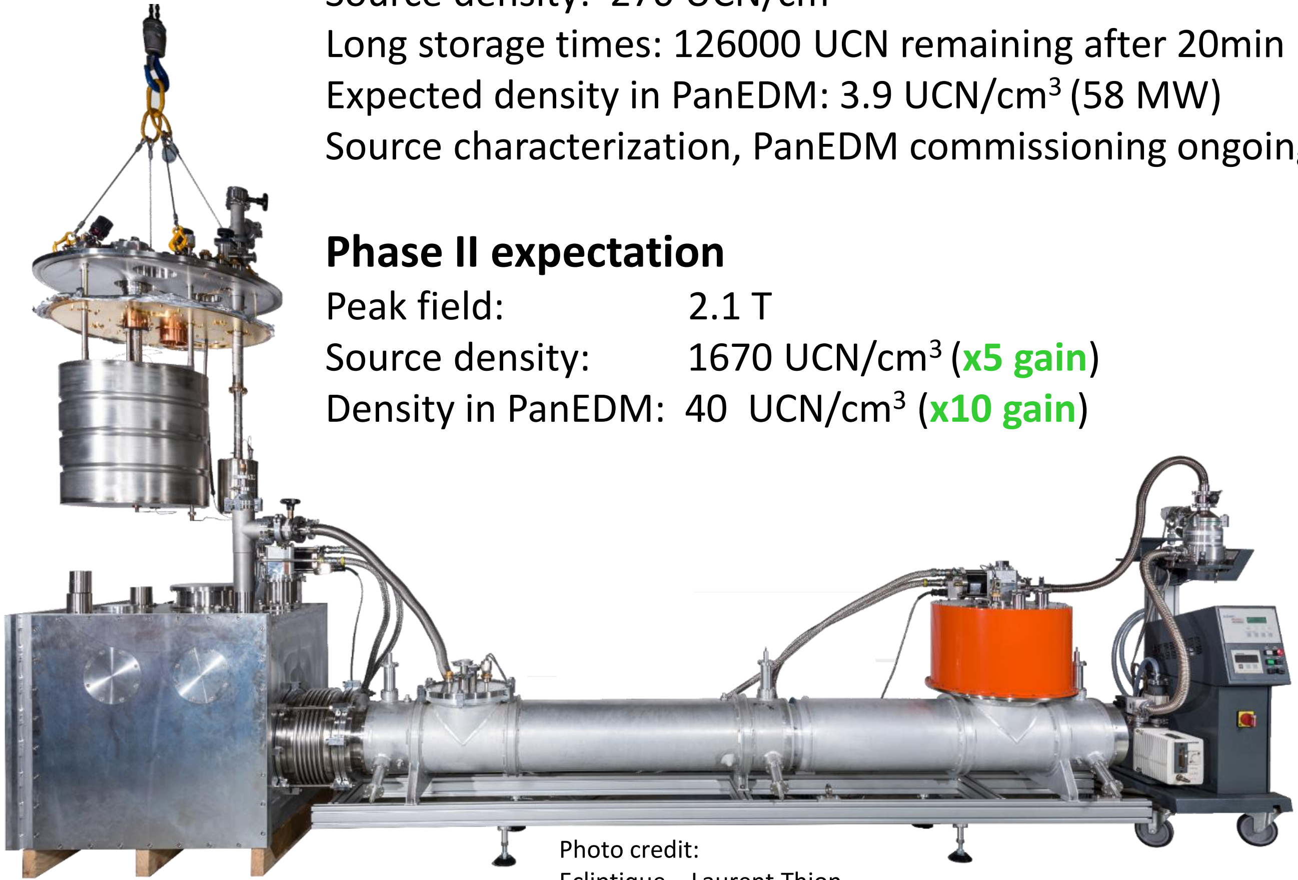

Photo credit:
Ecliptique – Laurent Thion.

Comparison to the prototype source SUN2

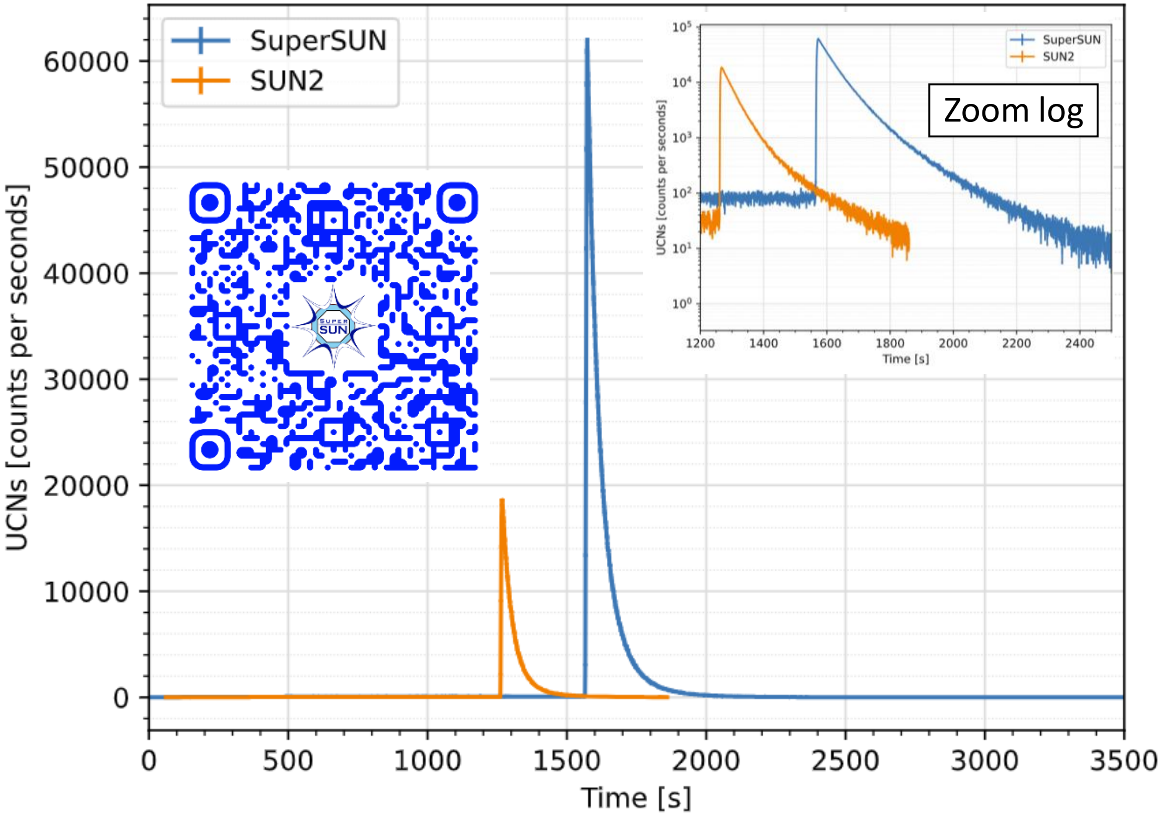

SuperSUN: High density UCN source

Phase I characterization

Measurement agrees with expectation (48 MW)

cf. [EPJ Conf. 219, 02006 (2019)]

Total UCN output: 3.8×10^6 (integral of blue peak)

Comparison to the prototype source SUN2

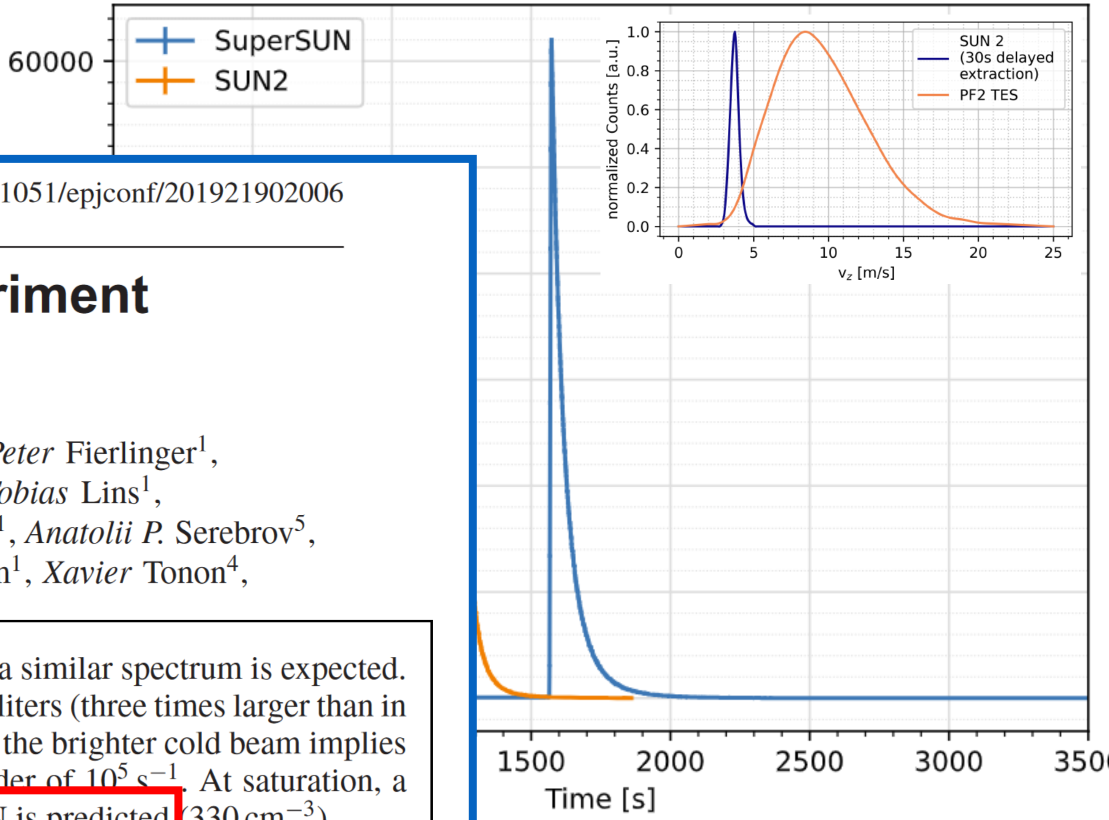

EPJ Web of Conferences **219**, 02006 (2019) https://doi.org/10.1051/epjconf/201921902006

PPNS 2018

The PanEDM neutron electric dipole moment experiment at the ILL

David Wurm[1], *Douglas H.* Beck[2], *Tim* Chupp[3], *Skyler* Degenkolb[4,a], *Katharina* Fierlinger[1], *Peter* Fierlinger[1], *Hanno* Filter[1], *Sergey* Ivanov[5], *Christopher* Klau[1], *Michael* Kreuz[4], *Eddy* Lelièvre-Berna[4], *Tobias* Lins[1], *Joachim* Meichelböck[1], *Thomas* Neulinger[2], *Robert* Paddock[6], *Florian* Röhrer[1], *Martin* Rosner[1], *Anatolii P.* Serebrov[5], *Jaideep Taggart* Singh[7], *Rainer* Stoepler[1], *Stefan* Stuiber[1], *Michael* Sturm[1], *Bernd* Taubenheim[1], *Xavier* Tonon[4], *Mark* Tucker[8], *Maurits* van der Grinten[8], and *Oliver* Zimmer[4]

Ongoing work: spectrum, transfer efficiency and storage in external volumes, etc…

by material walls only, and a similar spectrum is expected. The converter volume is 12 liters (three times larger than in SUN2); scaling for this and the brighter cold beam implies a production rate on the order of $10^5\,\mathrm{s}^{-1}$. At saturation, a total of 4×10^6 stored UCN is predicted ($330\,\mathrm{cm}^{-3}$).

3.8×10^6 UCN measured (fill-and-empty)

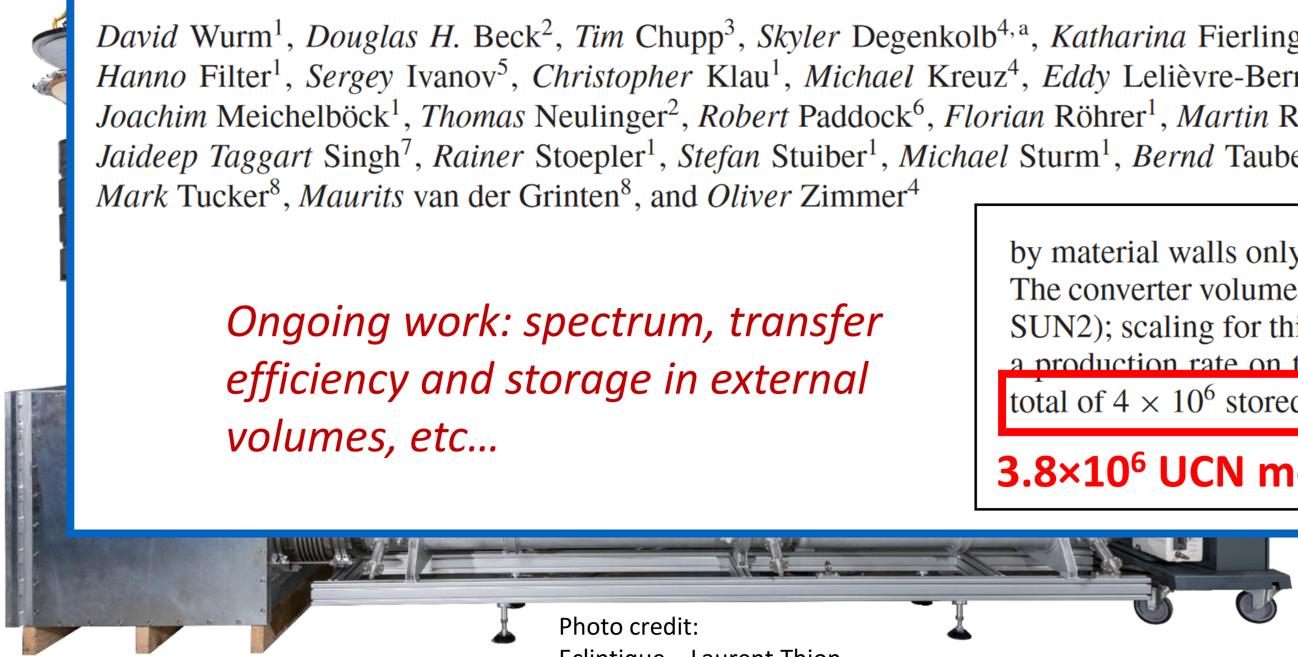

Photo credit:
Ecliptique – Laurent Thion.

SuperSUN phase II: polarized UCN and magnetic storage

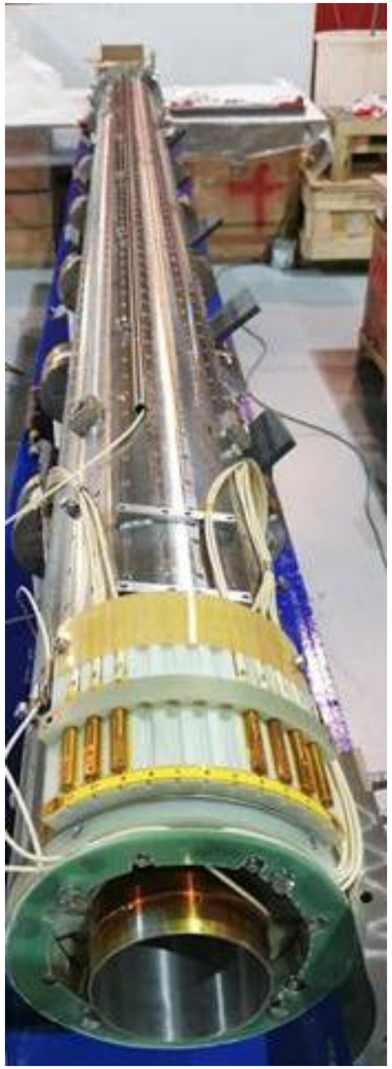

Benefits in phase II

- Increase storage potential for one spin state
- Decrease loss rate for stored UCN

→ UCN already polarized within the source

Phase II expectations (gain over phase I)

Peak field: 2.1 T

Source density: 1670 UCN/cm^3 (**x5 gain**)

Density in PanEDM: 40 UCN/cm^3 (**x10 gain**)

Status

Quench protection validated

Octupole trained up to 1 T

Preparing impregnation of the octupole, to reach nominal field

How much of the spectrum is extractable?

- Open converter / fill-and-empty
- Extraction / delivery efficiency

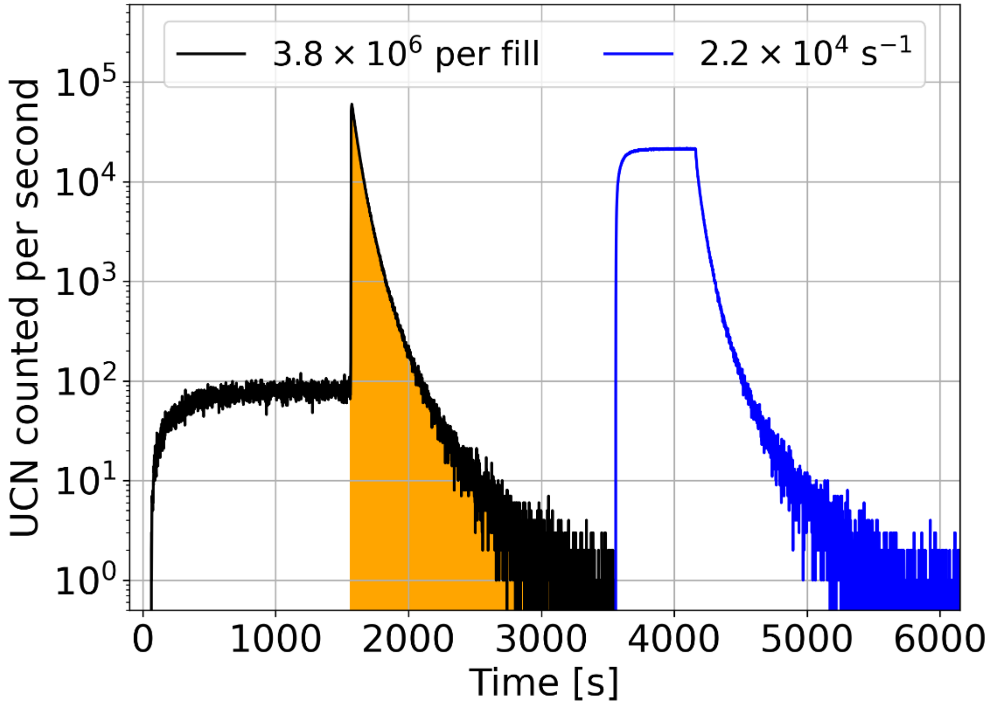

- Boost from leaving helium, vertical extraction
- E < 14.5 neV, ~4.5% of total

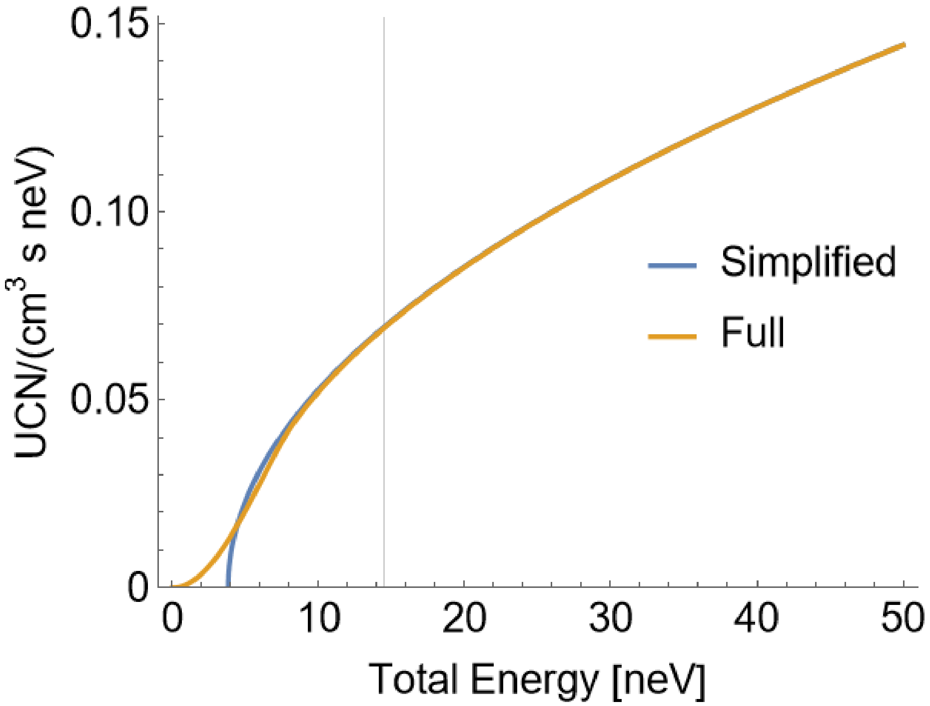

Source Characterization

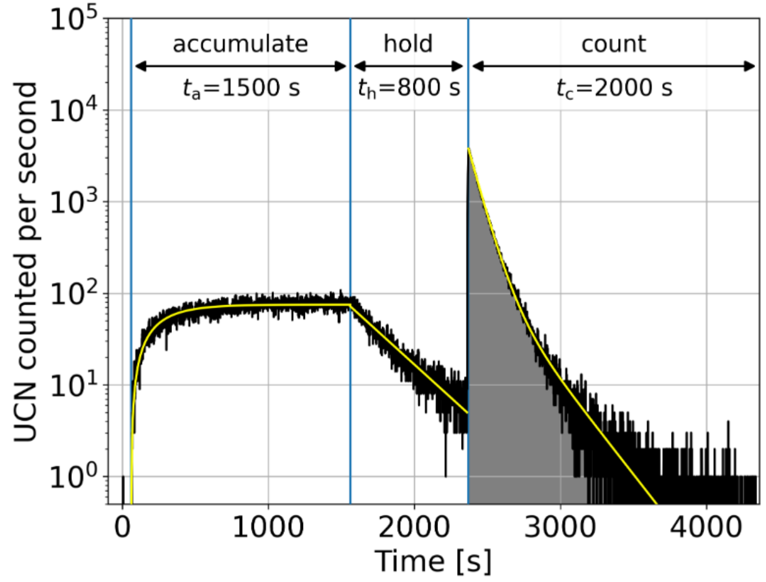

$$f_a(t;\tau_1) = \frac{1 - e^{-t/\tau_1}}{t_a - \tau_1(1 - e^{-t_a/\tau_1})}$$

$$f_h(t;\tau_2) = \frac{e^{-t/\tau_2}}{\tau_2\left(1 - e^{-t_h/\tau_2}\right)}$$

$$f_c(t;c,\tau_3,\tau_4) = c\frac{e^{-t/\tau_3}}{\tau_3} + (1-c)\frac{e^{-t/\tau_4}}{\tau_4}$$

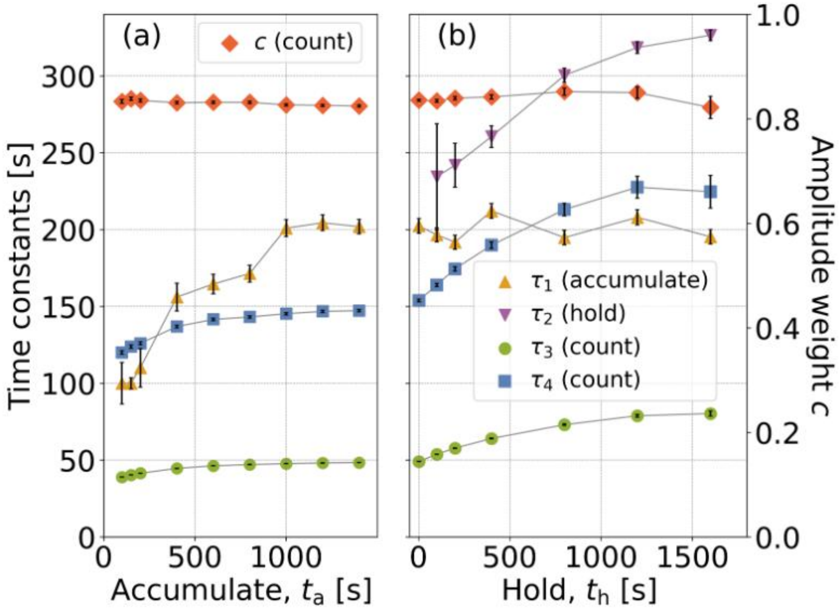

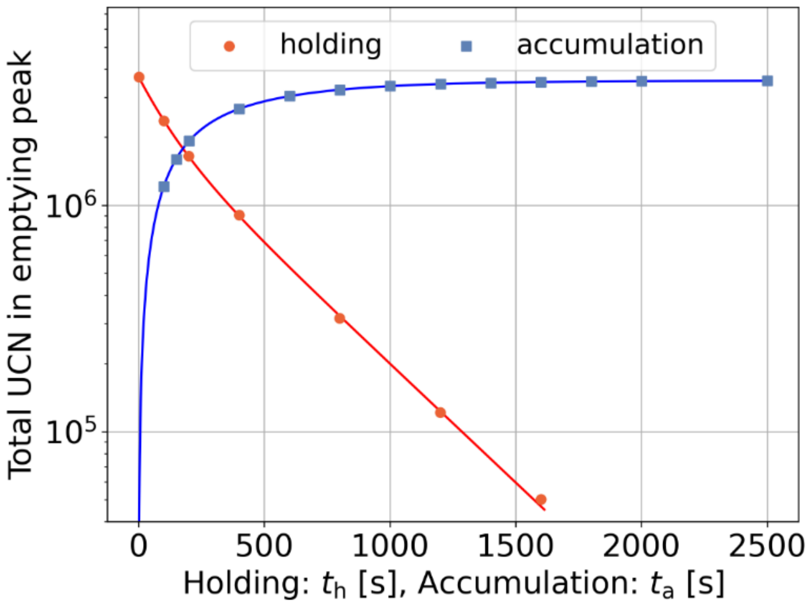

Complementary atoms/nuclei

$$S = s_N d_N + \frac{m_N g_A}{F_\pi}\left[a_0 \bar{g}_\pi^{(0)} + a_1 \bar{g}_\pi^{(1)} + \cancel{a_2 \bar{g}_\pi^{(2)}}\right]$$

We do *not* expect large Schiff moments in ^{129}Xe/ ^{199}Hg (suppressed by the screening effect)

$$\longrightarrow \; d_A(\text{dia}) = \kappa_S S - \underline{\left[k_{C_T}^{(0)} C_T^{(0)} + k_{C_T}^{(1)} C_T^{(1)}\right]}$$

But deformed nuclei can actually have **enhanced** EDMs:

$$\longrightarrow \; d_A(\text{dia}) = \underline{\kappa_S S} - \left[k_{C_T}^{(0)} C_T^{(0)} + k_{C_T}^{(1)} C_T^{(1)}\right]$$

$$S \propto \frac{\eta \beta_2 \beta_3^2 A^{2/3} r_0^3}{E_+ - E_-}$$

$$\frac{S_{Rn}}{S_{Hg}} = \frac{S_{Ra}}{S_{Hg}} \frac{S_{Rn}}{S_{Ra}} \approx 1000 \frac{\beta_2}{\beta_2} \frac{\beta_3^2}{\beta_3^2} \frac{\Delta E_{Ra}}{\Delta E_{Rn}} \approx 50-100$$

50 keV

400 keV

500-1000
(J. Engel et al.)

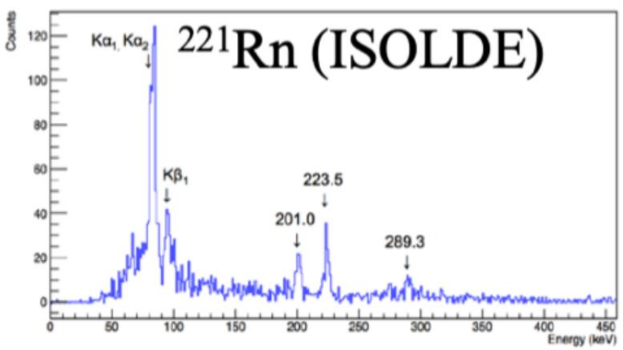

^{223}Rn: TBD

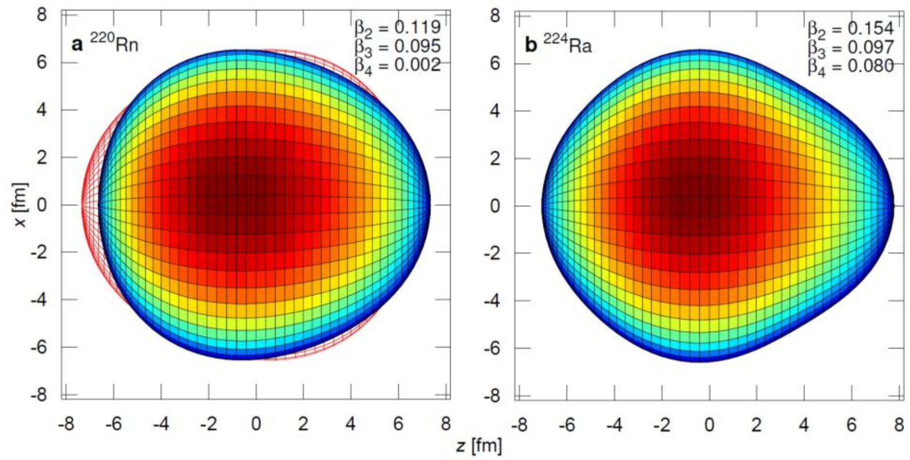

More nuclear structure